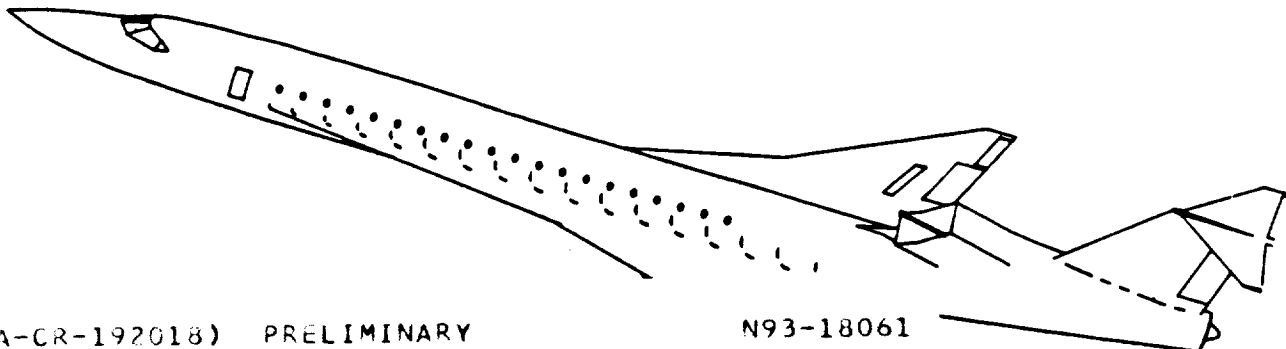


NASA-4435

IN-05-CR-
141654
P.103

Preliminary Design of a High Speed Civil Transport

The Opus 0-001



(NASA-CR-192018) PRELIMINARY
DESIGN OF A HIGH SPEED CIVIL
TRANSPORT: THE OPUS 0-001
(California Polytechnic State
Univ.) 103 p

N93-18061

Unclas

G3/05 0141654

The Opus 0-001 Design Team:

Joe Cannon
Jeff Frizzell
Fritz Anderson
Thomas Apgar
Farooq Ahmad
Asim Hameed

California Polytechnic State University
San Luis Obispo

Abstract

Based on research into the technology and issues surrounding the design, development, and operation of a second generation High Speed Civil Transport, HSCT, the Opus 0-001 team completed the preliminary design of a sixty passenger, three engine aircraft. The design of this aircraft was performed using a computer program which the team wrote. This program automatically computed the geometric, aerodynamic, and performance characteristics of an aircraft whose preliminary geometry was specified.

The Opus 0-001 aircraft was designed for a cruise Mach number of 2.2, a range of 4,700 nautical miles and its design was based in current or very near term technology. Its small size was a consequence of an emphasis on a profitable, low cost program, capable of delivering tomorrow's passengers in style and comfort at prices that make it an attractive competitor to both current and future subsonic transport aircraft. Several hundred thousand cases of Cruise Mach number, aircraft size and cost breakdown were investigated to obtain costs and revenues for which profit was calculated. The projected unit flyaway cost was \$92.0 million per aircraft.

List of Variables / Nomenclature

List Of Symbols

a.c.	Aerodynamic Center
AEO	All Engines Operating
APU	Auxillary Power Unit
C_D	Coefficient of Drag
$C_{D\alpha}$	Variation in Drag Coefficient due to Angle of Attack
$C_{D\delta_e}$	Elevator Trim Drag Coefficient
C_{D_u}	Variation in Drag Coefficient Due to Velocity
CG	Center of Gravity
C_L	Lift Coefficient
$C_{L\beta}$	Pitching Coefficient Due to Side-Slip
$C_{L\delta_e}$	Variation of Lift Coefficient with Elevator Deflection
$C_{L\delta_r}$	Variation of Lift Coefficient with Rudder Deflection
C_{Lq}	Lift Coefficient Due to Pitch Rate
C_{L_u}	Variation in Lift Coefficient Due to Velocity
$C_{L\alpha}$	Variation in Lift Coefficient Due to Angle of Attack
$C_{m\alpha}$	Variation in Pitching Moment Coefficient due to Angle of attack
$C_{m\delta_e}$	Variation in Pitching Moment Due to Elevator Deflection
C_{m_ih}	Variation in Pitching Moment Coefficient Due to the incidence angle of the Horizontal Stabilizer
C_{m_0}	Pitching Moment Coefficient at Zero Lift
C_{mq}	Pitching Moment Coefficient Due to Pitch Rate
C_{m_u}	Variation in Pitching Moment Due to Velocity
$C_{n\beta}$	Variation in Yaw Moment Due to Side-Slip
$C_{N\delta_r}$	Rudder Control Power
$C_{y\beta}$	Side Force Due to Side-Slip
$C_{Y\delta_r}$	Side Force Due to Rudder Deflection
HSCT	High Speed Civil Transport
FAA	Federal Aviation Administration
FAR	Federal Aviation Regulations
F.O.D.	Foreign Object Damage
ksi	Kilo pounds per square inch
L/D	Airplan Lift to Drag Ratio
OEI	One engine inoperative

psf Pounds Per Square Foot
RAT Ram Air Turbine

Table of Contents

1.0 Introduction	1
2.0 Mission Description.....	3
3.0 Preliminary Sizing	5
4.0 Aircraft Configuration	8
4.1 Options For Wing Layout.....	8
4.2 Engine Number and Location.....	10
4.2.1 Four Engines.....	10
4.2.2 Three Engines.....	12
5.0 Performance	13
5.1 Requirements.....	13
5.2 Aerodynamics and Performance	13
5.3 Performance Verification.....	16
6.0 Stability and Control	22
7.0 Wing Design	26
8.0 Fuselage Design	30
8.1 Cabin Arrangement.....	30
8.2 Safety Considerations.....	34
8.3 Flight Deck.....	35
8.4 Baggage Compartment.....	37
8.5 Fuel Tanks	37
9.0 Empennage design	39
10.0 Landing Gear	44
10.1 Landing Gear Position.....	44
10.2 Landing Gear Design	46
11.0 Propulsions	51
11.1 Engine Selection.....	51
11.2 Engine Position.....	53
11.3 Inlet Design.....	57
11.4 Engine Noise.....	59
11.5 Propulsion Development.....	59
12.0 Systems	60
12.1 Hydraulics.....	60
12.2 Electrical	65
12.3 Fuel.....	65

12.4	Oxygen.....	67
12.5	Anti-Ice.....	67
12.6	Fire Extinguishing.....	67
12.7	Potable Water.....	68
12.8	Waste Water.....	68
12.9	Air Conditioning / Pressurization.....	69
12.10	Engine Servicing and Inspection.....	72
12.11	Galley.....	72
13.0	Structures.....	73
13.1	Fuselage.....	73
13.2	Wing.....	75
13.3	Empennage.....	75
13.4	Structural Design Limits.....	78
14.0	Materials.....	80
15.0	Manufacturing.....	82
16.0	Cost and Profitability Analysis.....	85
17.0	Conclusions and Recommendations.....	90
18.0	References.....	91
19.0	Appendix.....	93

List of Figures

Figure 2.1	Mission Profile	4
Figure 3.1	Design Point Diagram.....	6
Figure 4.1	Aircraft Three-View	9
Figure 5.1	Area Distribution	15
Figure 5.2	Representative Drag Polars.....	17
Figure 5.3	Range versus Payload	20
Figure 6.1	CG Excursion.....	24
Figure 7.1	Wing Planform.....	27
Figure 7.2	Inboard and Outboard Airfoils.....	27
Figure 8.1	Cabin Layout	31
Figure 8.2	First Class Cross Section	32
Figure 8.3	Business Class Cross Section	33
Figure 8.4	Advanced Flight Deck.....	36
Figure 9.1	Empennage Detail.....	40
Figure 9.2	Longitudinal X-Plot	42
Figure 9.3	Directional X-Plot.....	43
Figure 10.1	Critical Landing Gear Angles.....	45
Figure 10.2	Ground Turning Capability	47
Figure 10.3	Main Landing Gear.....	48
Figure 10.4	Nose Landing Gear	50
Figure 11.1	Engine, Inlet, and Nozzle Placement.....	54
Figure 11.2	Inlet, Engine and Nozzle Diagram.....	58
Figure 12.1	Hydraulic System Schematic	61
Figure 12.2	Hydraulic Pumps and Reservoirs.....	62
Figure 12.3	Hydraulic Line Layout.....	63
Figure 12.4	Center Hydraulics and Powerplant Access	64
Figure 12.5	Fuel System Arrangement.....	66
Figure 12.6	Engine Fire Extinguishing	68
Figure 12.7	Potable Water Waste	69
Figure 12.8	Air Conditioning and Pressurization System.....	71
Figure 13.1	Structural Layout	74
Figure 13.2	Wing Structure Layout.....	76
Figure 13.3	Stress Analysis	77
Figure 13.4	Structural Design Limits.....	79
Figure 14.1	Skin Temperatures and Materials at Mach 2.2	81

Figure 15.1	Manufacturing and Assembly Breakdown.....	83
Figure 16.1	ROI vs Seating Capacity and Mach number.....	86
Figure 16.2	Aircraft Development Cost Breakdown.....	88
Figure 16.3	Manufacturing Cost Breakdown.....	88
Figure 16.4	Operating Cost Breakdown.....	89

List of Tables

Table 5.1	Performance Requirements.....	13
Table 5.2	Aircraft Performance.....	18
Table 5.3	Maximum Performance Capabilities.....	19
Table 6.1	Stability Derivatives.....	23
Table 7.1	Wing Geometry Summary.....	26
Table 7.2	Flap Deflection for Take-off and Landing.....	29
Table 9.1	Empennage Geometry.....	39
Table 10.1	Tire Data for Main and Nose Gear.....	49
Table 11.1	Engine Trade Study.....	52
Table 13.1	Design Limits and Design Ultimate Load Factors....	78

1.0 Introduction

Despite a somewhat troubled history (Reference 1), civilian supersonic passenger travel is on the verge of becoming a reality. Advances in propulsions, aerodynamics, and computer technology have reduced the obstacles from insurmountable to merely formidable. Twenty years ago, the U.S. undertook the design and development of a supersonic transport, but cancelled the project midway through (Reference 2). The reasons included environmental concerns and questions about the economic feasibility of such an aircraft. The French/British SUD/BAC Concorde was developed, despite these obstacles, but has been only a marginal economic success due to range limitations and the scarcity of airports willing to accommodate the excessive noise produced by the Concorde during takeoff and landing (Reference 1). These problems resulted in a small fleet size, which forced ticket prices up, limiting the number of travellers for whom supersonic flight was an option.

Ongoing research into the technologies and challenges of high speed flight by both government and civilian agencies have produced a number of innovative solutions to vexing questions. In particular, materials and propulsions for an HSCT have advanced enough to improve weight and range to the point of viability. The definition of viability is considered to be trans-Pacific flight since Pacific Rim traffic is projected to grow substantially in the next twenty years. Flights over this distance have the greatest time savings and therefore accentuate the advantages of supersonic flight. In addition, an aircraft that could fly trans-Pacific could also fly almost any other mission that an airline desired.

The environmental issues are somewhat more difficult to deal with. Sonic boom, for example, could be minimized by extensive tailoring of the aerodynamics of the vehicle. These modifications would adversely effect aircraft performance, thus reducing possible range. Since most countries currently forbid overland supersonic flight, overland routes were excluded from market considerations.

Takeoff noise is more difficult to resolve now, due to tightening of noise restrictions to the Federal Aviation Regulations FAR Part 36, Stage III level. NASA and several engine manufacturers have developed engines that reduce noise by reducing

exhaust velocity and by mechanical noise suppression. These engines are believed to be able to meet the Stage III restrictions (Reference 3).

A final environmental issue is the introduction of oxides of nitrogen into the upper atmosphere where they pose the danger of damaging the ozone layer. Again, improvements in combustion technology and the adoption of altitude restrictions make this problem manageable.

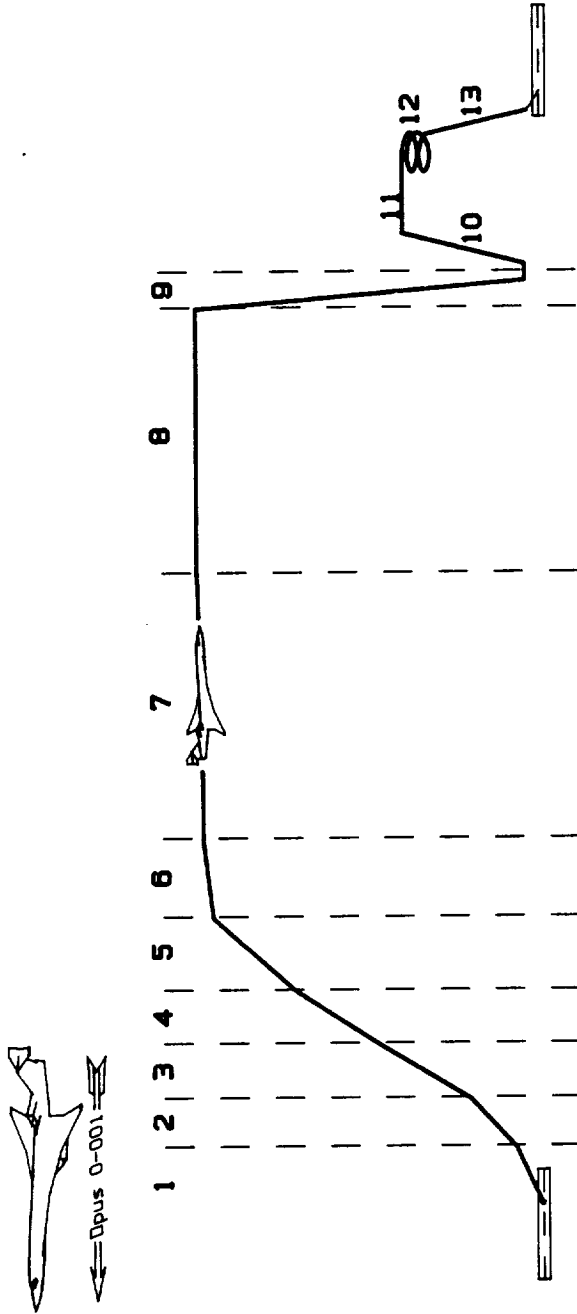
Given this background and the projected growth in world air traffic along lengthy over water routes, there is a definite market for a supersonic aircraft. However, before even an environmentally sound HSCT takes flight, the airlines and airframe manufacturers must be assured of making a profit. The Opus 0-001 economic analysis (Reference 4) included an in-depth study of the various costs involved in the design, development, manufacture, and operation of such an aircraft. Further, this analysis developed a revenue model which related ticket price by travel class to time savings and percentage market capture. Several hundred thousand cases of cruise Mach number, aircraft size and class breakdown were investigated to obtain costs and revenues from which profit was calculated. This analysis revealed that a the Opus 0-001 should be a sixty passenger, Mach 2.2 aircraft to provide maximum return on investment to the airline, while guaranteeing the airframer a profit margin. This small aircraft will be less expensive to develop, have less difficulty meeting takeoff noise requirements, and will fit into airports without requiring any of the modifications a larger HSCT would necessitate. Further, the Opus 0-001 is uses current technology -- unlike its larger competitors which are designed to optimistic technology levels projected ten to twenty years into the future -- ensuring that it will have a corner on the market for many years to come.

2.0 Mission Description

The Opus 0-001 HSCT is to be capable of supersonic cruise at Mach 2.2 with a design range of 4,700 nautical miles plus international reserves. The mission, including reserves, is illustrated in Figure 2.1.

The maximum balanced takeoff and landing field lengths are each 11,000 feet. The flight profile on climb is structured to remain below 250 knots while below 10,000 feet per FAR Part 91.70, followed by a relatively steep climb to 36,000 feet, at which point the aircraft levels off for acceleration to cruise speed and climbs to beginning cruise altitude. This acceleration begins approximately 25.5 miles from the point of takeoff, since this acceleration will take place over the ocean the chance that the sonic boom footprint will reach populated areas is reduced. The aircraft then cruise-climbs while remaining at the optimum lift coefficient for maximum range until it reaches the environmentally imposed altitude ceiling of 60,000 feet. Upon nearing its destination, the aircraft descends to land. No range credit is assumed for descent, as it may be necessary to spend some time in a holding pattern before landing. If at this point in the flight, it became necessary for the aircraft to divert to an alternate destination, the aircraft would climb to approximately 20,000 feet and fly subsonically one hundred nautical miles followed by the potential for thirty minutes loiter before final descent and landing.

This aircraft is capable of reasonably efficient travel at high subsonic speeds ($L/D = 14.5$), so if the takeoff or landing locations are inland, the aircraft can fly subsonically while overland without undue effect on range. Also, should one engine fail in cruise, the aircraft will be capable of either returning to its point of departure or continuing to its destination.



International Reserves:

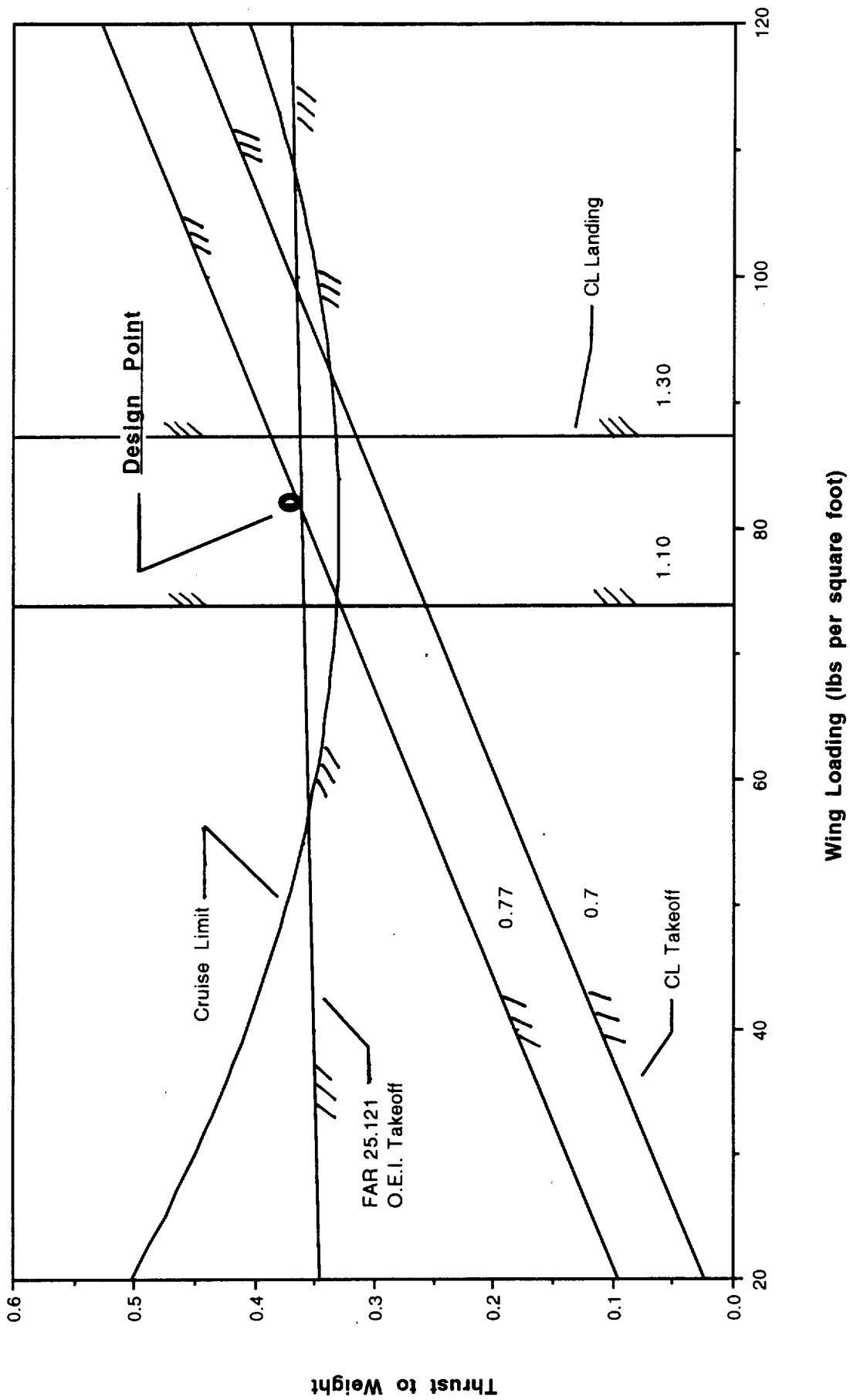
250 (0.43)
463 (0.76)

Figure 2.1: Mission Profile

3.0 Preliminary Sizing

In the preliminary sizing of the aircraft, it was presumed that the aircraft was a conventional, highly swept wing design incorporating turbine engines of some sort and fixed wing geometry (Reference 5). Comparisons with other supersonic cruise aircraft and research into the status of HSCT technology resulted in approximations of lift and drag. The design was constrained not only by the mission profile parameters described above (field length, range, speed) but also by FAR Part 91 concerning climb capability during takeoff, climb, and landing phases of flight with one engine inoperative, OEI. A trade study of wing loading (W/S), and takeoff thrust loading (T/W), resulted in the plot shown in Figure 3.1. The final design point was selected at $W/S = 80$ pounds per square foot, psf, and $T/W = 0.37$.

For low speed flight requirements such as field length and climb gradients, a trade study of various aspect ratios, wing loadings, and takeoff and landing speeds was carried out on an approximate basis to establish the design point chart (Appendix). The results of this analysis indicated that higher aspect ratios and lower wing loadings were desirable from a low speed point of view. Conversely, a high wing loading was preferred for high speed flight. This is due to reduced wetted area for parasite drag, and passenger comfort. Another advantage of a high wing loading is that for a given aircraft geometry and flight condition, there is a unique C_L which produces the best L/D ratio: for low wing loadings, this value is achieved at the altitudes of highest ozone concentration. A wing loading of 80 psf was selected as a compromise which retained low speed performance, but did not have excessive drag in cruise.



Wing Loading (lbs per square foot)

Figure 3.1: Design Point Diagram

An aspect ratio of 2.4 was selected as a compromise between low speed and high speed flight. A wing aspect ratio of three would have been best for low speed flight, but would have presented structural and aerodynamic difficulties. To reduce drag, a sweep angle of 70 degrees would be required to keep the wing within the Mach cone of 61 degrees. With this leading edge sweep, a W/S of 80 psf, and an aspect ratio of three, simple geometric constraints would have dictated a highly swept arrow wing which would result in poorly supported wing tips. That would be structurally inefficient and produce other difficulties such as potential ground strike at takeoff and landing due to the aft extension of the wing.

Thus a compromise was struck between low speed and high speed performance by adopting a double delta/arrow wing combination with an aspect ratio of 2.4 and a W/S maintained at about 80 psf.

4.0 Aircraft Configuration

The airplane configuration is determined both by internal and external constraints. The requirement to carry sixty passengers comfortably suggests a large fuselage diameter. On the other hand, aerodynamic constraints dictate a slender, area-ruled fuselage. By iteratively balancing these two constraints a refined fuselage geometry was settled upon. This geometry is shown in Figure 4.1. One criterion which the design team would not compromise was the requirement that a tall person (6'-6") should be able to wall upright in the aisle.

4.1 Options For Wing Layout

Alternative configurations for the Opus 0-001 included variable wing geometry, either symmetrically swept or skewed. A variable sweep wing, much like that of the Rockwell B-1 and the original Boeing SST proposal (Reference 6) would easily meet takeoff and landing requirements due to its aerodynamic similarity to standard subsonic transports in those flight regimes. In addition, compromises in W/S and aspect ratio would not be required, since aspect ratio and wing planform area both vary with sweep angle, resulting in an aircraft optimized for both cruise and low speed flight.

As attractive as this is, the design burden would have only been shifted to structural weight -- reducing the mission payload and range. The pivot mechanism and associated carry through structure for bending moments would be overly heavy and complex. Such systems are safety critical and for civilian use must be very reliable and intensively maintained (Reference 6). The structure necessary to carry bending moments through would impinge into the cabin as well, reducing the flexibility of the internal layout of the aircraft. The aforementioned Boeing SST proposal won against its fixed geometry Lockheed competitor for essentially the performance reasons listed above. However, midway through the design process, Boeing was forced to admit that the pivot weight was untenable and revised its design to a fixed geometry, (Reference 3). Thus, while it is certainly possible to make a variable geometry aircraft, the advantages are outweighed by the added complexity and weight.

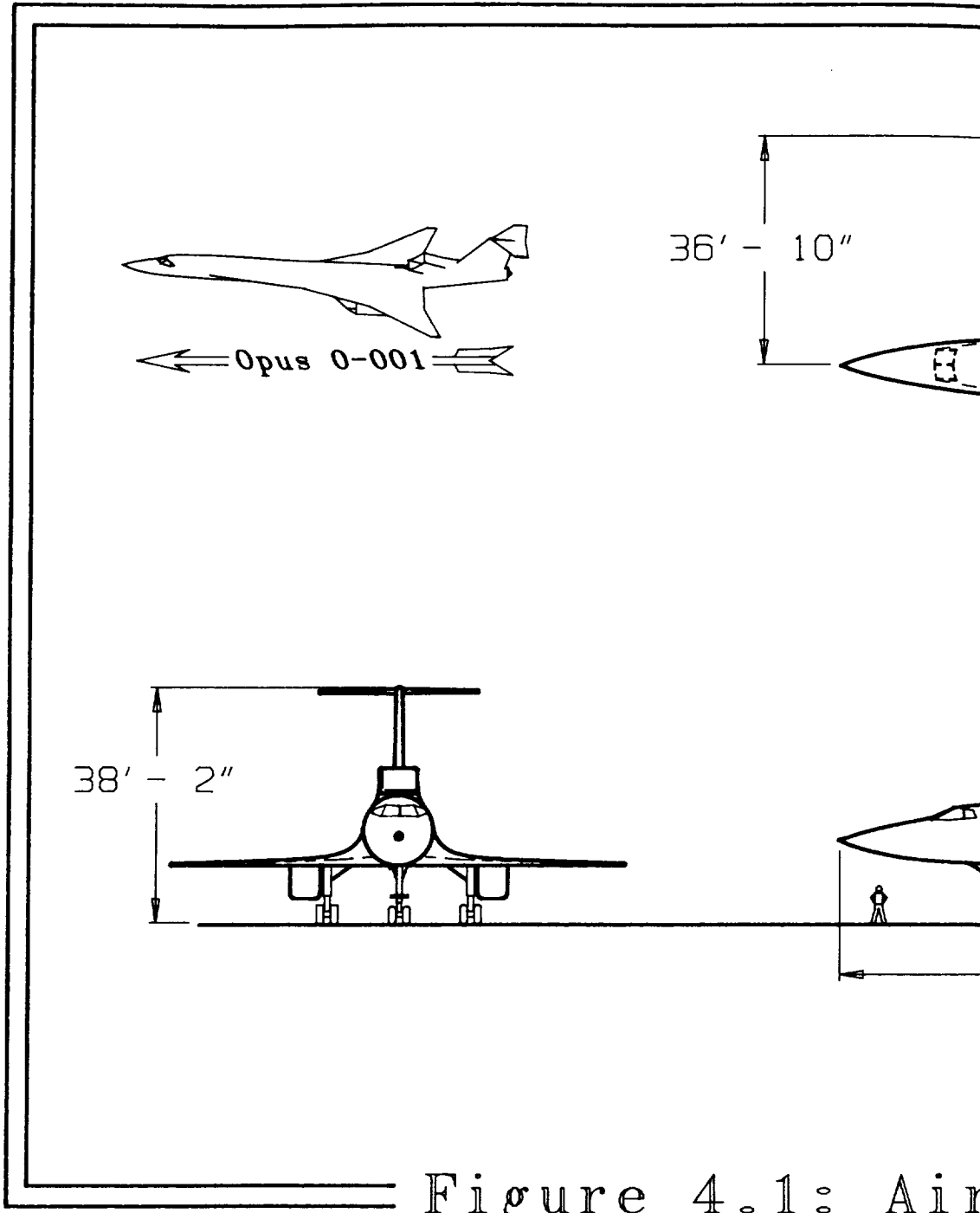
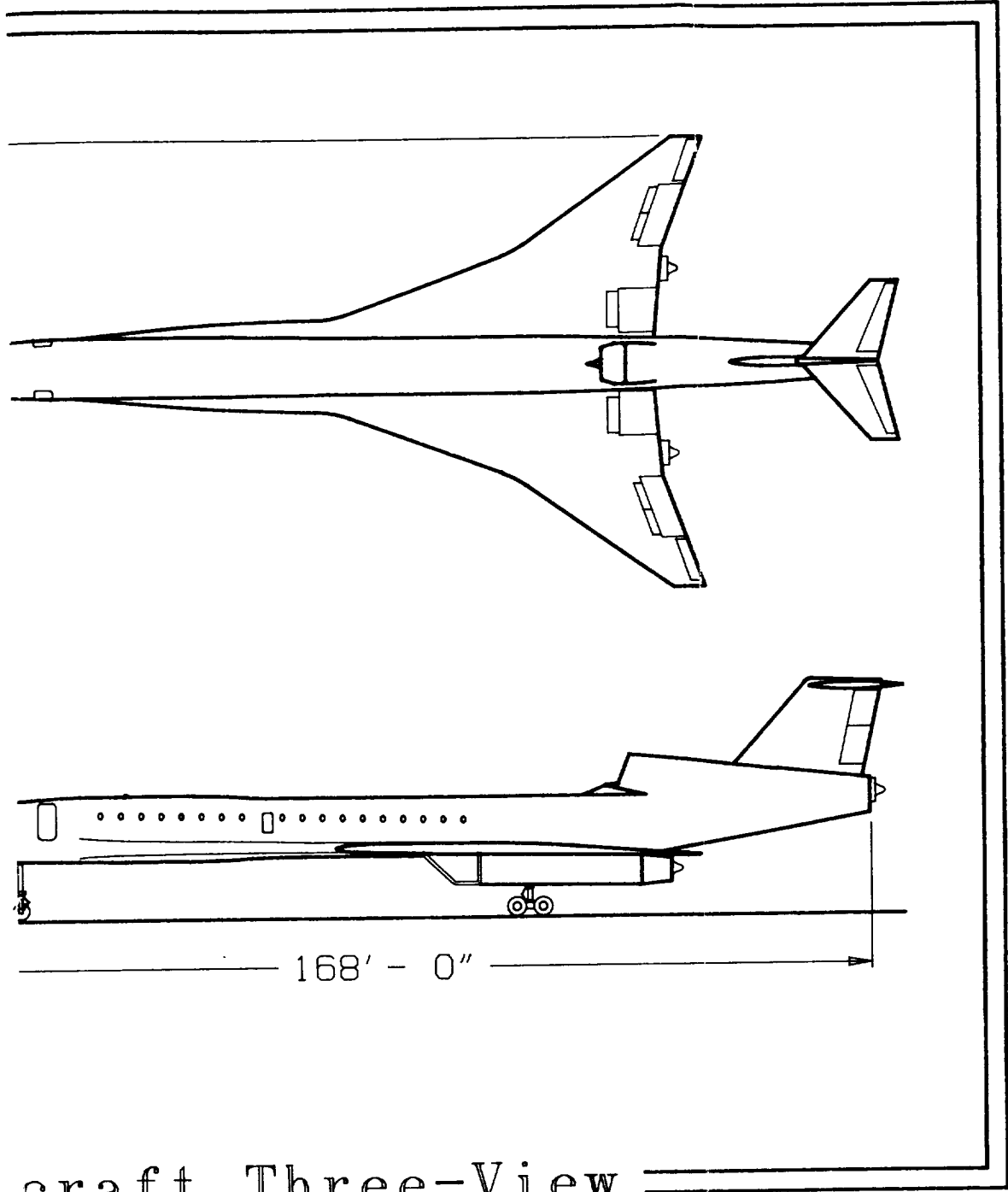


Figure 4.1: Air



craft Three-View

An oblique skewed wing design possesses many of the merits of the symmetric variable geometry design without the bending moments to carry through the pivot structure and wing. However, the relatively small size of Opus 0-001 meant that any fuselage mounted pivot mechanism (if mounted near the CG, as would be expected for a design with low trim drag in mind) would impinge into the passenger cabin and produce a maintenance burden by being difficult to access. These together with the possible marketing difficulties of the unconventional asymmetric aircraft effectively ruled this option out.

4.2 Engine Number and Location

The next major configuration item to be determined by performance requirements was the number and location of the engines. Key issues in the selection of these parameters were T/W requirements, OEI flight conditions, cost, maintenance, and airframe integration. At first, the small size of the Opus 0-001 (due to small payload weight) and cost and simplicity issues suggested a two engine configuration. However, the climb requirements for OEI for a two engine aircraft with such a low aspect ratio would have resulted in the need for a takeoff T/W of 0.60. This is comparable with many combat aircraft, but is highly unattractive due to the excess weight and costly operation of an engine that oversized. Further, a major advantage of the Opus 0-001 design -- its ability to meet Stage III noise requirements -- would likely have been compromised by engines of this size. Consequently, both three and four engine designs were considered. Both were satisfactory in terms of the T/W ratios.

In the discussion that follows, the combination of engine and inlet integration considerations are used interchangeably to refer to propulsion/airframe integration, which plays an important role in the aerodynamic efficiency of the aircraft as a whole.

4.2.1 Four Engines

A four engine layout would provide for favorable lift interference if the engines were to be located far aft on the wing. Unfortunately, four engines require more maintenance and leave less span for high lift devices (which are

a necessity for a highly swept, low aspect ratio wing). In addition, four wing mounted engines would require wide separation between the engines to reduce interference drag in supersonic cruise. Supersonic interference drag can result in variations of L/D by as much as 1 full point (Reference 7).

For drag reasons, most four engine HSCT designs incorporate podded axisymmetric engines (Reference 8). Podded engines need to be mounted well away from the wing, and each other, in order to realize the benefits of the podded installation. Typically, small aircraft like the Opus 0-001 do not possess the ground clearance required to suspend engines on pods, so the engines would have to be mounted directly on the wing, negating many of the benefits of the axisymmetric inlet. Consequently, two dimensional inlets (2-D) were selected. These inlets can be mounted directly under the wing. To provide adequate pressure recovery in supersonic flight and present uniform air flow to the compressor face the inlets themselves become quite long. This results in lengthy nacelles. By mounting four such separated nacelles under the wings, far enough outboard to allow for landing gear retraction, the outboard engine would present structural difficulties due to the length of unsupported engine trailing behind the wing.

Spacing problems led to consideration of other engine arrangements. An over-under arrangement of pairs of engines on each wing, while reducing spacing problems and potentially reducing takeoff noise through shielding of the upper exhaust by the lower, added certain other complications. For example, commonality between nacelles would be reduced because the inlet conditions over and under the wings are substantially different. Also, maintenance accessibility to the upper engine would require special equipment.

Under fuselage or inboard under wing engine positions also alleviate engine spacing problems, but both would require that the engines be aft of the landing gear in order to position the gear correctly with respect to center of gravity. Placing inlets aft of the gear increases the likelihood of ingesting debris resulting in Foreign Object Damage, FOD, to the engine. Also, landing gear retraction would disrupt the airflow into the inlet.

The shortcomings associated with a four engine configuration can be minimized with a three engine configuration. For these reasons, the four engine arrangement was set aside.

4.2.2 Three Engines

The three engine arrangement (two wing mounted, one tail mounted) appears to be ideal in many ways. The weight of the aft engine pushes the CG range aft, decreasing instability. The main landing gear position moves aft with the CG location, increasing the rotation angle for a given fuselage ground clearance. The center engine is mounted so that its exhaust leaves from the aft tip of the fuselage. The exhaust from this engine effectively extends the aft end of the fuselage to produce a "fill in" effect. This fill in effect increases the fuselage fineness ratio, which in turn improves supersonic efficiency, without sacrificing fuselage diameter. Since the exhaust of the center engine takes the place of physical structure, a lighter fuselage is possible. There are some potential disadvantages in mounting an engine beneath the tail. They are:

- boundary layer ingestion
- flow separation over the fuselage at high angles of attack stalling the compressor
- inlet blanketing of the vertical stabilizer at high angles of attack
- easy access to the tail engine

These potential problems are addressed in the Propulsions section of this report.

Another possible three engine configuration was two wing mounted engines with one under the aft end of the fuselage. This layout was discarded due to the limited rotation angle afforded, FOD to the engine, and aerodynamic interference with the landing gear.

5.0 Performance

5.1 Requirements

The performance requirements of the HSCT were specified in part in Reference 4 and in part are set in accordance with FAR Part 25. The following is a brief list of some of the major performance requirements:

1. Takeoff - Balanced Fieldlength = 11,000 feet, (Reference 4)
2. Climb - Climb Gradients (Reference 9)
 - Takeoff and climb phases, OEI
 - a. Transition : 0.3 %
 - b. Takeoff Climb: 1.5 %
 - c. 2nd Segment: 2.7 %
 - d. En route Climb: 1.5 %
 - Landing, OEI: 2.4 %
 - Landing, all engines operating: 3.2 %
3. Cruise - Speed: Mach 2.2 (Reference 4)
 - Altitude: 50-60,000 feet (Reference 4)
 - Range: 5,000 nm with reserves (Reference 4)
 - Payload: 60 passengers with bags, 5 crew (Reference 4)
4. Landing - Balanced Fieldlength: 11,000 feet (Reference 4)
5. Load Factor - +2.5 g, -1.0 g structure limit (Reference 9)

Table 5.1 Performance Requirements

5.2 Aerodynamics and Performance

There are conflicting aerodynamic considerations involved in designing to meet the performance requirements. These play a major role in the layout of the wing and fuselage and in particular the nacelle/airframe integration. The aircraft is designed for efficient supersonic flight which requires a high $L^{0.5}/D$. During takeoff and landing conditions, the low airspeed and associated high induced drag significantly increased the required thrust.

In supersonic cruise, the L/D for the Opus 0-001 is 8.0 (Appendix). This is somewhat less than the maximum supersonic L/D of 8.5. The reason for the difference is that the L/D for maximum range in cruise corresponds to the maximum value of $L^{0.5}/D$, rather than the maximum L/D. Wave drag is a major component of supersonic drag. Wave drag results from variations in pressure due to shock wave formation. For minimum wave drag, the area distribution should be smoothly varying and the maximum area should be as small as possible. These considerations required careful tailoring of the Opus 0-001 fuselage area. This area ruling imposed constraints on the internal seating layout. Area distribution issues also result in thin, highly swept wings, which pose structural and fuel volume limits. The empennage should be small for minimum skin friction drag. The actual and ideal area distributions for the Opus 0-001 are presented in Figure 5.1. The ideal curve is based on a Sears-Haack distribution at Mach 1. A more complex three dimensional approach to area ruling would be required to optimize the aircraft shape for the design cruise of Mach 2.2.

The takeoff and landing L/D's are 5.7 and 5.3, respectively. During takeoff and landing, induced drag and parasite drag are greater because of the deployment of high lift devices and landing gear. High lift devices are necessary to increase $C_{L \text{ takeoff}}$. Lower lift coefficients would require lower W/S or higher takeoff speeds. The first option is ruled out because of altitude restrictions; the second is excluded because higher takeoff speeds require longer runways. The efficiency of the wing is determined by a parameter known as leading edge suction (Reference 10). Leading edge suction (and efficiency) improves with low sweep angles, rounded leading edges, and the deflection of high lift devices. The horizontal and vertical stabilizers should be large to provide the control authority for low speeds, particularly rotation on takeoff to counter the nose down pitching moment caused by the flaps. These guidelines are in conflict with those outlined for supersonic flight and resulted in compromises for almost every aspect of the design. These compromises are discussed in the individual sections of the report (e.g. Design Point, Aircraft Configuration, Wing Design, etc).

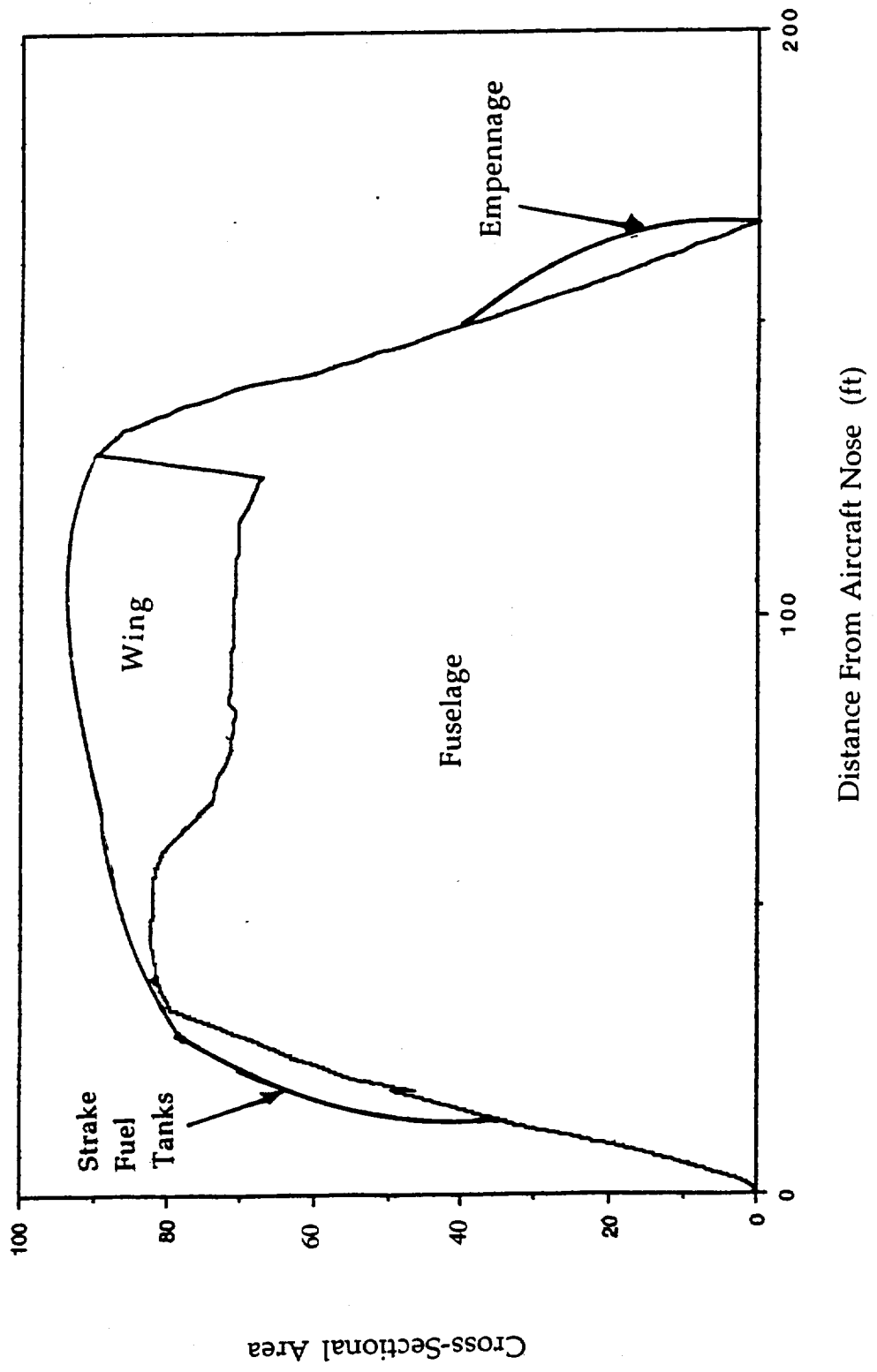


Figure 5.1 Area Ruling

5.3 Performance Verification

Once the wing and engine layout was determined from performance considerations, verification of the performance requirements in a more detailed set of calculations was possible. The T/W necessary and thus the engine size required was determined for various flight regimes and a comprehensive fuel burn calculation was performed to determine the true fuel burn necessary (Appendix).

The engine type was selected by the desire to maintain a low T/W while still meeting the performance requirements for all mission phases. Included in this analysis was the variation of engine performance with altitude and Mach number and the effect of altitude and Mach number on dynamic pressure (and thus C_L required for level flight as well as the actual drag force generated). For some of the engine types examined, T/W was sized by takeoff and landing climb requirements; for others it was sized for cruise due to rapid drop-off in engine performance with increasing altitude. Obviously, it is undesirable to have to carry the extra weight of an engine that is oversized for a particular flight regime simply because of the requirements of another flight regime. In general, the effect of these variations in engine characteristics would be to shift the compromise point on the design point plot. For example, an engine that is underpowered at high altitudes would tend to shift the airplane design to higher wing loading and lower the aspect ratio. By selecting an engine optimized for the high speed regime, the low speed requirements become more difficult to meet.

In the example given, the improvement made by shifting the balance between high speed and low speed design may simply make the aircraft less bad rather than acceptable. The improvements made for cruise would be overshadowed by the large T/S to meet takeoff requirements. Instead, an engine was selected that came closer to matching the desired performance characteristics.

Initial sizing estimates for aircraft weight together with approximate drag polars had resulted in the design wing loading and aspect ratio list above (Reference 11). These results also included values of 0.37 for T/W and 2,000

cubic feet of fuel. More accurate calculations give final values of 0.37 and 2,400 respectively, and the following trimmed drag polars for several flight conditions. The trimmed drag polar can be seen in Figure 5.2. The drag was computed based on a component drag build up, including trim and wave drag.

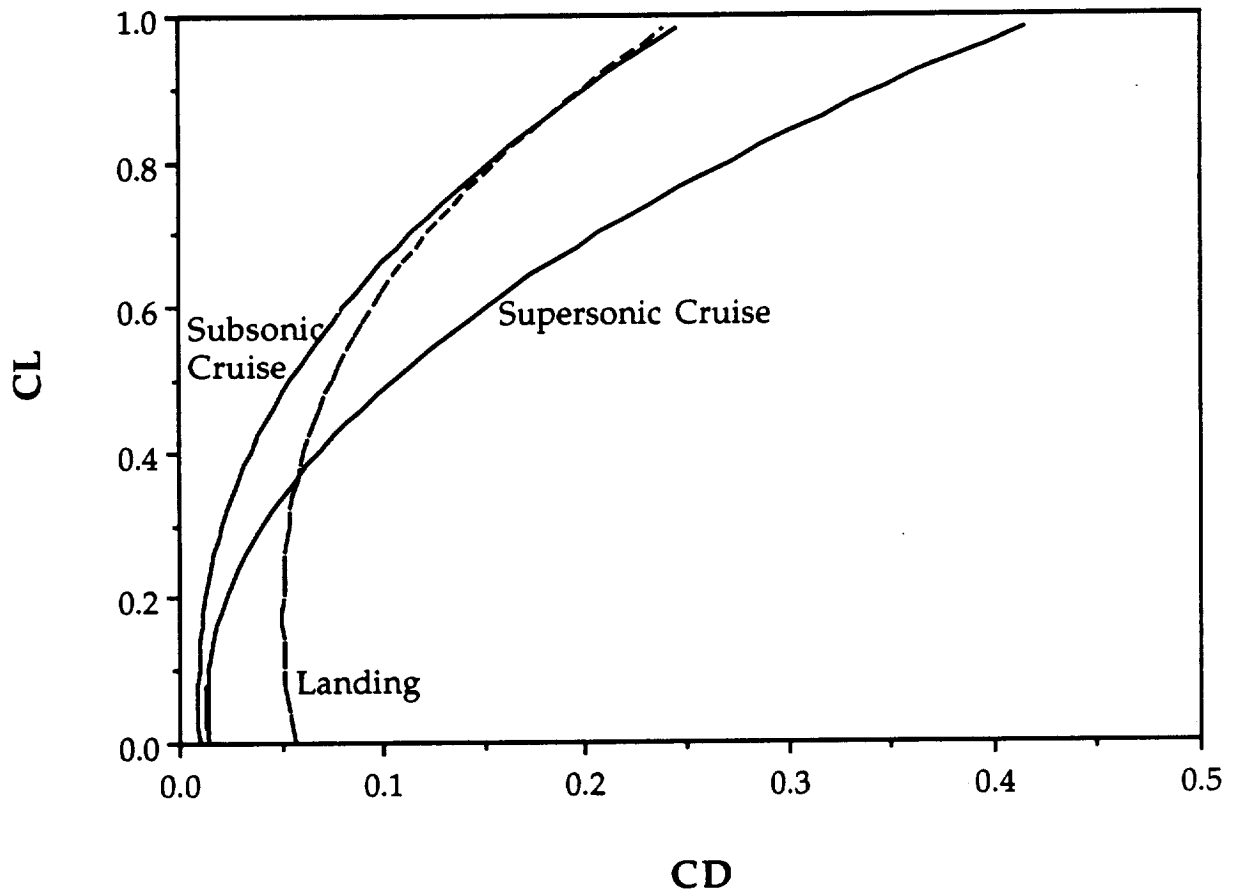


Figure 5.2 Representative Drag Polars

The compliance of the design to the performance requirements given is contained in the following discussion and tables.

	Required	Achieved
	=====	
1. Takeoff Field Length (OEI):	11000 ft.	10700 ft.
2. Climb:		
Transition (OEI):	0.3%	0.3%
Initial Climb (OEI):	1.5 %	14.0%
2nd Segment (OEI):	2.7 %	17.0%
En route Climb (OEI):	1.5 %	13.0%
Landing (OEI):	2.4 %	11.0%
Landing (AEO):	3.2 %	15.0%
3. Cruise		
Mach Number:	2.2	2.2
Altitude (ft):	<60,000	<60,000
Range (plus int'l reserves):	4700 nm	4900 nm
4. Landing Fieldlength:	11,000 ft	9,800 feet
5. Load Factor :	+2.5 g to -1.0 g	Met

Table 5.2 Aircraft Performance

The majority of these climb gradients are requirements for OEI at maximum weight. For AEO flight, the climb gradients are significantly steeper. In fact, were it not for speed restrictions and noise problems, this aircraft could accelerate transonically at about 12,000 feet above sea level while in a 12% climb (Reference 12). To remain below 250 knots while below 10,000 feet altitude, it would be necessary either to throttle the engines down or increase the climb gradient to nearly 25%. This sort of climb would probably not be acceptable from the viewpoint of passenger comfort (both physical and psychological). Maximum rate of climb in the flight envelope is approximately 13,800 feet per minute. Computations of excess power for various configurations indicate sufficient excess power throughout the

required flight envelope. Table 5.3 gives a brief overview of the performance capabilities of the Opus 0-001.

1. Takeoff Field Length :	6800 ft
2. Climb:	
Transition	2.0%
Initial Climb:	16.0%
2nd Segment:	27.0%
En route Climb:	25.0%
3. Cruise	
L/D Supersonic, 55,000 ft.	8.0
L/D Subsonic, 22,000 ft.	14.5
Range Max Payload (nm):	4700
Range Ferry flight (nm):	5700
4. Landing Field Length ($0.8 \cdot W_{to}$):	8970 feet

Table 5.3 Maximum Performance Capabilities

The range versus payload diagrams seen in Figure 5.3, shows that the aircraft is capable of meeting the design range fully loaded. For more typical load factors for first and business classes, the range is approximately 5,200nm. The aircraft possesses a ferrying range of 5,700 nm.

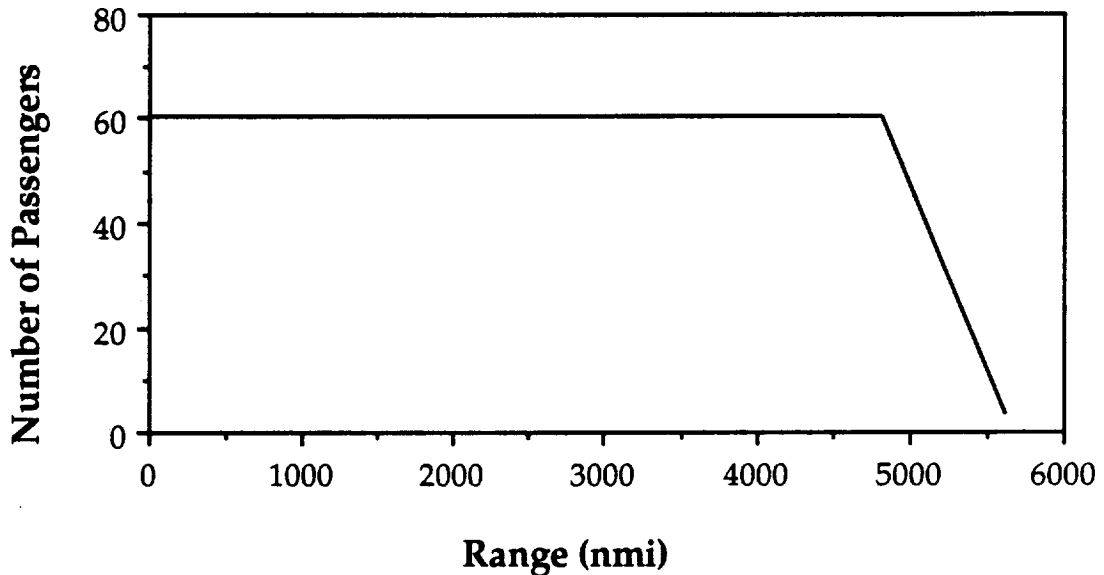


Figure 5.3 Range versus Payload

These ranges were computed by progressively integrating fuel burn through climb, cruise, and the appropriate reserve fuel flight phases in 30 second increments, including variation of L/D and sfc at each time increment (Appendix). These calculations also include the 60,000 foot altitude limit and climb gradients specified previously. In each case, the limitations of maximum gross weight and maximum available fuel volume were used to determine available weight. These ranges are limited by the maximum gross weight of the aircraft, not by available fuel volume. There are two benefits to this limitation. First, with reinforced landing gear and a longer takeoff fieldlength, it may be possible to add more fuel and fly yet further in future models of this aircraft. Second, with the current model retains spare fuel volume for CG management, depending upon passenger load and current fuel load.

The landing distance was found to be 9,970 feet. Landing distance was computed using a wet asphalt surface with braking power provided by the main wheels and the drag of the aircraft.

As shown above, the aircraft is capable of meeting or exceeding all of the performance requirements set out in the Request For Proposal as well as the pertinent Federal Aviation Regulations.

6.0 Stability and Control

The stability of an aircraft is a complex function of its geometry, flight condition, and flight control system. Consequently stability and control was analyzed only for certain representative conditions, namely landing, and subsonic and supersonic cruise (Reference 13). The stability characteristics of the Opus 0-001 aircraft are summarized for these flight conditions in Table 6.1.

Condition	Landing	Subsonic Cruise	Supersonic Cruise
Mach	0.25	0.76	2.20
Altitude	500	25,000	55,000

Longitudinal Stability Derivatives:

C_{L1}	0.9187	0.2648	0.1316
C_{D1}	0.2062	0.0178	0.0164
$C_{m\delta}$	-0.0969	-0.0006	0.0017
$C_{L\alpha}$	3.2467	3.5650	2.1471
C_{Lu}	0.0142	0.0434	-0.8593
$C_{d\alpha}$	1.5777	0.3074	0.1527
C_{du}	-0.00049	0.0013	0.0051
C_{mu}	0.0238	0.0063	0.0034
$C_{m\alpha}$	0.1036	0.2206	0.0234
C_{mq}	-69.16	-83.49	-41.43

Lateral-Directional Stability Derivatives

$C_{y\beta}$	-0.2912	-0.3056	-0.2494
$C_{n\beta}$	0.1441	0.1547	0.1184
$C_{l\beta}$	-0.1035	-0.0597	-0.0477

Control Derivatives

$CL_{\delta e}$	0.1801	0.2821	0.1368
CM_{i_h}	-0.5339	-0.6455	-0.3130
$CM_{\delta e}$	-0.2470	-0.3863	-0.1918
$CD_{\delta e}$	0.01817	0.00664	0.000624
$CY_{\delta r}$	-0.1301	-0.1301	-0.1301
$CN_{\delta r}$	0.1020	0.1016	0.1085

Table 6.1 Stability Derivatives

Approximately 3% static instability in the longitudinal mode was selected for subsonic flight to give near neutral stability in supersonic cruise due to the shift in the aircraft aerodynamic center with Mach number. This desire for neutral stability sized the horizontal stabilizer. Since the stabilizer was designed to be unloaded in cruise trim drag was reduced cruise, which boosted range. A smaller tail, with less weight and wetted area, could improve range even more but only at the expense of longitudinal control power. Since the aerodynamic center of the wing shifts aft approximately 1% of the Mean Aerodynamic Chord transonically, the level of instability is a function of CG position. As seen in the CG excursion diagram, Figure 6.1, the CG is essentially the same at takeoff and landing (positions 10 and 19) and thus, by pumping fuel between tanks, the CG position may be held constant. The variations of the CG excursions are deceptively large, since they represent adding or removing fuel from individual tanks. In practice, the CG can be constrained between the forward and aft CG locations indicated on the CG excursion. For ferry flight or other low passenger loads, the tendency for the CG to shift aft can be overcome by adding ballast in the aircraft nose. Thus, this aircraft possesses the nearly same level of static stability throughout its flight regime which simplifies the design of the stability augmentation portion of the flight control system. Stability augmentation will be required for this marginally unstable aircraft to provide adequate handling qualities. Such a system is not unprecedented in commercial transports as evidenced by the Airbus aircraft (Reference 14). Fly-by-wire controls will be used to allow for electronic variation of control laws for various flight phases. For safety and reliability reasons, the system is multiply redundant.

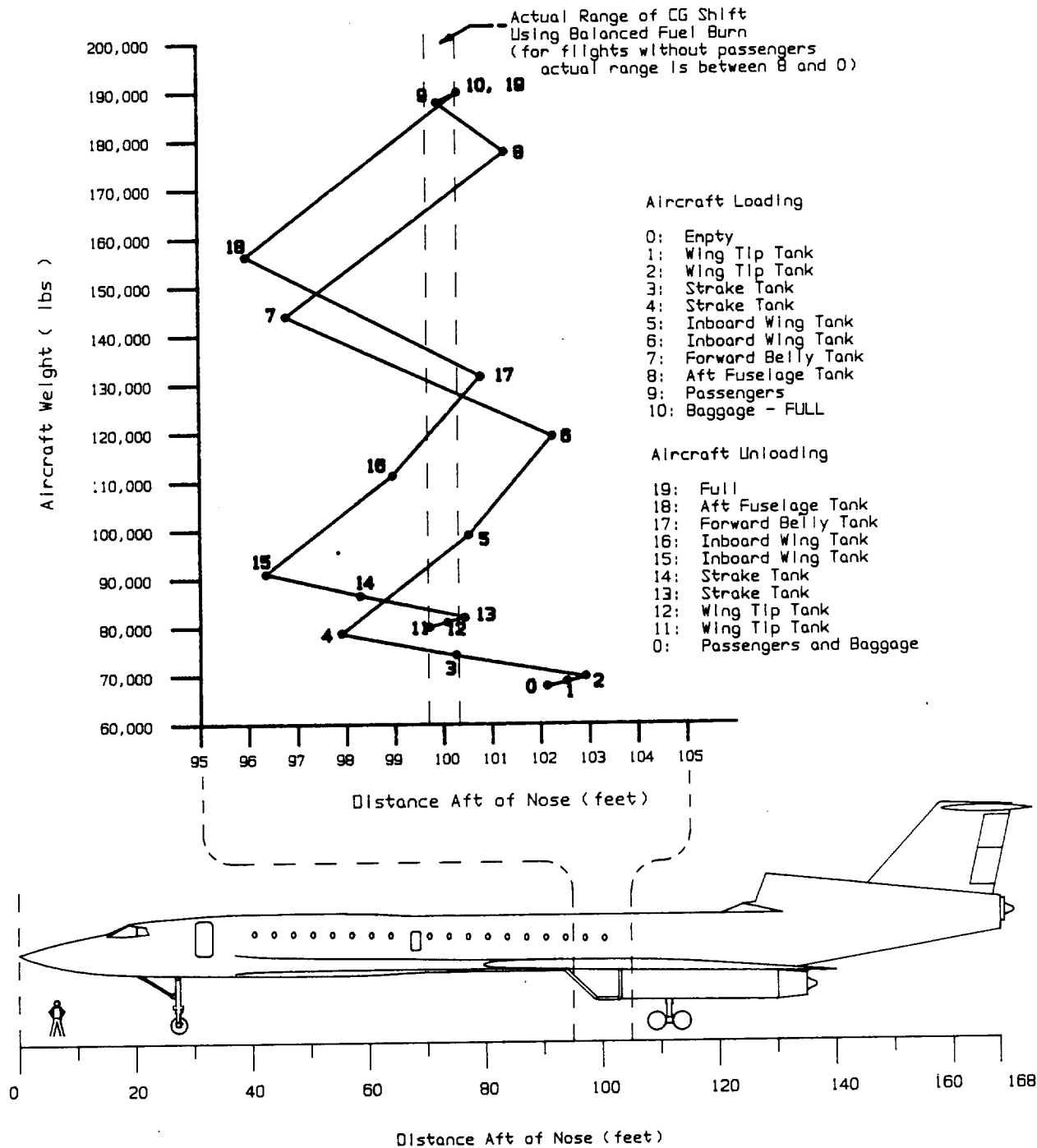
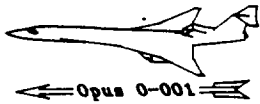


Figure 6.1: Center of Gravity Position Excursion With and Without Fuel Balancing

The elevator is sized to rotate the aircraft on takeoff. The incidence angle of the entire horizontal tail surface can be adjusted to reduce the elevator deflections necessary for a given flight condition, and reduce the associated control deflection drag. A stabilizer incidence angle of -10 degrees is required for takeoff and landing, due to the large nose down pitching moment contribution of the flaps. Since the horizontal stabilizer is at a much lower angle of attack than the wing, the horizontal surface will not stall until well after the maximum angle of attack permitted by the ground strike criterion. In cruise configuration, the small camber of the wing and fuselage results in near zero pitching moments, so that the elevator does not need to be deflected at all for trimmed flight in supersonic cruise. This reduces the drag and was a determining factor in the selection of the 0 degree tail incidence angle for that regime (Appendix).

The lateral control power is limited by the available dynamic pressure. Therefore the rudder deflection required to maintain sideslip of less than 5 degrees for a failure of an outboard engine is a function of Mach number. The critical case is the landing configuration, which requires 17 degrees rudder deflection to counter the yawing moment due to unbalanced engine thrust (Appendix).

The droop of the flaperon in takeoff and landing configurations necessitates asymmetric aileron deflection. That is, there is not much room left for aileron deflection downward, so more deflection occurs on the up going aileron. The outboard panel of the aileron is used at high speed, where dynamic pressures could cause aeroelastic control reversal if the entire aileron surface were deflected. These outboard ailerons provide adequate control power for supersonic flight because of the high dynamic pressure, low rolling moment of inertia, and the lack of a requirement for high maneuverability supersonically for this type of aircraft. The spoilers may be used subsonically to provide proverse yaw in subsonic cruise, but cannot be used on approach or takeoff, due to the reduction in lift coefficient and L/D which size the engines. Once on the ground, the spoilers are deployed to destroy the lift of the wing and flaps, adding weight to the wheels. This weight improves brake power to reduce landing roll.

7.0 Wing Design

The wing planform shown in Figure 7.1 was selected largely on the basis of comparison with experimental work done in other HSCT design programs and with previous supersonic cruise designs. For Mach 2.2, the Mach cone angle is 61 degrees. It is desirable to have at least a part of the wing swept inside the Mach cone for minimum cruise drag. The geometry of the wing is summarized in the table below:

Parameter	Inboard	Outboard
Area (ft ²)	1775	500
Leading edge Sweep (deg):	70	55
Trailing edge Sweep (deg):	5	21
Root Chord (feet):	73.4	23.2
Tip Chord (feet):	23.2	4.3
Thickness/Chord:	3 %	3 %
Airfoil Section:	NACA 63-103	Supersonic Biconvex

Table 7.1 Wing Geometry Summary

The wing area and aspect ratio were determined to meet performance criteria from the design point diagram, Figure 3.1. Once these basic parameters were selected, the planform shape of the wing had to be designed. The basic planform is a highly swept inboard portion, with substantial taper and an outboard portion that is at a sweep angle such that its leading edge is supersonic in cruise. This results in a higher aspect ratio than is possible on a straight leading edge wing design. The span break location was chosen to be as far outboard as possible to minimize the drag of the supersonic outboard part, while still maintaining enough tip chord to insure structural strength against flutter and room for fuel and control surfaces. As described previously, weight growth occurred midway through the design due to the addition of more fuel. Since the weight increase was roughly 6%, a decision occurred to leave the wing size the same and simply let the W/S increase slightly to its current value of 84. The aerodynamic center (ac) shift for this wing planform is approximately 1% MAC. This value is remarkably small, and demonstrates one of

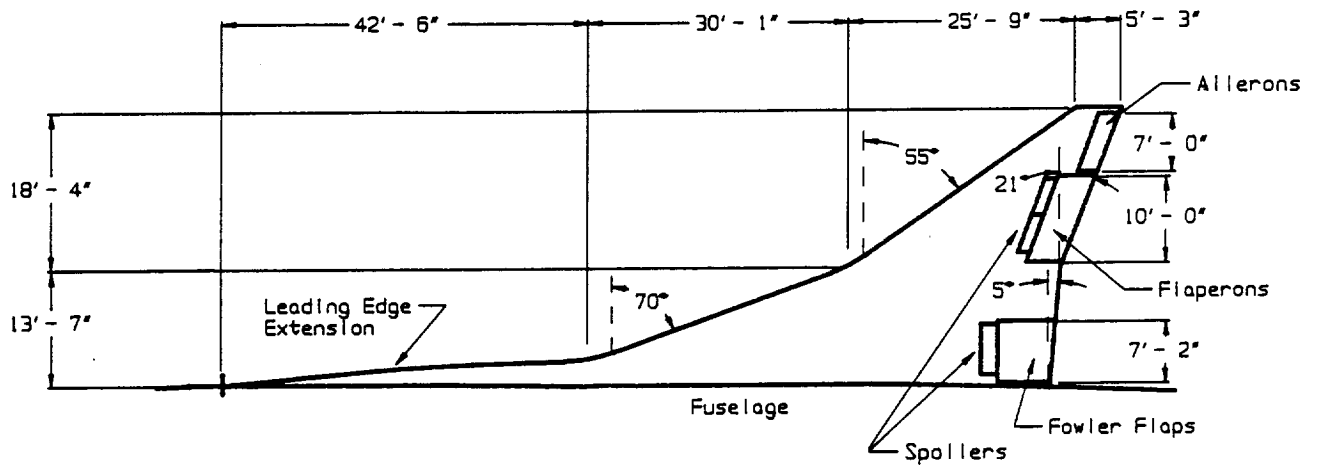
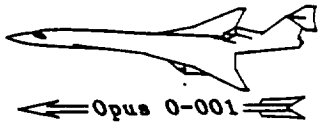
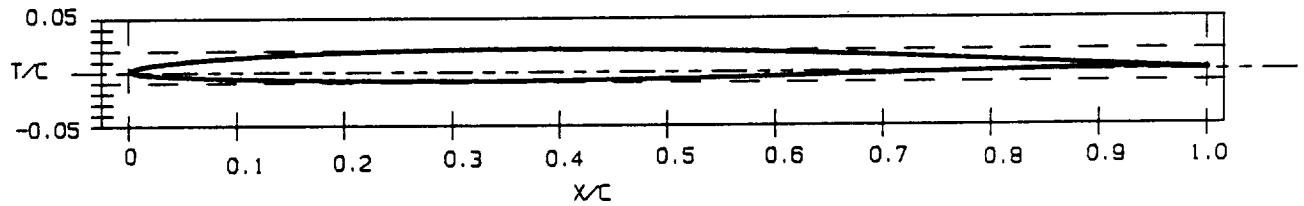
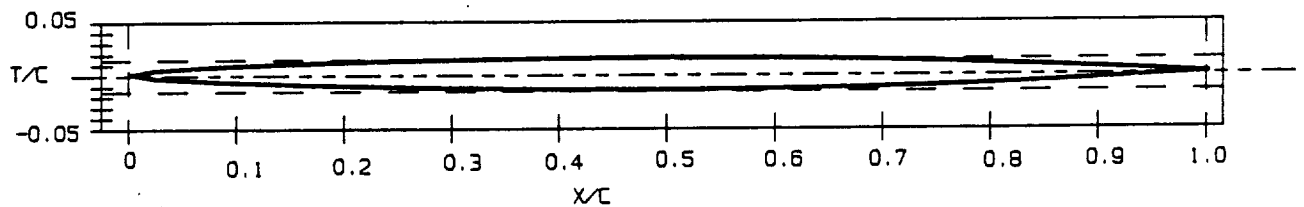


Figure 7.1: Wing Planform, Controls, and High Lift Devices



Inboard Airfoil: NACA 63-103



Outboard Airfoil: Bi-convex, 3% Thick, Symetric Airfoil With Supersonic Leading Edge

Figure 7.2: Inboard and Outboard Airfoils

the advantages of a cranked wing planform: this small ac shift means that the stability of the aircraft does not shift dramatically transonically. The airfoil sections can be seen in Figure 7.2.

Note that the wing seems to appear small in with respect to the fuselage, compared to other HSCT concepts. In reality, such a comparison is deceptive. Wing area is a function of the aircraft weight and wing loading. The wing's linear dimensions (span, chord) are proportional to the square root of the weight, while fuselage dimensions are roughly proportional the cube root of the weight. Therefore, the relative proportions are not going to be the same for the Opus aircraft as it is for larger HSCT proposals. Also, a portion of the reference wing area is buried in the fuselage. All aerodynamic calculations were based on the exposed and reference wing areas as appropriate (Appendix).

The airfoil selection is highly preliminary, since aeroelastic and wave drag computations are generally used to tailor airfoils for high speed applications. The primary factor in selecting the airfoil sections for this aircraft is thickness; wave drag considerations weigh heavily against thick airfoils, though such airfoils have better low speed performance (particularly in stall angle). Tentatively, the inboard wing section will be a NACA 63-103 cambered subsonic airfoil. The pitching moment and zero lift angle of attack were based on linear extrapolations of data for slightly thicker airfoils. This source data was fairly linear in the region of interest, but lacked data for such thin airfoil sections (Reference 15). Also, the pitching moment and zero lift angle for an airfoil are largely a function of camber, so the preliminary assumptions used should be reasonable in the absence of aerodynamic modelling. The normal component of the leading edge is subsonic throughout the flight envelope. Slight camber was provided to result in lift at near zero degrees angle of attack to reduce required wing incidence and cabin floor slope angles in cruise, as well as to unload the outer wing, which has a higher lift curve slope due to lower sweep. The wing is also mounted at 1.5 degrees incidence to the fuselage. The outboard airfoil, essentially an uncambered biconvex supersonic section, was selected because the leading edge will be outside the Mach cone. The characteristics of this airfoil were presumed to resemble the NACA 0003 symmetric airfoil, with a supersonic leading edge. Three degrees of washout are used to augment the inboard camber in unloading the outboard portion of the wing.

Due to the highly swept wing and low aspect ratio, the lift curve slope for this aircraft is fairly low. Consequently, high lift devices were required. The inboard section of the wing included Fowler flaps, which extend -- effectively increasing the lift curve slope -- and deflect to provide a lift increment. The outboard wing panels utilize flaperons. The flaps were sized to provide a CL range of 0.6 to 1.0 at angles of attack around 10 to 15 degrees.

	Takeoff	Landing
Inboard Deflection (deg):	20	10
Outboard Deflection (deg):	30	20
Inboard Extension (feet)	3	4
CL increment:	0.171	0.263

Table 7.2. Flap Deflection and CL Increments for Take-off and Landing

Since the wing is thin, it cannot contain the amount of fuel necessary for the Opus 0-001 to meet its design range. This led to the addition of extensions of the root of the leading edge along the fuselage as a fuel strake and the inclusion of fuel tanks in the blending of the wing/fuselage intersection. This blending serves to reduce interference drag between the two surfaces as well.

8.0 Fuselage Design

The important components of fuselage design discussed below are the cabin layout, the flight deck, the baggage compartment, and the fuel stored in the fuselage and the leading edge extensions.

8.1 Cabin Arrangement

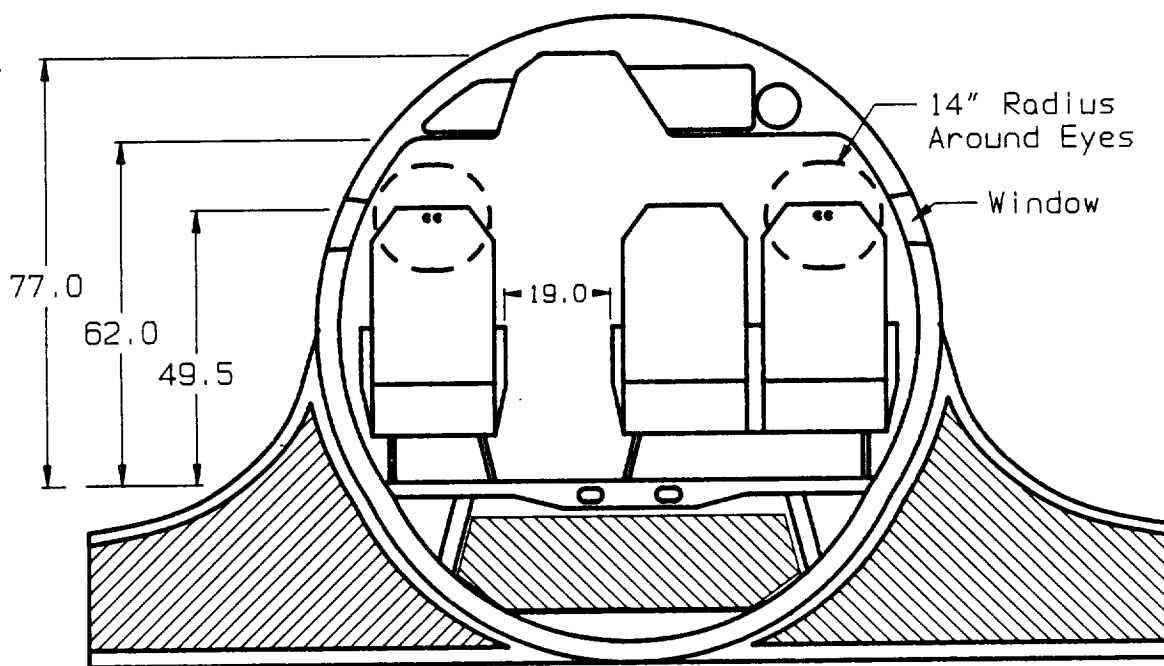
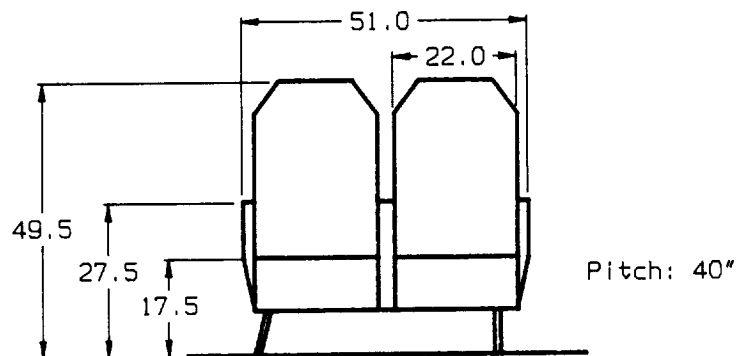
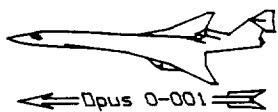
The cabin arrangement of the Opus 0-001 was designed to be competitive with the current subsonic aircraft interior for similar flight lengths. The primary drivers for the interior arrangement were to maximize customer comfort and operator efficiency without sacrificing aerodynamics by increased cabin diameter.

Aerodynamic considerations would dictate as slender a fuselage as possible.

A final concern with the interior layout was that it could be manipulated to suit airline requirements. There was a limit to how much flexibility could be incorporated into the design due to area ruling for minimum supersonic drag. One proposed layout, presented in Figure 8.1, shows a sixty passenger cabin with a 50/50 split between business and first class.

The first class compartment is arranged for three across seating as shown in Figure 8.2. The first class seats are 22 inches wide with a pitch of 40 inches. The business class is seated four across as shown in Figure 8.3. The business class seats are 18.5 inches wide with a pitch of 38 inches. These cross sections show the changes in diameter for area ruling. Note that the hull utilizes a double-bubble to maximize the height of the cabin and under floor volume while minimizing cross sectional area.

The most unusual feature of this layout is that the first class seating is located aft of the business class. This cabin configuration was the compromise of area ruling and seat dimensions in an attempt to maintain good aerodynamics and maximize cabin class volume. With this configuration, first class passengers will not be disrupted by other class passengers moving through their section. The interior noise in first class due to the aft engine was a concern, but it should not be excessive since a large fuel cell and the baggage hold separate the cabin from the engine location.



 - Fuel Tanks

Figure 8.2: Opus 0-001 First Class Cross Section

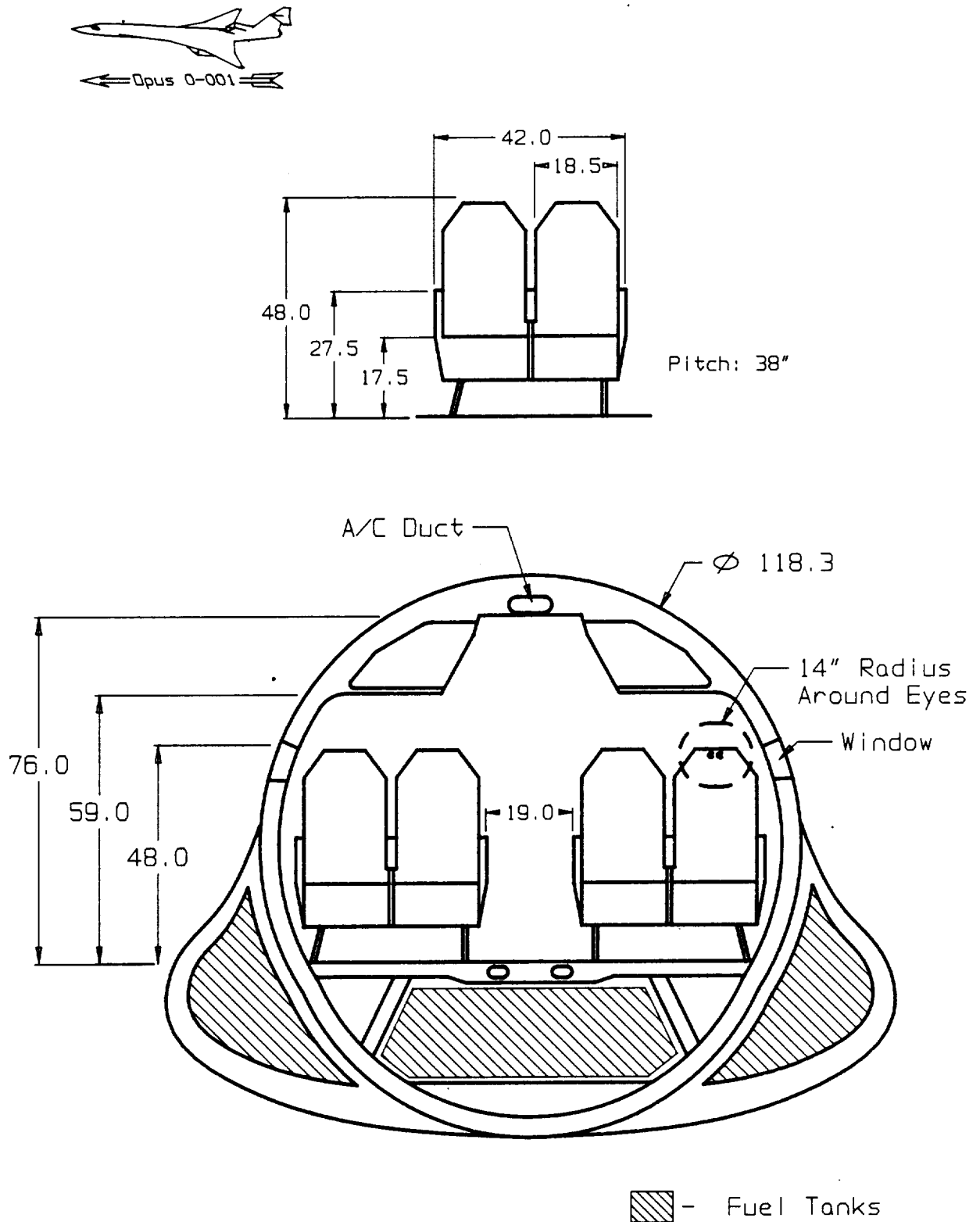


Figure 8.3: Opus 0-001 Business Class Cross Section

FOLDOUT FRAME

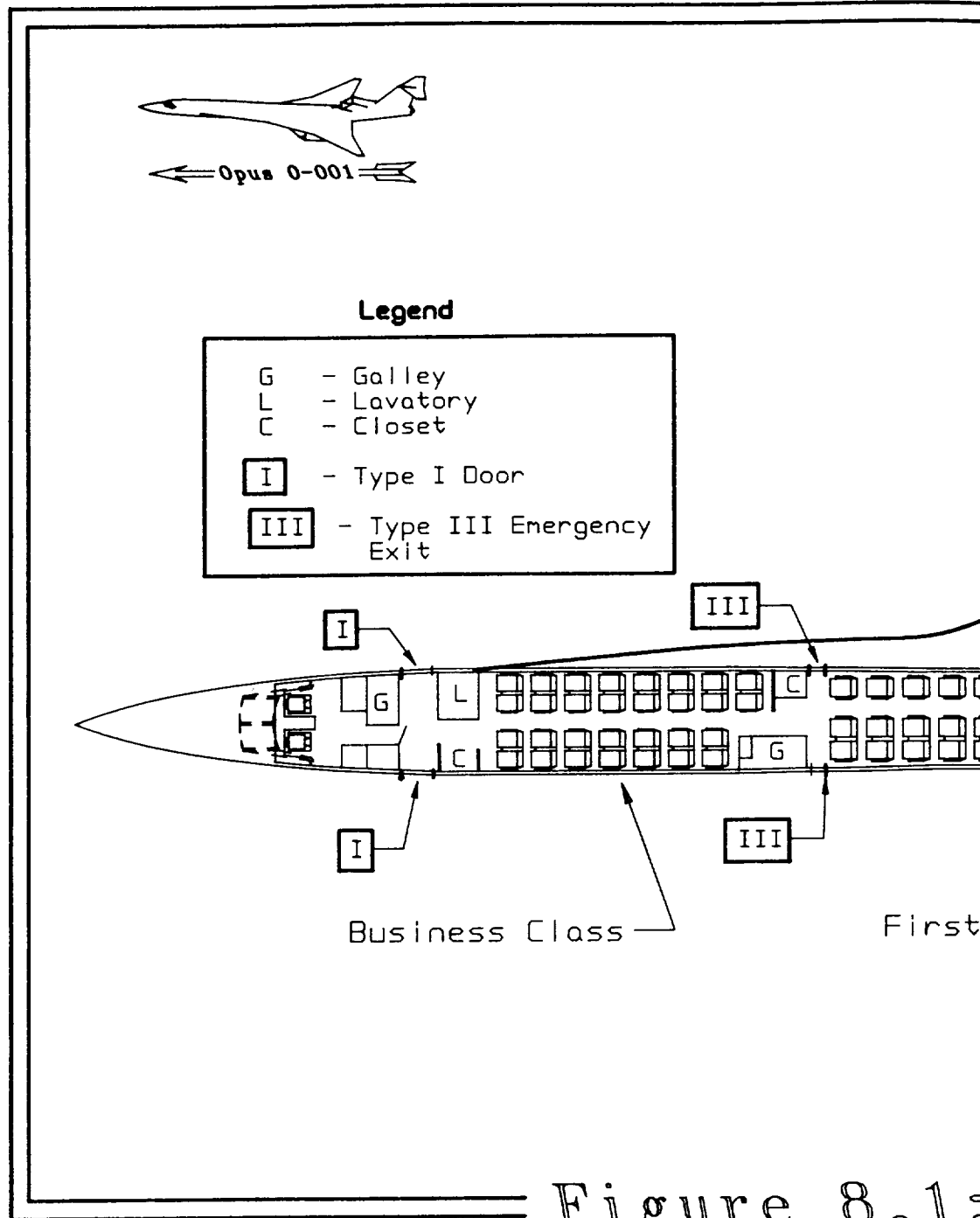
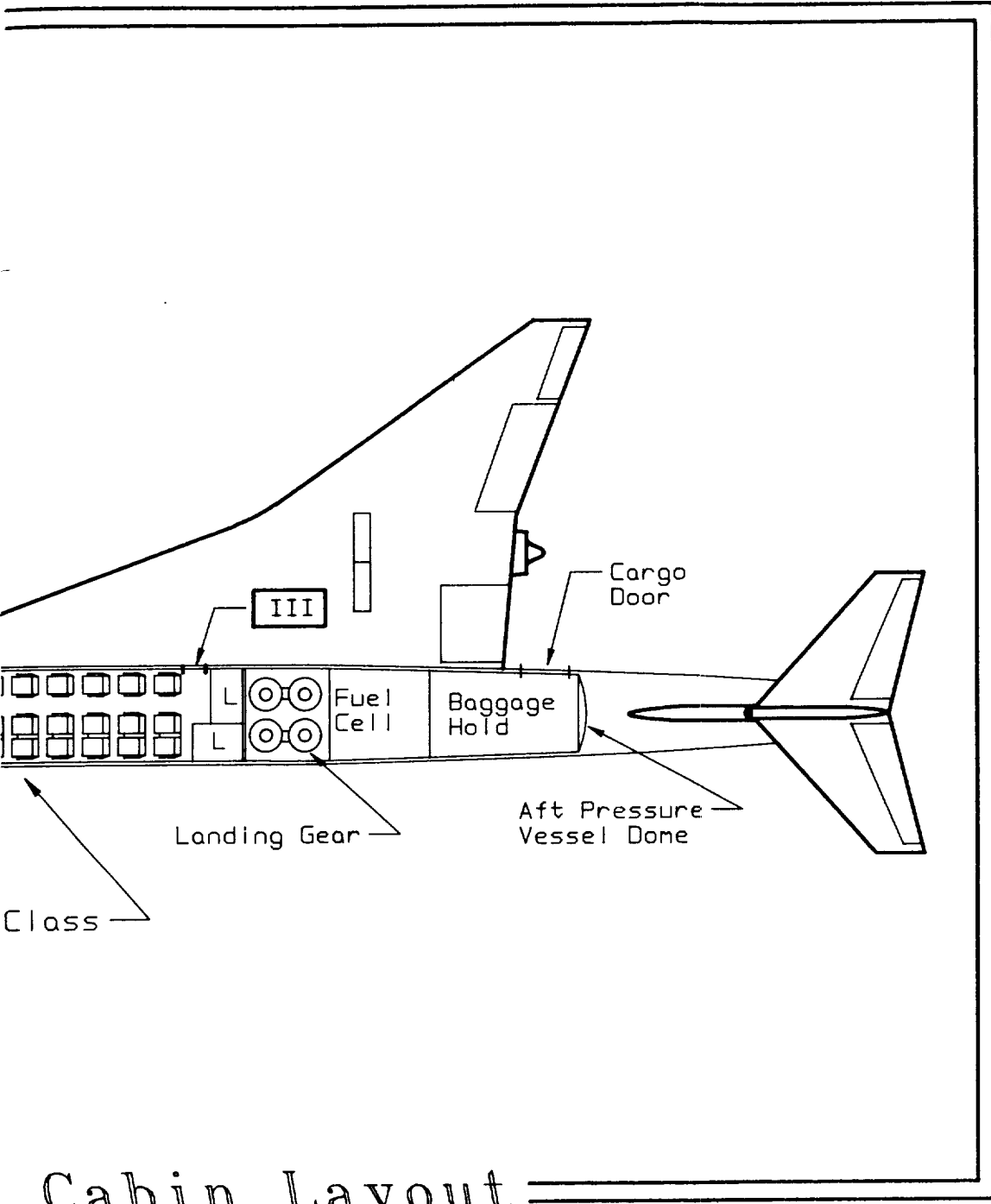


Figure 8.1:



Cabin Layout

The passengers this aircraft will carry demand a high level of customer comfort. For this reason all amenities available on a subsonic transport will be made available to the Opus 0-001 customer. These include closets, lavatories, and a galley for each class. Each seat will have a personal entertainment system including a small LCD video screen located in the back of each seat. The closets are located at the front of each class section. There are two first class closets, one measuring 35 x 24 inches, the other is 20 x 24 inches. The business closet measures 45 X 24 inches. There are a total of three lavatories, one in the front of the business section, and two aft of the first class section. A galley is positioned at the front of each section to provide quick service to all passengers. The galley is to be equipped to serve one in flight meal and provide drinks throughout the flight. The galleys and lavatories were positioned to avoid having to make major changes to the water and waste systems should an airline wish to reconfigure the interior. The passengers will be serviced by three flight attendants, two for first class and one for business. Flight attendants will use fold down seats on both Type I doors, and on the Type III door aft of the first class section.

8.2 Safety Considerations

The cabin was designed to comply with all Federal Aviation Administration, FAA, safety requirements. There are a total of four exits to be used in case of an emergency, in compliance with, FAR 25.807. Two Type I emergency doors are located in front of the business section on either side of the aircraft and are used for loading passengers, and galley servicing. Two Type III doors are located before the first class section on either side. The access to these doors is between the first row of seats and the closet and galley. Recent changes to the FAA requirements may require this route be widened or the seats removed. Currently there is a 38 inch wide clearance. An additional Type III emergency door is located on the right side behind the first class section forward of the lavatory. This door is not required by the FARs but will decrease the emergency deboarding time of the aircraft and thus make it safer. The exit doors are thirteen feet above the ground so inflatable evacuation slides are incorporated under all emergency exits, with the exception of the most aft door which opens over the wing. The Type III doors will have to open through an area where some wing blending occurs. The blending can be cantilevered off the door such that little interference will exist when it opens. The fuel cells in the blended area will stop two feet to either side of the doors where life

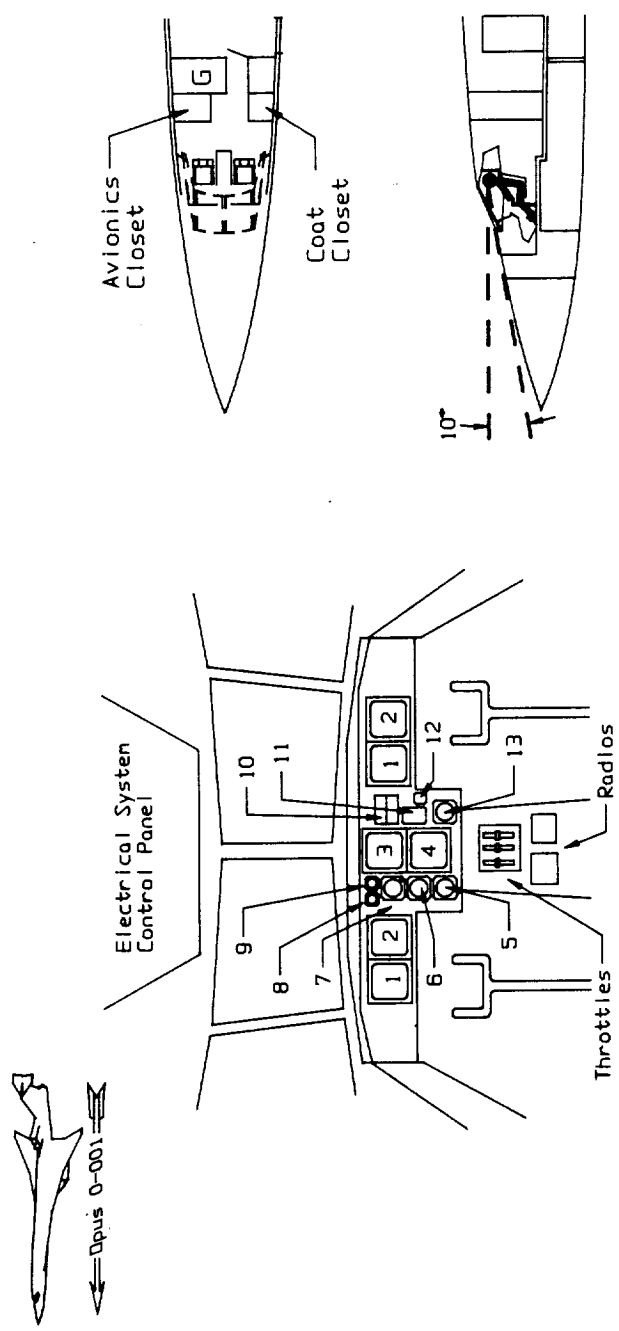
rafts will be stored. Life rafts are stored in the forward closets for the Type I doors. These safety considerations meet all FAA requirements and should be able to provide reasonable evacuation times and passenger safety.

8.3 Flight Deck

The Opus 0-001 is following the current trend of having a two member flight crew (Reference 16). A full CRT display cockpit will be available at the airlines request to minimize pilot workload. Figure 8.4 shows the flight deck and the CRT instrument panel, which is very similar to the Airbus A320's. The avionics computers will be stored under the floor in front of the landing gear bay. Due to the volume that the nose gear occupies extra room for the computers was made available inside the cockpit. The type of guidance avionics will be dictated by FAR minimum required equipment, and the airlines preference.

Extra seating for airline and FAA observers is available in the cockpit. One seat is located beside the pilot closet, and the other beside the avionics bank. The seats will fold up to save room.

Centerline visibility from the cockpit is limited to a downward angle of 10° from the horizontal. This is less than ideal but should be sufficient for safe operation. When looking a few degrees to the side of centerline the downward vision angle increases to 15° (Reference 16). Due to the slenderness of the fuselage more than enough visibility is available on either side of the cockpit. A drooping nose was not used to improve the vision angles because the weight penalty was too severe. As synthetic vision systems are developed they will be incorporated into the available avionics.



Instrument Panel Cockpit Layout

Key

- 1 Horizontal Situation Indicator and other Flight Information
- 2 Radar and Flight Information
- 3 Engine Reading and Warnings
- 4 Engine and System Readings
- 5 Automatic Direction Finder
- 6 Distance Measuring Equipment/VOR
- 7 Standby Attitude Indicator
- 8 Standby Airspeed Indicator
- 9 Standby Altimeter
- 10 Landing Gear Indicator and Auto Brake/Anti-Skid Control
- 11 Landing Gear Control
- 12 Brake Pressure
- 13 Clock

Figure 8.4: Opus 0-001's Advanced Flight Deck

8.4 Baggage Compartment

The combination of a minimum cabin aisle height of 76 inches and a slender fuselage for aerodynamic considerations made storing baggage under the floor impractical. It was possible to increase the size of the double bubble fuselage cross section enough to store the baggage under the passengers, but the increased area would have made the area distribution far from ideal, especially if the leading edge extension fuel tank (discussed under Fuel Cells) were included. The center of gravity also had a much greater excursion between flying with and without passengers and baggage causing difficulty in manipulating the stability margin for minimum trim drag. The baggage was therefore placed aft of the passenger cabin in a full fuselage diameter baggage hold giving a storage volume of 710 cubic feet. The compartment is accessed through a 60 x 60 inch cargo door located on the right side of the fuselage just behind the wing. It is expected that due to the small number of passengers the baggage can be hand loaded, but where required, containers can be used. However, this will decrease the amount of baggage that can be carried.

8.5 Fuel Tanks

Typically small aircraft have shorter ranges than large aircraft because of the limited amount of fuel they can store in the wings. For this reason it was necessary to store much of the fuel inside the fuselage and in leading edge extension fuel tanks. There are three major fuel tanks inside the fuselage. One under the business section, one under the first class section, and one aft of the cabin.

The fuel tank aft of the cabin separates the cabin and the baggage hold. This aft fuel cell holds 750 cubic feet of fuel, it is the largest single tank on the aircraft. The tank is housed inside the pressure vessel to avoid needing a second pressure vessel for the baggage compartment.

The walls on either side of the fuel cell are designed to withstand any forces that would be exerted by the fuel, or pressure differences should the cabin and baggage compartment depressurize.

The under the floor fuel cells are shown in the cross sections. These tanks will hold 500 cubic feet of fuel. Note that a "crumple zone" has been left for safety. The crumple zone is 14 inches deep under the business section and 10 inches deep under the first class section. The wing structure and engines will decrease the amount of damage under the first class section in the event of a gear-up landing. These tanks are also to be lined for safety considerations. The idea of putting fuel under the floor is not new. It has been used safely and effectively on the Concorde as well as on many extended range subsonic aircraft (Reference 1).

The final fuel cells discussed here are the fuel tanks located in the leading edge extensions. They can be seen in the fuel tank layout diagram: Figure 8.4. The leading edge extension was added to increase the fuel capacity of the aircraft so they are not shaped for lift production. The extensions were positioned to smooth the area distribution. These tanks are outside the pressure vessel and should pose little safety risk. Approximately 85 cubic feet of fuel can be stored in each of these tanks.

Overall the fuselage and leading edge extensions hold more than 60% of the total fuel capacity and are thus necessary to meet the range requirements.

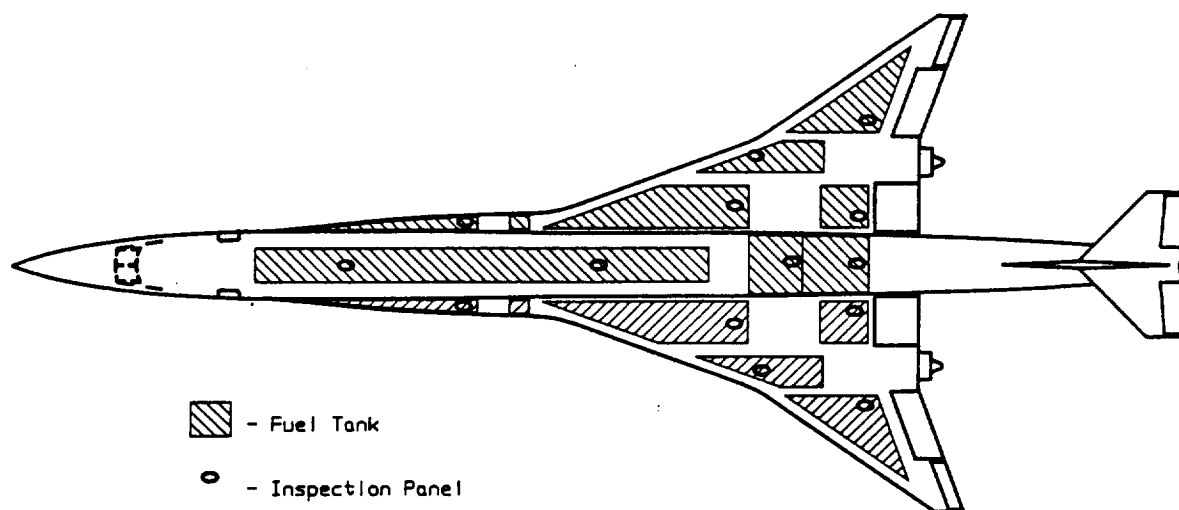


Figure 8.5 Fuel Tank Layout

9.0 Empennage design

The empennage of the Opus aircraft consist of conventional vertical and horizontal stabilizers in a T-tail configuration. These surfaces were sized for stability and control power. The basic geometry of the horizontal and vertical stabilizers are summarized in the Table 9.1, and depicted in Figure 9.1. The thicknesses were designed to provide structural strength while maintaining low wave drag. The sweep angles and aspect ratios were selected based on a combination of considerations: minimum drag, structural strength, the effect of geometry on lift curve slope, and control effectiveness.

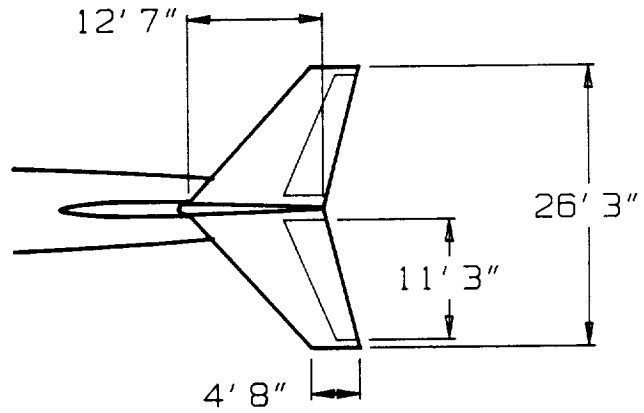
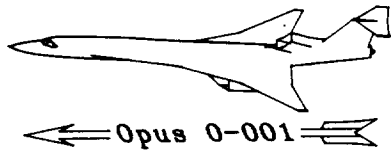
Horizontal Stabilizer

Area:	220 ft ²
Aspect Ratio:	3.5
Span:	26.25 feet
Thickness:	5%
Volume Coefficient:	0.138

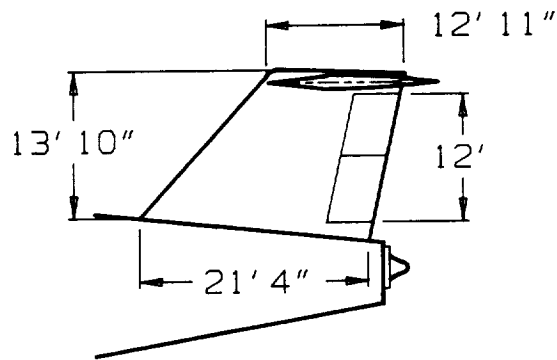
Vertical Stabilizer

Area:	220 ft ²
Aspect Ratio:	1.0
Span:	13.8 feet
Thickness:	6%
Volume Coefficient:	0.117

Table 9.1 Empennage Geometry



Top



Side

Figure 9.1: Empennage Close Up

The original design concept of the Opus 0-001 called for a canard aircraft with winglets instead of a vertical tail for directional control. Further evaluation proved that the winglets were aerodynamically inadequate to provide the control forces necessary to counter OEI yawing moments. In place of the winglets, a canting the canard was considered as a means to produce yaw as well as pitch control (a V-canard design). An advantage of this type of configuration is the possibility of small stabilizer surfaces due to their long moment arm. Unfortunately, this configuration would be both directionally and longitudinally unstable and require stability augmentation for yaw and pitch control. Since the aircraft CG was behind the a.c., the canard would be down loaded in flight, negating the trim drag advantages of incorporating instability into a design. Also, the interaction of the canard trailing vortex on the wing and engine inlets was a point of uncertainty. These two factors led to the switch to conventional horizontal and vertical stabilizers. A T-tail arrangement was chosen to reduce aerodynamic, mechanical and structural interference with the number tail-mounted engine and provide direct access to the engine and the control surface. Other advantages of the T-tail are an increased horizontal stabilizer effectiveness (due to a position out wing wash) and vertical stabilizer effectiveness (due to the capping effect of the horizontal). Further, the T-tail configuration keeps the horizontal surface out of the thermal and acoustic loads produced by the wing-mounted engines.

The sizes of the empennage components were estimated initially using volume coefficients of similar aircraft and then refining them by longitudinal and directional X-plots. The plots are shown in Figure 9.2 and Figure 9.3, respectively. The final values of horizontal and vertical stabilizer areas are 220 and 220 square feet respectively. The longitudinal X-plot shows the aircraft to be slightly unstable subsonically and nearly neutrally stable supersonically, resulting in low trim drag. The size of the horizontal stabilizer also determines the control effectiveness of the elevator; therefore, the size was verified for takeoff rotation. The directional X-plot shows that the aircraft is very nearly neutrally stable in yaw even without a vertical stabilizer because of the presence of the fuselage mounted nacelle. In this case, the requirement for one engine inoperative restoring moment and the need for a reasonably large surface for rudder control power resulted in the selected vertical stabilizer area. Also, the height was sized to keep the horizontal stabilizer well clear of blanketing by the wing at high angles of attack.

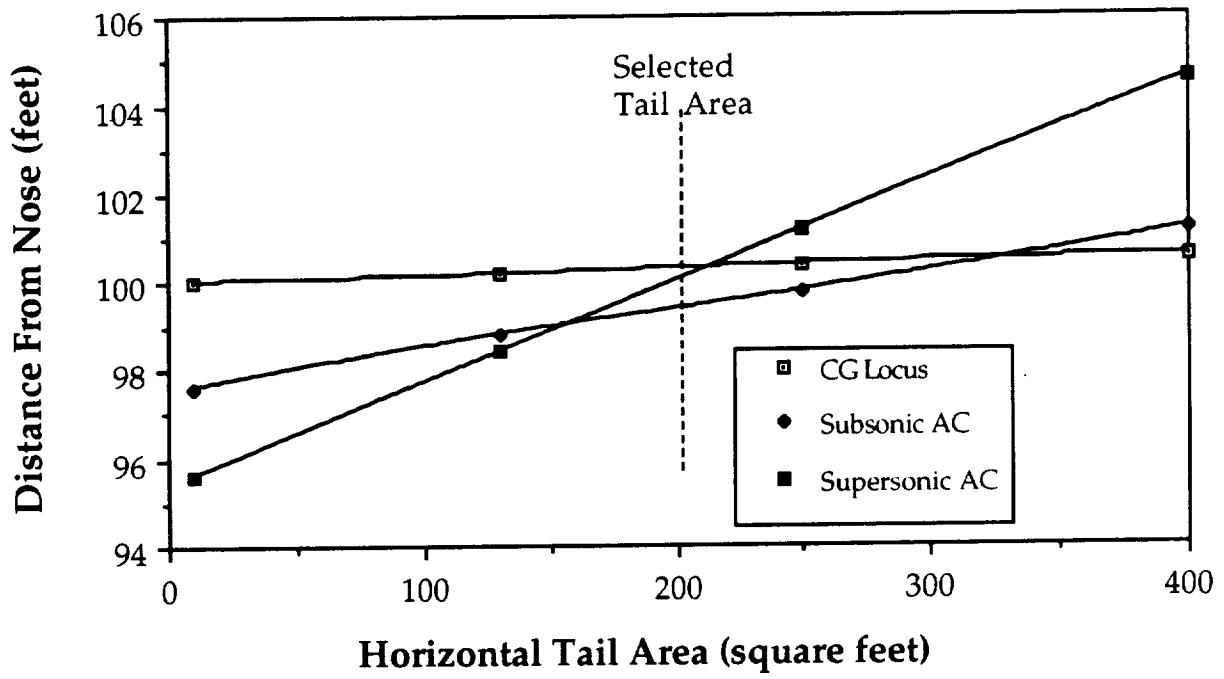


Figure 9.2 Longitudinal X-Plot

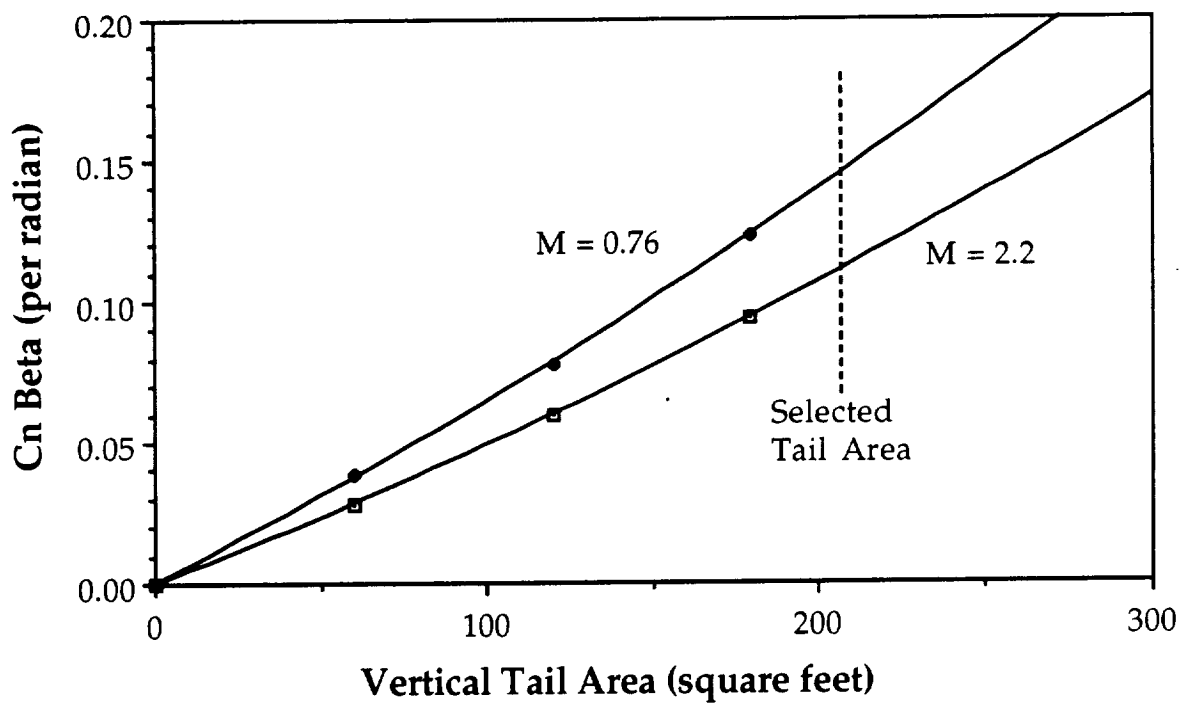


Figure 9.3 Directional X-Plot

10.0 Landing Gear

The critical factors for the landing gear are their position and their design. Their design includes their ability to retract using as little volume as possible. The conventional tricycle arrangement is used.

10.1 Landing Gear Position

The possible landing gear positions were limited for the Opus 0-001 because the volume under the floor is too small to store the landing gear under the passenger cabin area. For this reason, the main gear are located aft of the passenger cabin below the fuel cell area where the floor level could be raised. The nose gear is located far forward so the wheels can be retracted forward under the cockpit where the floor can also be raised a small amount. The step up for the main gear occurs at a large bulkhead and wing spar to avoid additional structural weight. The bulkhead and spar were already required as hard points for the main landing gear strut and wing box.

The position of the main gear with respect to the CG is shown in Figure 10.1. This figure shows that the main gear are 18° behind the most aft CG location to avoid instability during ground operations. At this position the nose gear carries 8% of the total load. The tip over angle was calculated to be 48° , well under the 55° limit (Reference 17). The maximum rotation angle before tail strike is 14.8° with deflated tires, this is sufficient for takeoff and landing rotation. A preliminary concern was the small angles, with respect to centerline, between the wing mounted engine inlets and the nose gear. This condition may cause a problem with FOD of an engine. This however is misleading since the damage statistically appears to be more of a function of the engine's susceptibility to FOD rather than these angles (Reference 17). Since the engine has a relatively small diameter and a long inlet, susceptibility to FOD should be low. Also, the length between the nose gear and engine inlets is relatively long compared to typical subsonic transports so debris should settle below the inlet before reaching it.

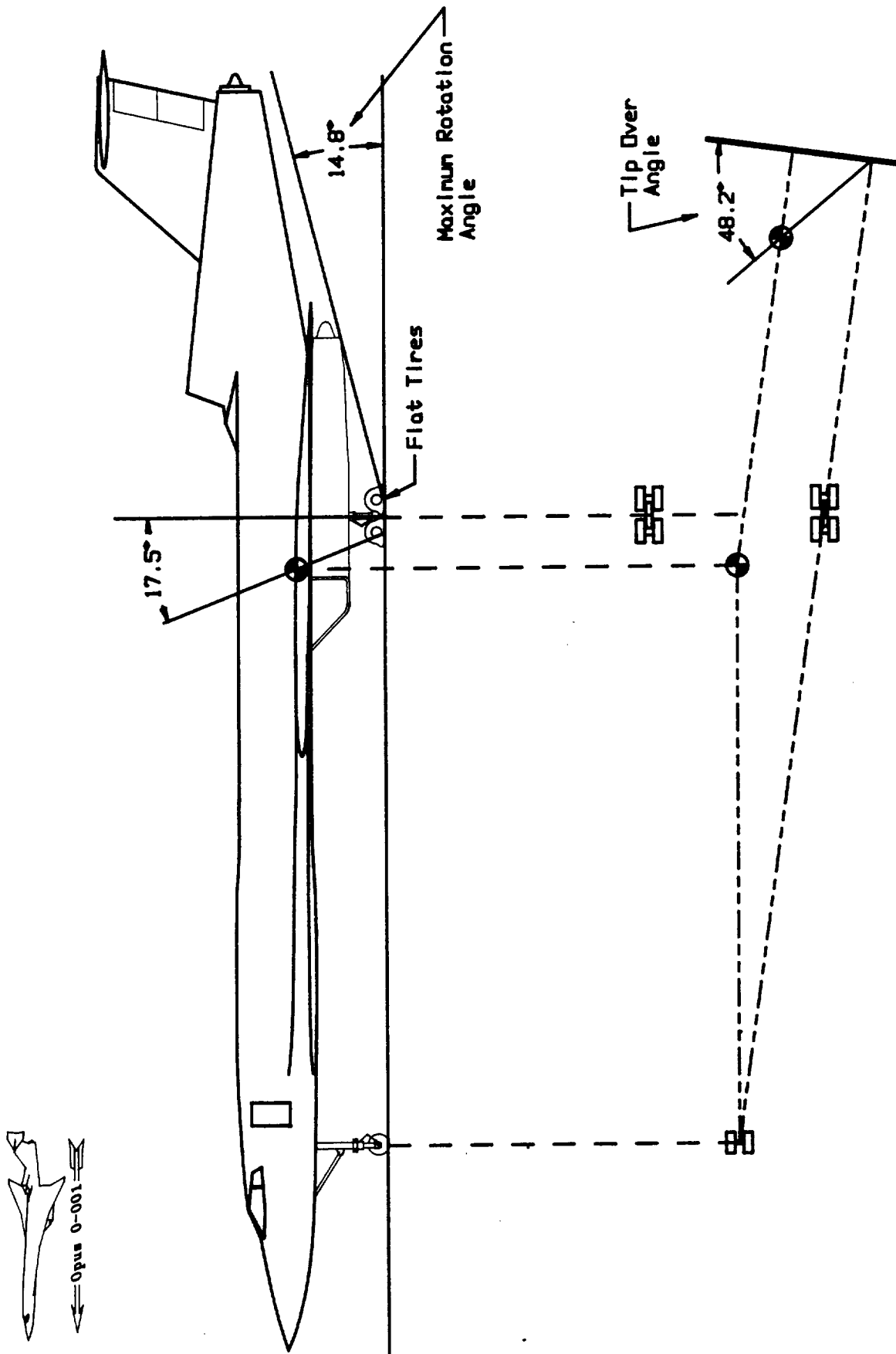
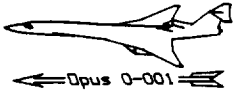


Figure 10.1: Critical Landing Gear Angles

The turn radius is dependent on the gear position and the nose gear steering angle. The nose gear is capable of steering to an angle of 75° degrees which is fairly typical of modern subsonic transports. This allows a turn radius of 127.7 feet as shown in Figure 10.2. The aircraft is thus capable of doing a low speed 180° turn on the typical 150 foot wide runway found at international airports. The concern about turning distance is critical for many of the larger HSCT which may require the addition of high cost fillets to existing runway and taxiway intersections.

10.2 Landing Gear Design

The gear are designed to be typical of those in service today to minimize development costs and maximize reliability. They are also designed to meet all FAA requirements and airport limitations. The volume of the retraction mechanism was critical since it must be housed in a thin wing. The main gear are shown in Figure 10.3. The design is very similar to that used on the Concorde. The major features of the design are its relative simplicity and its ability to shorten by eight inches during retraction to minimize moving the pivots (and the engines) farther out on the wing. The retraction sequence shown allows the struts and actuator to fit in the wing. The gear will be cooled during flight by vented cabin air. This will allow the brakes to absorb more heat during landing without risking damage to the tires.



180° Turn on 150 Foot Runway

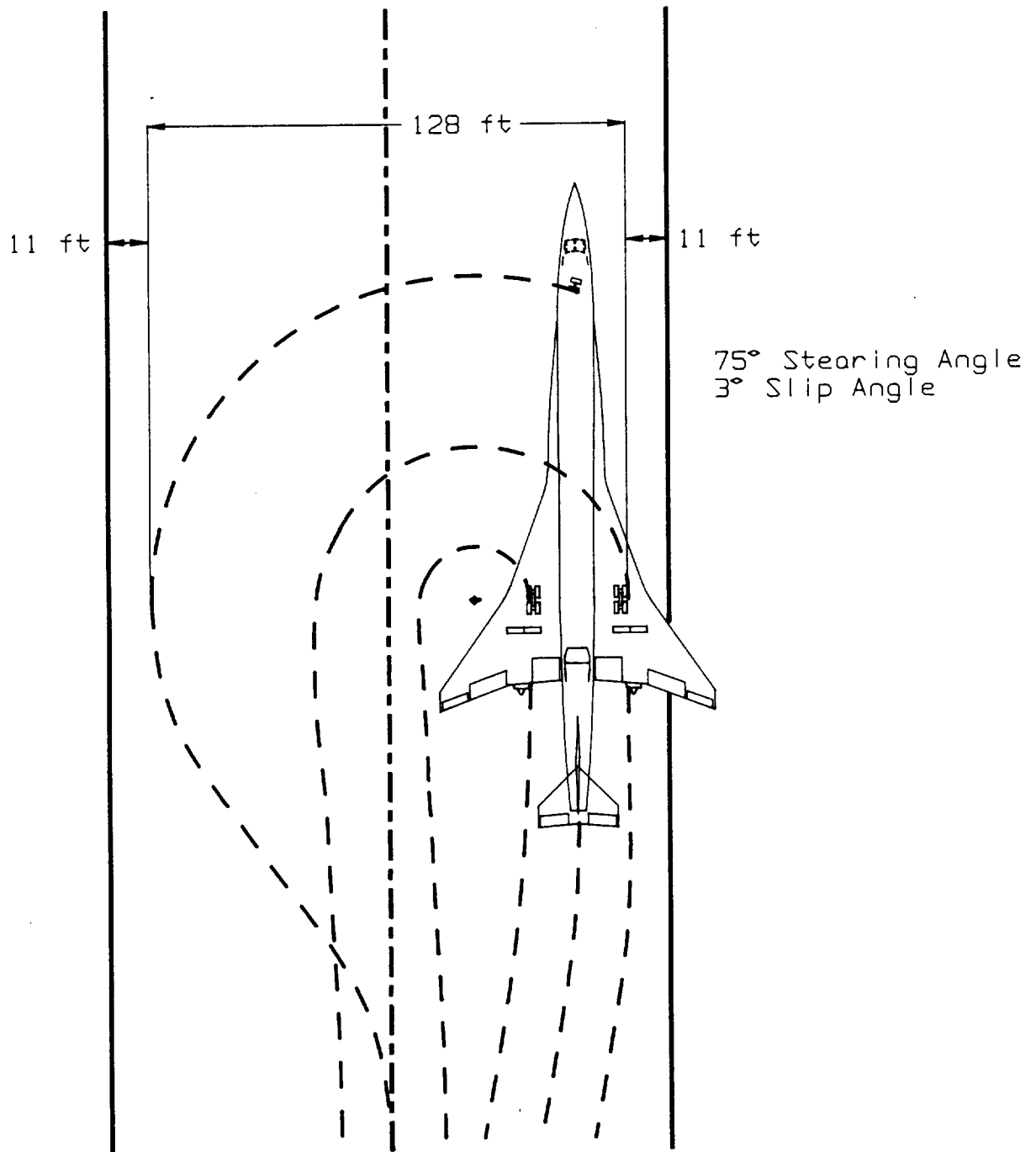
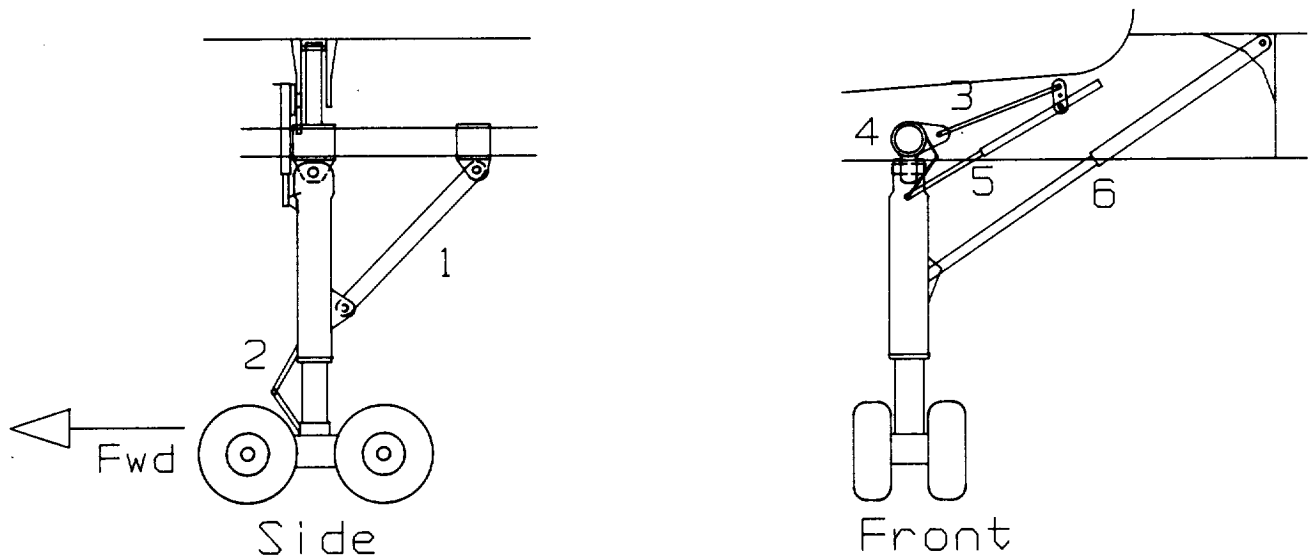
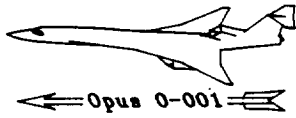
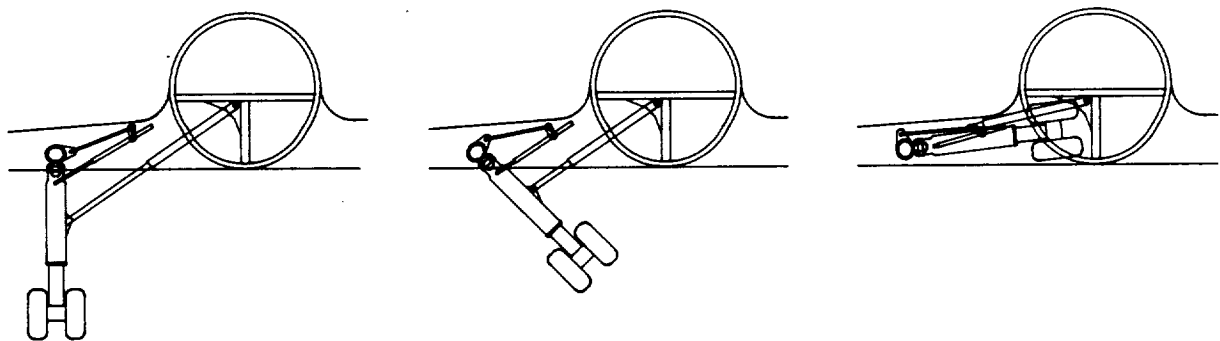


Figure 10.2: Ground Turning Capability



- 1 Longitudinal Brace
- 2 Torque Link
- 3 Compensating Linkage for final retraction
- 4 Leg-shortening Linkage
- 5 Retraction Jack
- 6 Telescopic Side Brace



Retraction Sequence

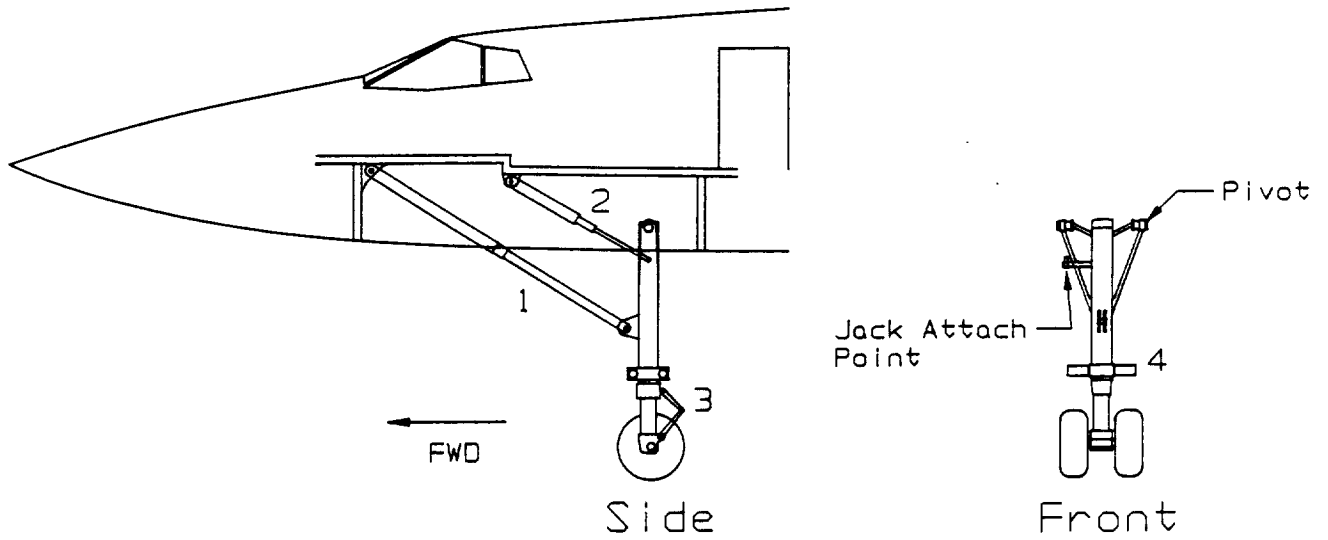
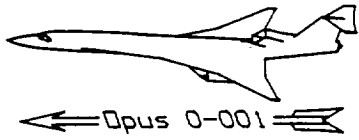
Figure 10.3: Main Landing Gear

The nose gear is shown in Figure 10.4. It is very similar to the Airbus 300D nose gear. The turn angle on this gear is approximately 75°. The retraction sequence shown allows the gear to be stowed under the cockpit without striking the floor. The tires used are advanced Type VIII which carry relatively high loads for small tires and which are better for high speed takeoff and landings. Table 10.1 displays the tire parameters for the main and nose gear. Note that the tires are the same size and type for main and nose gear which reduces replacement stock.

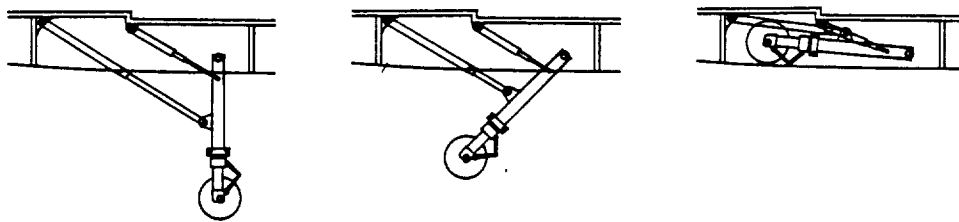
Tire Size:	37 x 14 - 14
Ply Rating:	24, Tubeless
Type:	VIII
Max. Loading (lbs):	25,000
Unloaded Press. (psi):	160
Tread Pattern:	Rib
Max. Speed (MPH):	225
Max. Diameter (in):	37
Loaded Radius (in):	15.1

Table 10.1 Tire Data for Main and Nose Gear (Reference 17)

The landing gear load classification number, determined using this tire data, was found to be 54 for the nose gear and 67 for the main gear. This number is well below the limit for current runways and is typical of many other subsonic transports which range between 30 and 90 (Reference 17). Again this is an area where the larger supersonic transports, which weigh nearly one million pounds, may have trouble and have to pay for runway upgrades.



- 1 Telescopic Drag Strut
- 2 Retraction Jack
- 3 Torque Link
- 4 Steering Jack



Retraction Sequence

Figure 10.4: Nose Landing Gear

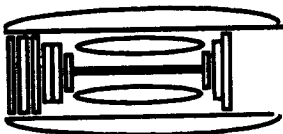
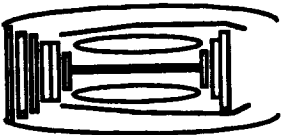
11.0 Propulsions

The failure of efforts to design and build a successful high speed civil transport in the early 70's was due in large part to limitations in propulsive system technology. Many of the factors driving the current designs are still dependent on engine developments. These drivers include noise, operating efficiency, emissions and specific fuel consumption. A weakness in any of these areas would cause an aircraft to be considered a failure. For this reason, the latest developments in propulsion technology were incorporated into the Opus 0-001 design.

The propulsion system design for the Opus 0-001 aircraft included selecting a powerplant, determining the engine locations, designing the inlet, and minimizing noise to meet at least Stage III requirements.

11.1 Engine Selection

Four basic turbine engine configurations were considered for the Opus 0-001. These were a conventional turbojet, a low by-pass turbofan, and two variable cycle engines (VCE): the tandem fan (Reference 18) and the NASA Lewis mixed flow engine (Reference 19). The engines were evaluated primarily on their efficiency, their thrust profile versus Mach number and altitude, and their noise output. The results of this trade study are shown in Table 11.1. Information on emissions was so scarce that comparison on the limited data would have been inaccurate.

Engine Type	Advantages	Disadvantages
 <p>Turbojet</p>	<ul style="list-style-type: none"> • fair supersonic efficiency • good thrust availability throughout altitude and Mach number range • proven reliability and maintainability 	<ul style="list-style-type: none"> • poor subsonic efficiency • excessive noise • excessive emissions
 <p>Low Bypass Ratio Turbofan</p>	<ul style="list-style-type: none"> • good supersonic efficiency • good thrust availability throughout altitude and Mach number range • proven reliability and maintainability 	<ul style="list-style-type: none"> • poor subsonic efficiency • excessive noise • excessive emissions

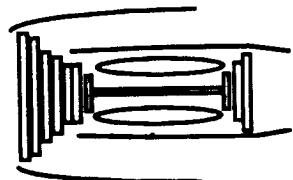
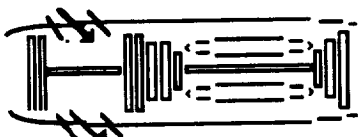
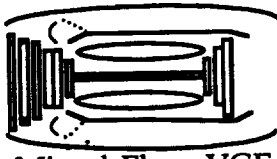
 <p>High Bypass Ratio Turbofan</p>	<ul style="list-style-type: none"> • good subsonic efficiency • low noise emissions 	<ul style="list-style-type: none"> • poor supersonic efficiency • large engine size and weight
 <p>Tandem Fan VCE</p>	<ul style="list-style-type: none"> • good efficiency for subsonic and supersonic regimes • low noise production, near Stage III requirements with no augmentation. 	<ul style="list-style-type: none"> • loss of thrust at altitude • large engine size and weight • new expensive technology • higher maintenance time and costs
 <p>Mixed Flow VCE</p>	<ul style="list-style-type: none"> • good efficiency for subsonic and supersonic regimes • low noise production, near Stage III requirements with some augmentation. 	<ul style="list-style-type: none"> • new expensive technology • higher maintenance time and costs

Table 11.1 Engine Trade Study

The variable cycle engines, both the tandem fan and the mixed flow, attempt to get good subsonic and supersonic properties by changing the effective bypass ratio for different flight regimes. The bypass ratio is increased for subsonic flight by opening vanes or auxiliary flow doors. The bypass ratio is then reduced for fuel efficient supersonic cruise. The basic difference between the tandem fan and the mixed flow engines is the means of varying the bypass ratio.

The tandem fan has two compressor sections. In low by-pass mode the air from the first compressor is fed into the second compressor. In high by-pass mode the air from the first compressor is directed out of the engine while the second compressor section draws in fresh air from auxiliary inlets to the engine core. The amount of flow through the two compressor sections is varied to change the bypass ratio.

The mixed flow engine has a single compressor section. The mass ratio of bypass flow to core flow is varied by changing internal engine geometry and opening

auxillary inlet doors to increase flow through the nozzle. There are a number of other configurations of the variable cycle concept but most are similar to those discussed here.

Engine efficiency was considered paramount in deciding on engine type. For this reason, the selection was quickly limited to one of the variable cycle engines. The decrease in thrust at cruise altitude of the tandem fan was so great, that a T/W ratio of 0.6 would have been necessary. This value of T/W was far too high for this type of aircraft. The mixed flow variable cycle engine did not have this problem. The noise, however, was higher than the tandem fan and would require more suppression. Even with the thrust losses incurred in noise suppression (Reference 20), the fuel consumption would be less for the mixed flow engine than the tandem fan with a T/W of 0.6.

The mixed flow variable cycle engine was selected for the Opus 0-001 to meet the mission requirement for thrust and efficiency. With some oversizing and mechanical noise suppression, FAR Part 36 Stage III restrictions could be met. The only drawback to this engine -- its increased costs due to its recent development -- was not critical.

11.2 Engine Position

A three engine layout was selected as described in the Aircraft Configuration section to minimize T/W and to avoid problems associated with four engines. A number of factors influenced the placement of the three engines. These factors included landing gear position, stability and control, inlet position, nacelle length, and structural considerations (Reference 21). The engine placement can be seen in Figure 11.1.

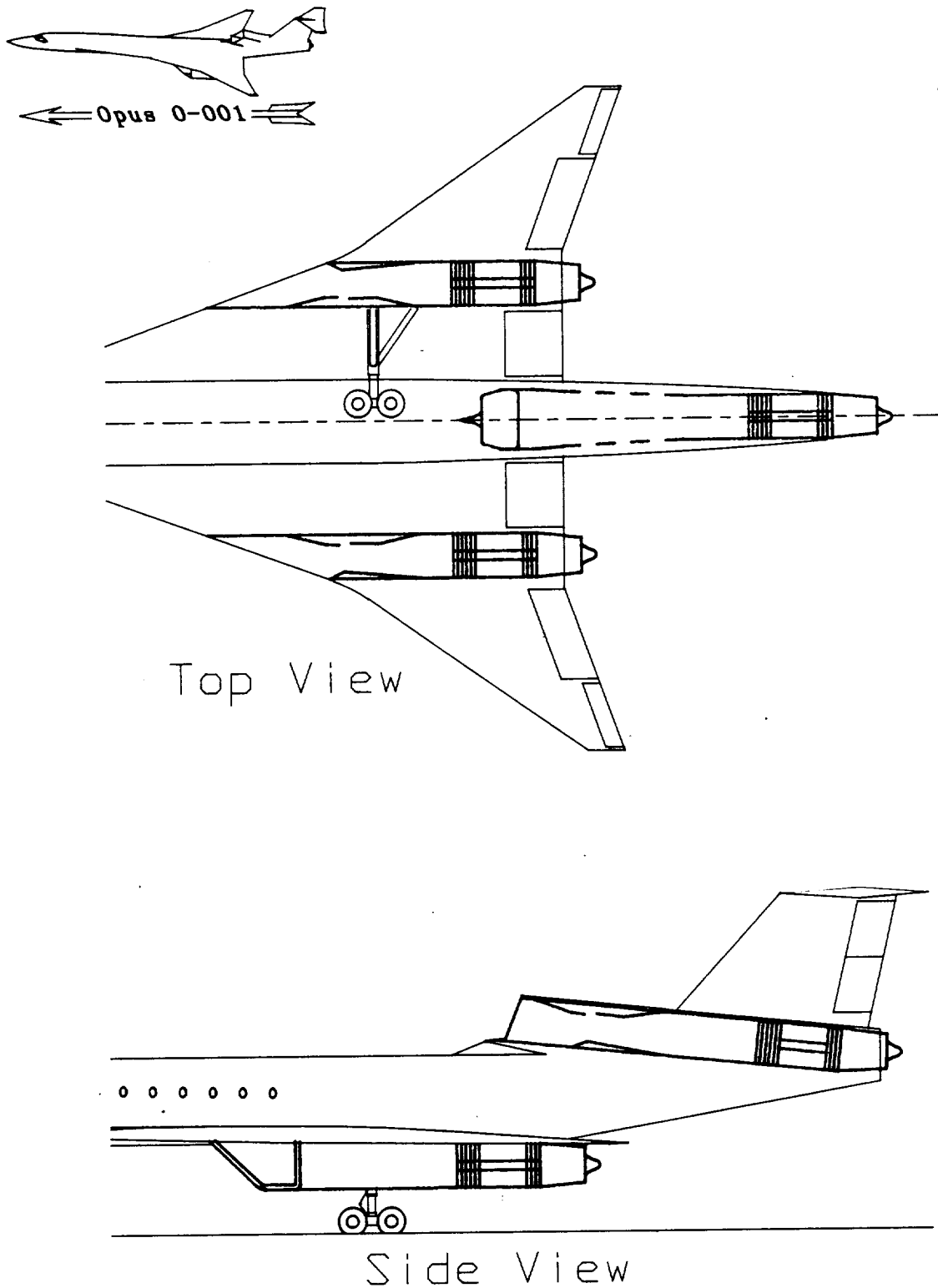


Figure 11.1: Engine, Inlet, and Nozzle Placement

The two wing-mounted engines were positioned as far inboard as possible to reduce the adverse effects of a critical engine failure on lateral stability. The landing gear however had to be sufficiently long to allow a 14° rotation during takeoff and landing. Since the landing gear could not have been retracted through the engine or in front of it, the engines were mounted outboard of the gear. These constraints put the final location of the engines just inboard of the wing span break. This position allowed the inlet to be located near the leading edge of the wing and be long enough for effective pressure recovery. The structure of the inboard portion of the wing was able to support the engine weight with minimal addition of structural weight and reinforcement.

The third engine was placed on the fuselage at the base of the vertical stabilizer as stated in Aircraft Configuration. A ventral position was considered but abandoned due to FOD problems and landing gear interference with the airflow into the inlet during gear retraction. The engine was oriented to keep a straight inlet aligned with the engine center line. The nozzle was then canted at a 5° angle to keep the thrust vector lined up with the aircraft longitudinal axis. This canting of the nozzle should cause little loss in thrust and seems to be typical for many HSCT design proposals (Reference 22).

The third engine position raised some concerns that were investigated, including:

- boundary layer ingestion
- flow separation over the fuselage at high angles of attack, stalling the compressor
- inlet blanketing of the vertical stabilizer at high angles of attack

The problem of degradation in engine performance and compressor stalls due to boundary layer ingestion were addressed by including a 1.4-foot boundary layer diverter. The maximum boundary layer thickness was calculated to be approximately 1.2 feet at Mach 0.1 (Reference 23). This value decreased with increasing Mach number. For Mach numbers below 0.1 the velocity gradient was small enough to cause negligible degradation in engine performance.

The concern of flow separating from the fuselage and stalling the compressor could not be addressed directly with mathematical or empirical means. Instead a review

of other jet aircraft with tail mounted engines was conducted to determine if any such problems existed. The aircraft considered were the McDonnell Douglas DC-10, Boeing 727, Lockheed L-1011, Handley Page HP-115, and Tupelov Tu-22 (Reference 14). Two other aircraft designs, were the supersonic NASA SCAT 16 and the proposed Gulfstream/Sukhoi supersonic business jet. None of these aircraft displayed any problems with the engines located similarly to the Opus 0-001 center engine. The HP-115 even demonstrated high angle of attack capabilities even with a large delta wing which would contribute to problems of ingesting turbulence.

The flow separation problem was further addressed by considering Navier-Stokes flow predictions for high angles of attack used on the McDonnell Douglas F/A-18 (Reference 24). These predictions showed that appreciable turbulence occurred at angles of attack greater than 20° , which is 10° beyond those expected for the Opus 0-001. At lower angles of attack some diversion of the flow across the fuselage was induced but not enough to cause any problems with the engine inlet. Therefore it is very unlikely that compressor stall will occur at the angles of attack the Opus 0-001 will achieve during normal flight.

Blanketing of the vertical stabilizer by the inlet at high angles of attack is not expected to be a problem. Assuming the airflow were to separate off the inlet and no flow was induced downward by the center engine the vertical stabilizer would still have only one half of its area blanketed. The vertical stabilizer is oversized by approximately 200% for OEI safety margin and should therefore have plenty of control power even at low speeds. Also at low speeds auxiliary doors, used to increase the mass flow rate through the inlet, will have an effect similar to boundary layer suction and should force the flow to reattach to the fuselage. The strong vortices trailing off the wing also forces the flow to follow the fuselage. Both of these effects will tend to cause less blanketing of the tail.

Wind tunnel testing or computational aerodynamics would have to be done to better refute the potential problems, but this is beyond the scope of the preliminary design. Based on the evidence given, the three engine configuration should be successful.

11.3 Inlet Design

The Opus 0-001 employs a two dimensional inlet on all three engines. The inlet is similar to the Concorde inlet, employing an adjustable isentropic ramp to decelerate the flow. A strong oblique shock then forms to bring the flow to subsonic speeds with minimal loss of total pressure. Total pressure recovery should be over 90%. A typical inlet cut-away is seen in Figure 11.2.

The inlet of the wing engines is positioned just behind the leading edge to maximize inlet length, take advantage of compression from the shock wave off the leading edge, and maximize L/D. According to Reference 25, L/D performance is maximum for inlets beginning near the wing trailing edge. L/D decreases for inlets near mid-chord, and increases again for inlets near leading edge. Structural considerations eliminated the possibility of placing the inlet near the trailing edge. The inlet for the aft engine was designed the same as the wing inlets so as to have nearly the same pressure and velocity at the compressor face. A podded axisymmetric inlet was considered but the structural problems and interference drag made this an impractical alternative. Since the 2-D inlet has been used successfully on the Concorde for years, development costs and unforeseen problems should be minimized.

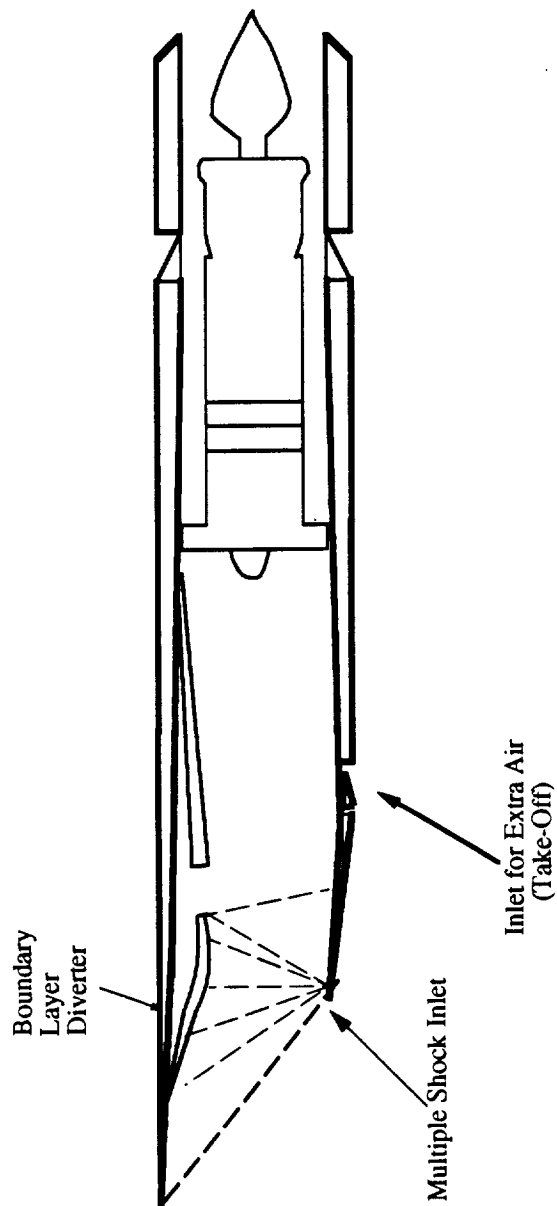


Figure 11.2 Inlet, Engine, and Nozzle Diagram

11.4 Engine Noise

To be a certifiable transport aircraft, the Opus 0-001 will have to meet at least FAR Stage III noise requirements. The mixed flow engine is close to meeting the requirements but further noise reduction must be achieved to increase this likelihood. The Opus 0-001 has an advantage over larger HSCT because data indicates a three engine aircraft will be 3-5 dB quieter than a four engine aircraft (Reference 26). The lower weight should also lower the noise a few decibels although experimental data confirming this is scarce. Jet exhaust noise is the largest contributor to total noise for the mixed flow engine. The engine is oversized approximately 15% to decrease the exhaust velocities. This oversizing should bring the velocities down to an acceptable level. Should further reduction in noise be necessary, a plug in the nozzle will invert the exhaust velocity profile. It has been shown that the inverted velocity profile will decrease the noise without a substantial loss in engine performance. Currently developments in engine noise suppression are making the likelihood of a small aircraft meeting Stage III requirements much more likely.

11.5 Propulsion Development

With current engine technology the Opus 0-001 can operate economically and meet Stage III noise requirements. Information on emissions was not available but should emissions be a problem, the selected NASA-Lewis mixed flow variable cycle engine is equipped with a clean combustor which minimized NO_x emissions. There continues to be many developments to decrease specific fuel consumption, noise, and emissions. New developments could continually be added to the Opus 0-001 to increase range and efficiency or decrease economic impact. Due to the advantages a smaller aircraft has in meeting noise limitations the Opus 0-001 will be able to operated effectively while the larger supersonic transport proposals are grounded waiting to somehow be certified.

12.0 Systems

12.1 Hydraulics

The Opus 0-001 incorporates a fly-by-wire system that is interfaced with a hydraulics system. This interface package is placed in the fuselage central to all flight controls. An advantage of having fly-by-wire to hydraulics system is to reduce hardware from the cockpit to the flight controls. A hydraulics system was used instead of an electrohydrostatic system since heat generated in the electrohydrostatic actuators would not be readily dissipated due to aerodynamic heating. Heat generated in the hydraulic system can be dissipated in the system.

The 8,000 psi hydraulics is composed of three separate systems following the Boeing 767 layout. Each system is distributed throughout the flight control actuators so that the loss of any two systems will not impair the ability to safely fly the aircraft to an emergency landing. The system layout is seen in Figure 12.1. Each engine pressurizes a system with two pumps in parallel as a redundancy. The reservoirs are set up for gravity feed to the pumps. The three hydraulic system pump layouts are seen in Figure 12.2. Each system contains an emergency accumulator which is normally uncharged. In the event of total loss of engine power each system has a dedicated nitrogen bottle that charges the emergency accumulator to allow control of the aircraft until the aircraft has decelerated to subsonic speeds, at which time a ram air turbine, RAT, is deployed to pressurize the center system. The landing gear may be deployed by free fall. The nose gear will lock down due to dynamic pressure since it folds down, and to the rear (Reference 27).

The hydraulic line layout to the flight controls is seen in Figure 12.3. Hydraulic system checks, engines off, will be accomplished by a single pump on the auxiliary power unit, APU, which cannot be operated in flight.

The hydraulic system reservoirs are accessed through the right and left main landing gear bays for the right and left systems respectively, and through an access door on the side of the rear of the fuselage for the center system. The rear system requires the use of a ladder, or scaffolding to access the reservoir as seen in Figure 12.4. The flight control to hydraulics interface is accessed through a plate on the bottom of the fuselage.

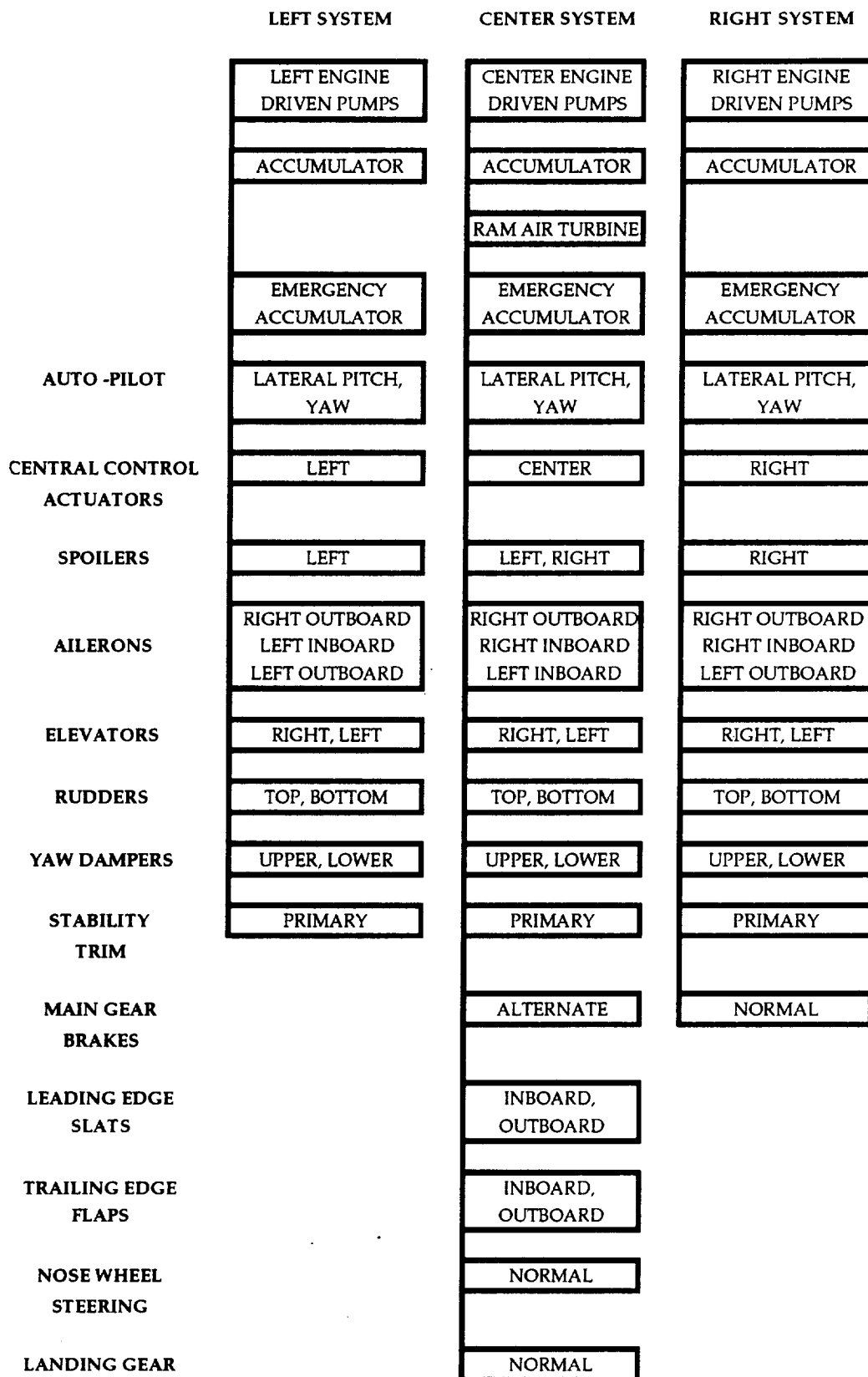


Figure 12.1 Hydraulics Schematic

Legend

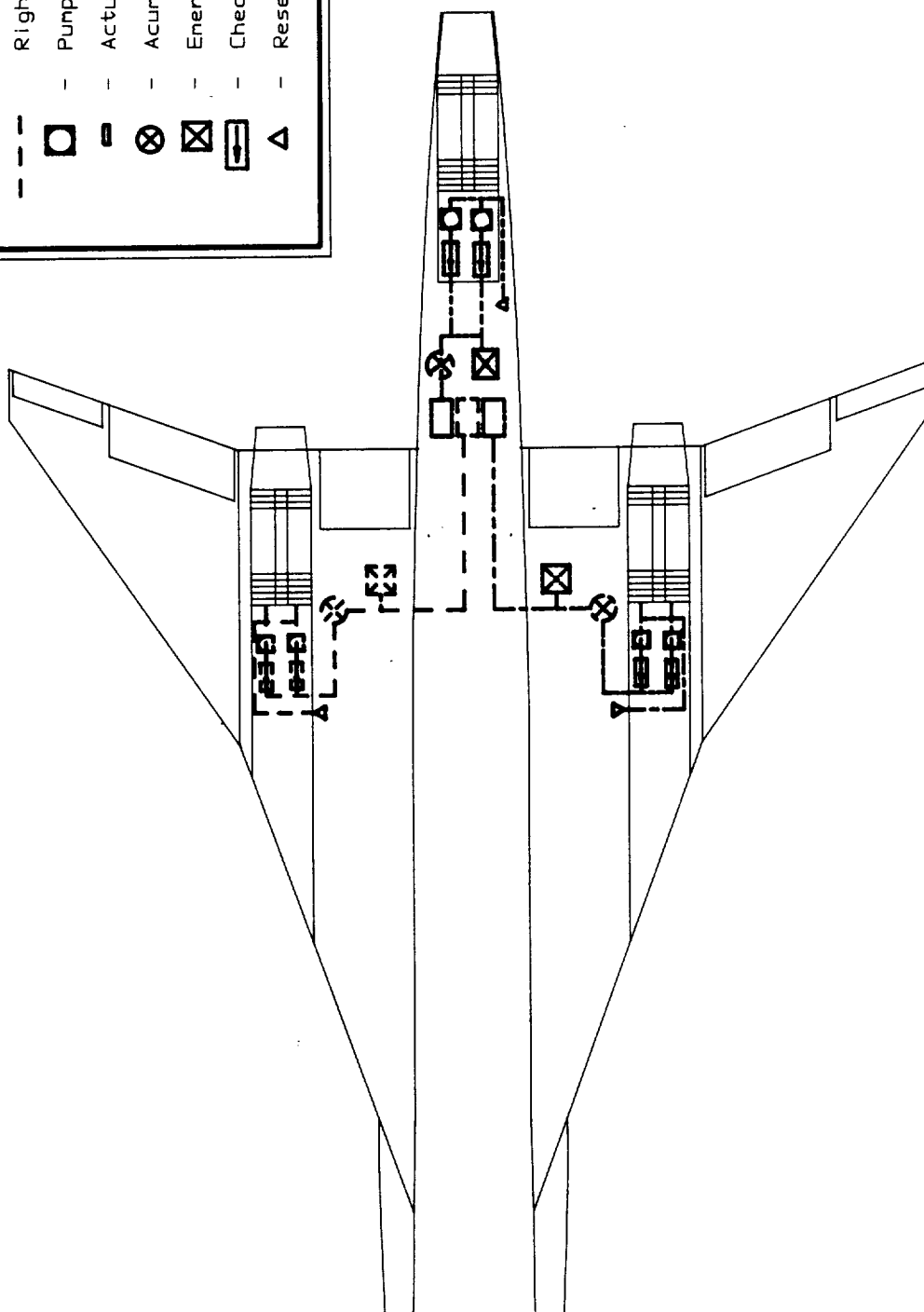
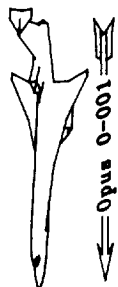
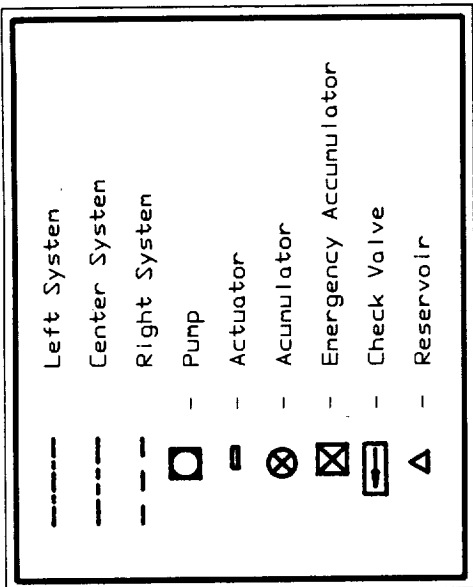
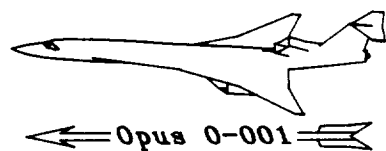


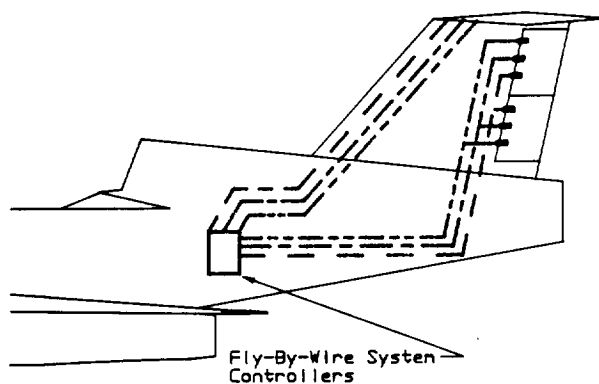
Figure 12.2: Hydraulic Pumps and Reservoirs



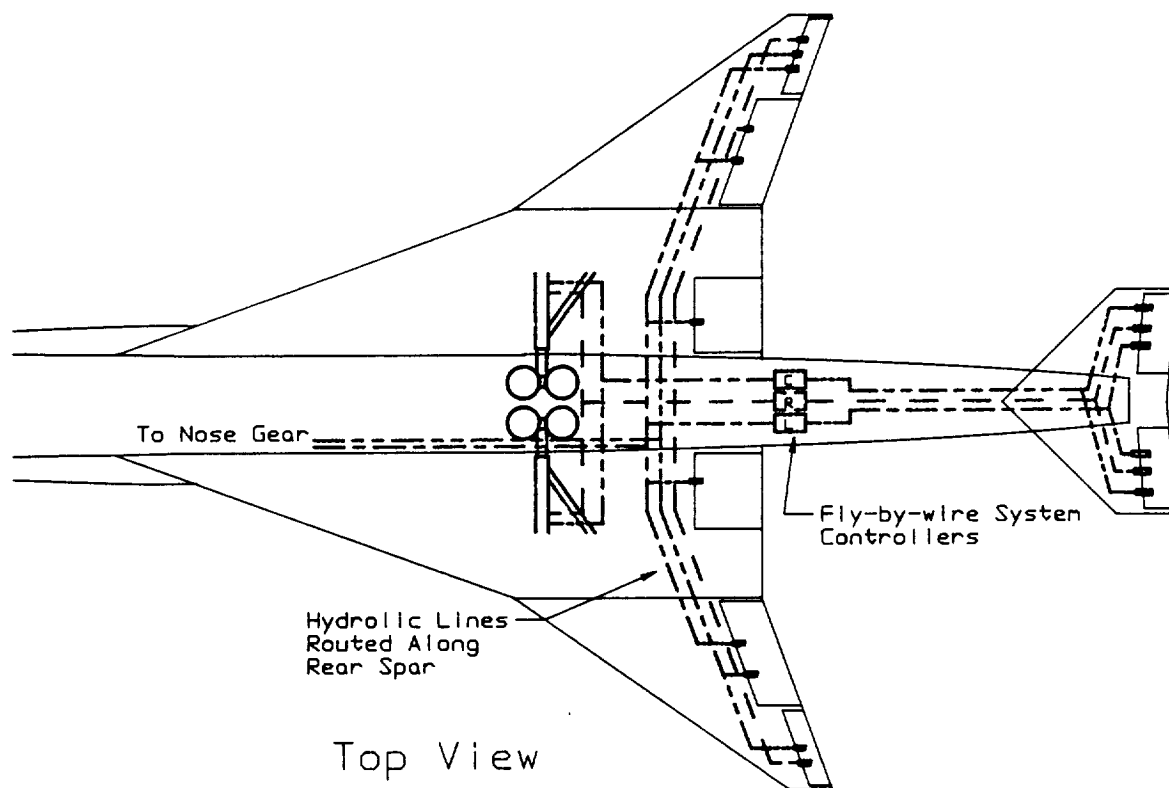
Legend

---	Left System
- - -	Right System
----	Center System
□	Actuator

Note: lines are shown joining together to simplify drawing. In reality each line is independent and distanced from other lines.



Side View
Empennage



Top View

Figure 12.3: Hydraulic Line Layout to Controls

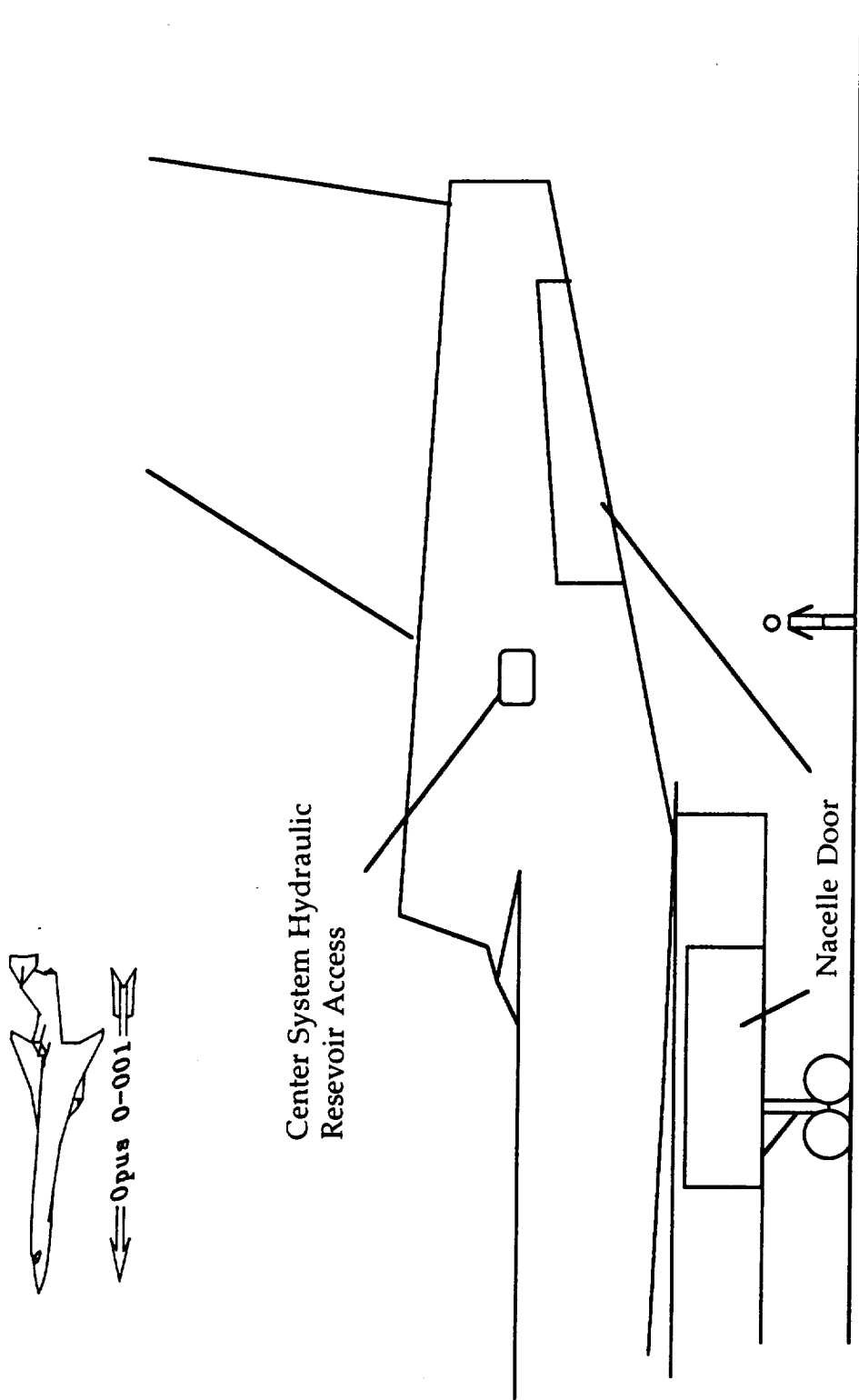


Figure 12.4 Center Hydraulics and Powerplant Access

12.2 Electrical

The electrical system is powered by three 80kVA alternators operating at 400Hz. An alternator is mounted on each engine, and one on the APU for ground power. In the event of total loss of engine power a gel type battery system is used for essential load electrical power which is then supplemented by the RAT at subsonic speeds.

Servicing, and inspection of the APU is possible via a door on the bottom of the fuselage adjacent to the APU. Service of the engine mounted alternators is possible through the nacelle doors, also seen in Figure 12.4.

12.3 Fuel

The total maximum engine thrust is 75,000 lbs. with a thrust specific fuel consumption of 1.2 lbs. fuel/lb. thrust/hour which sizes the maximum fuel flow required of the system to 90,000 lbs. fuel hour.

Fuel management is handled by computer for center of gravity adjustment, and distribution of fuel throughout the fuel tanks. Refueling is accomplished by pressure feeding from below each wing.

The wing tanks are wet wing type. The strake, and fuselage tanks are reinforced in the event of a gear up landing. All fuel tanks will be pressurized to avoid the possibility of fuel pump cavitation at the high altitudes that the Opus 0-001 will operate at. All tanks incorporate electric primary boost pumps in the tanks to further insure positive pressure in the fuel lines.

The wing, and strake fuel tanks are accessible for inspection through plates on the top of the strakes, and wings. The fuselage tanks are accessible for inspection from the bottom of the fuselage through plates. The access panel can be seen in Figure 12.5 along with the fuel cell arrangement. All tanks incorporate internal baffles to restrict fuel surging caused by aircraft accelerations, and all tanks are lined to ensure integrity in the sealing of the tanks.

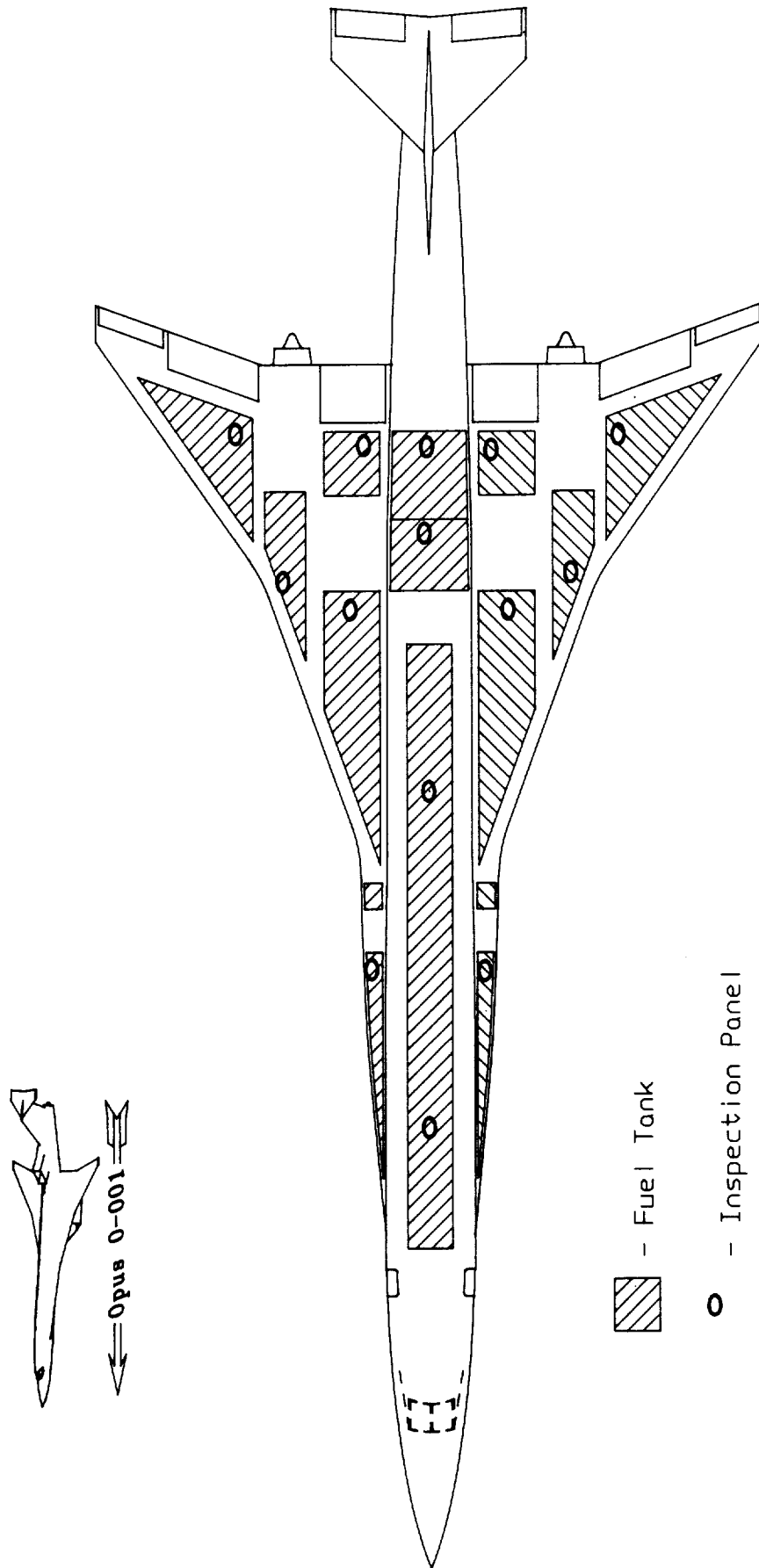


Figure 12.5: Fuel System Arrangement

12.4 Oxygen

The emergency oxygen system is composed of a chemical type for passengers and flight attendants, and bottled oxygen for the flight crew. There are chemical oxygen masks above each passenger seat, each lavatory, and each galley. The masks are stored in the ceiling, and drop down in the event of depressurization. The chemical oxygen is dispersed to a mask only when the mask is used. In case of a medical emergency there are two portable oxygen tanks, one in the forward galley and one in a dedicated cabinet at the end of the cabin across from the Type III emergency door.

Access to the chemical supplemental oxygen system is accomplished through the doors that store the masks. Servicing of the crew oxygen is accomplished through the nose gear well. The portable oxygen tanks are removed from the aircraft for servicing.

12.5 Anti-Ice

The engine inlet leading edges, vertical stabilizer leading edge, horizontal stabilizer leading edge, and the wing leading edges will incorporate anti-icing equipment in the form of an electrical resistance heating mat. This will be implemented when waiting for take-off, and flight in holding patterns in ice prone conditions. The elements are timed to heat eight seconds every minute, and alternate to different portions of the above mentioned points to reduce electrical loading.

12.6 Fire Extinguishing

Each engine nacelle, and the APU compartment, contain a high pressure fire bottle. The fire bottle is connected to plumbing that surrounds the engine with six "legs". This can be viewed in Figure 12.6. The extinguisher agent is discharged by either a two shot possible method by twisting the engine's T-handle in the cockpit, or by pulling the T-handle which cuts off the hydraulics, electrical, and the fuel while discharging the fire extinguishing agent to that engine. Each nacelle incorporates rate-of-temp-rise, and over-temp sensors. The APU extinguishing agent is discharged by a handle in the cockpit. A over-temp sensor is incorporated in the fire proof APU compartment.

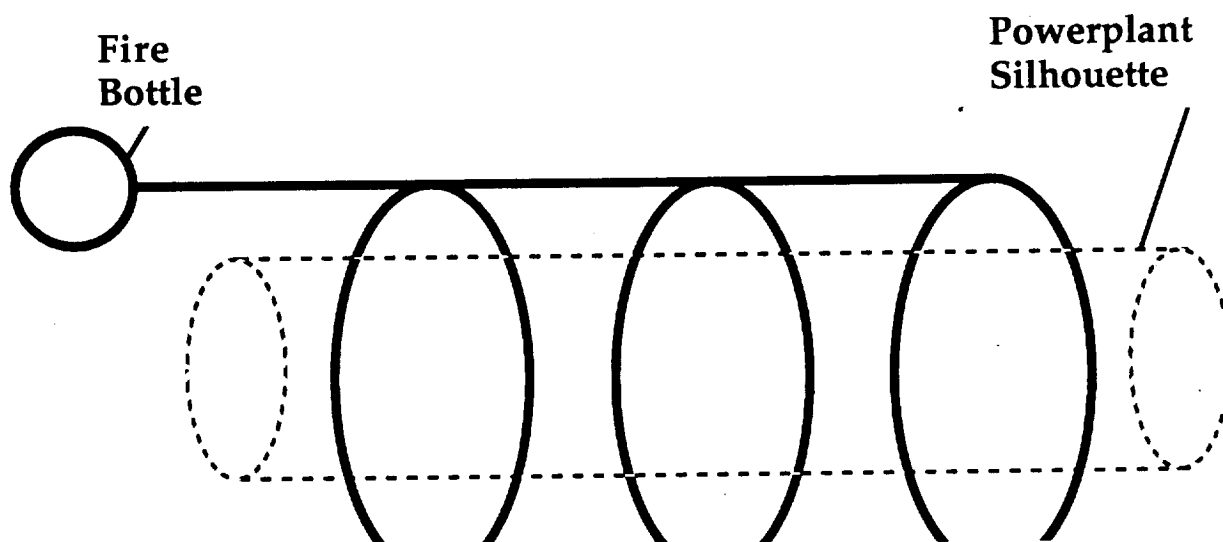


Figure 12.6 Engine Fire Extinguishing

The fire extinguishing bottles are serviced through the nacelle doors, or the APU access for the respective system.

12.7 Potable Water

The potable water is sized at 0.4 gallons per person which requires a 26 U.S. gallon reservoir placed aft of the nose landing gear bay. The reservoir is pressurized with air to allow for water system pressure. Plumbing connects the water tank to each lavatory, and galley. At each location the plumbing splits to hot and cold outlets, and to the commode in the case of the lavatories. An electrical heating element surrounds the hot water pipe for hot water at the sinks.

Servicing of the potable water tank is accessed the nose landing gear bay.

12.8 Waste Water

Waste water from the sinks of the lavatories, and galleys is piped to a holding tank in the rear of the aircraft. The holding tank incorporates a float that electrically controls valves at the inlet to the tank, and the outlet to overboard as seen in Figure 12.7. When the tank level reaches 1.5 gallons the float triggers the inlet valve to close. After the inlet closes the outlet to overboard opens. Due to differential pressure of the airspace in the tank with the outside air pressure, the tank is force

drained. When the float drops down the outlet is closed and then the inlet opens slowly and draws any accumulated water in the line into the tank while equalizing with the tank air pressure with the cabin air pressure.

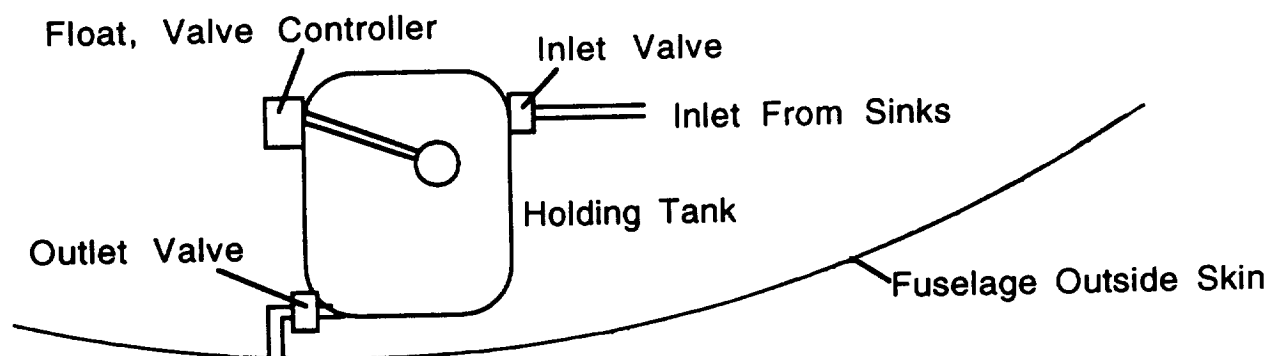


Figure 12.7 : Potable Water Waste

Waste from the commodes is handled in a similar manner. When a commode is flushed a valve that vents the holding tank overboard closes, and waste from the commode is drawn into the holding tank by differential pressure. A separator at the top of the tank restricts any waste from exiting overboard. Potable water is used to rinse the commode. The holding tank has a 40 U.S. gallon capacity, and is serviced through the main landing gear bay.

12.9 Air Conditioning / Pressurization

Sizing the system at 20 cu.ft./person/minute requires a circulation of 180 cu.ft./min. The pressurization and air conditioning system is fed by engine bleed air. After the air passes through a catalytic converter to disassociate the high ozone content into oxygen, the hot bleed air is fed through a primary heat exchanger and cooled partially by outside air. The air is then fed through a filter to remove radioactive

particles on its way to the compressor of the cold air system. The air leaves the compressor and flows through the secondary heat exchanger (again cooled by outside air), a fuel/air heat exchanger, and water separator before entering the turbine of the cold air system. The air leaves the cold air system and the temperature is regulated by mixing it with the air on the inlet side of the compressor of the cold air system. From there the air is piped throughout the cabin, and the baggage compartment. The avionics bay, and fly-by-wire to hydraulics interface temperatures are regulated independently from the cabin air. The air is dumped overboard via the landing gear wells. (Reference 1). A layout of the cabin air conditioning plumbing is seen in Figure 12.8.

Ground operation of the air-conditioning system is accomplished by tapping into the bleed air of the APU. Since the heat generated during flight is much greater than that on the ground the APU will deliver sufficient bleed air pressure for ground operation. The A/C system is accessed through a plate on the bottom of the fuselage.

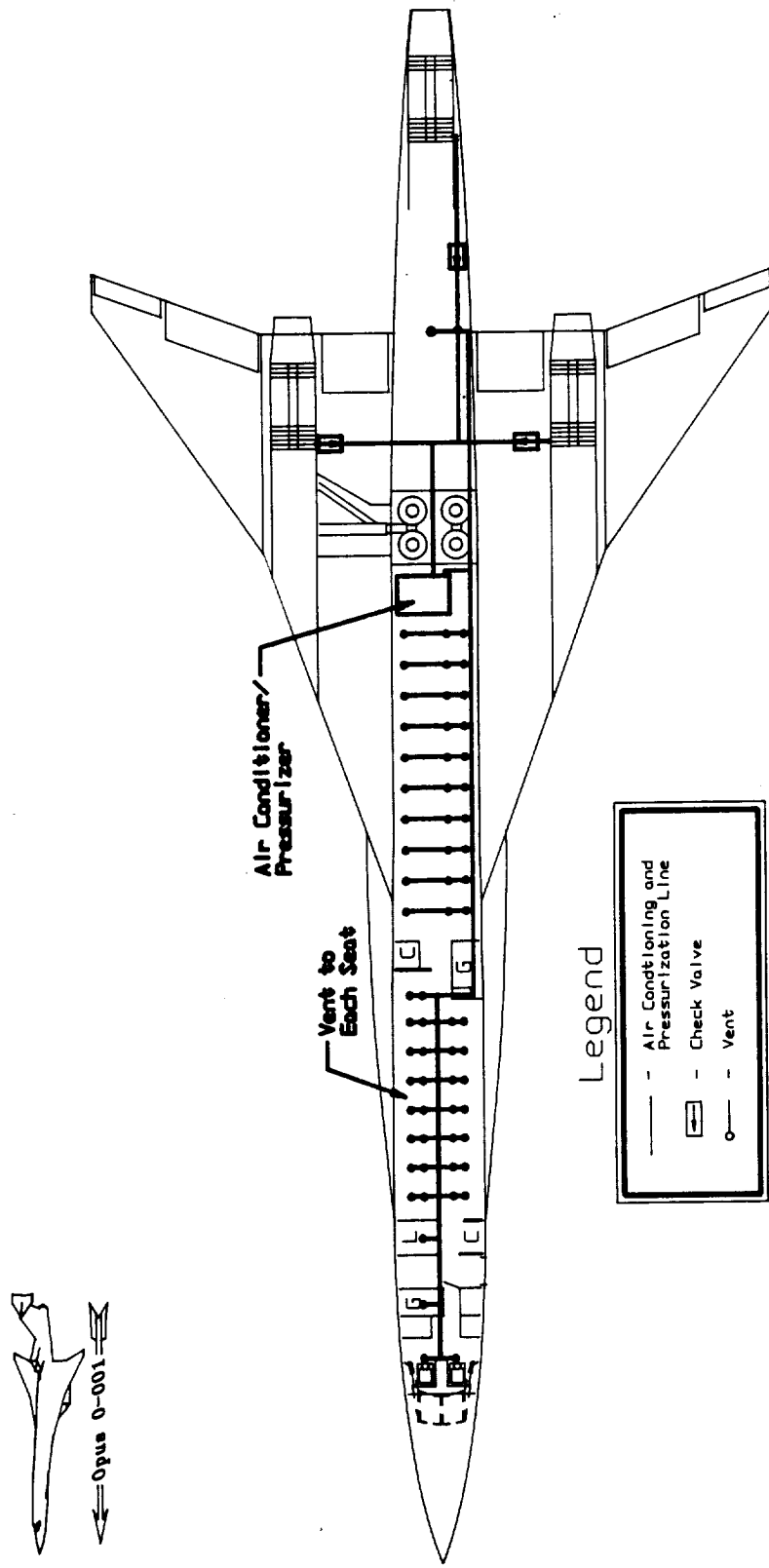


Figure 12.8: Air Conditioning and Pressurization System

12.10 Engine Servicing and Inspection

Servicing, and inspection of the wing mounted engines is possible through the nacelle doors. The nacelle immediately surrounding the core engines is removable for engine removal and replacement with conventional engine jacks. Servicing, and inspection of the rear engine is possible through clam shell type doors that open to completely expose the engine. A hoist is built into the structure above the engine for raising and lowering the engine to and from the engine mounts. All three engines are identical to reduce the number of specialized parts.

12.11 Galley

Galley serving is accomplished through the loading door across the from the passenger loading door. If turn around time proves to be a problem, the first class galley can be serviced through the Type III emergency exit located on the right side of the fuselage.

13.0 Structures

13.1 Fuselage

The fuselage was developed using conventional design and construction methods (Reference 28). The cross section is constructed in a double bubble layout. The load-carrying skin is supported on longitudinal stringers located at six inch intervals which are in turn mounted on hoop frames spaced at twenty inches on center. The frames are notched at their circumference to accept the stringers, which are T-section at the front of the aircraft and Z-section aft of the wing. These stronger Z-section stringers are needed due to the tail-heavy nature of the Opus 0-001. The forward skins are riveted to the hoop frames on a single flange while those aft of the wing are riveted to a double flange to increase stress resistance, and resistance to vibration fatigue caused by engine acoustic loading. (Appendix). Figure 13.1 shows the Opus 0-001 structural layout.

The cabin window frames in the Opus 0-001 needed particularly careful design. The windows are mounted in panels which are milled from plate aluminum to provide integral stiffening webs around the openings.

The cabin floor consists of balsa wood sheets sandwiched between aluminum alloy sheets. The floor is supported by floor spars set on the same spacing interval as the hoop frames. The floor spars are connected to the hoop frames at the intersection of the hoop double bubble. The portion of the fuselage under the floor contains fuel tanks. This area is reinforced to withstand a gear up landing.

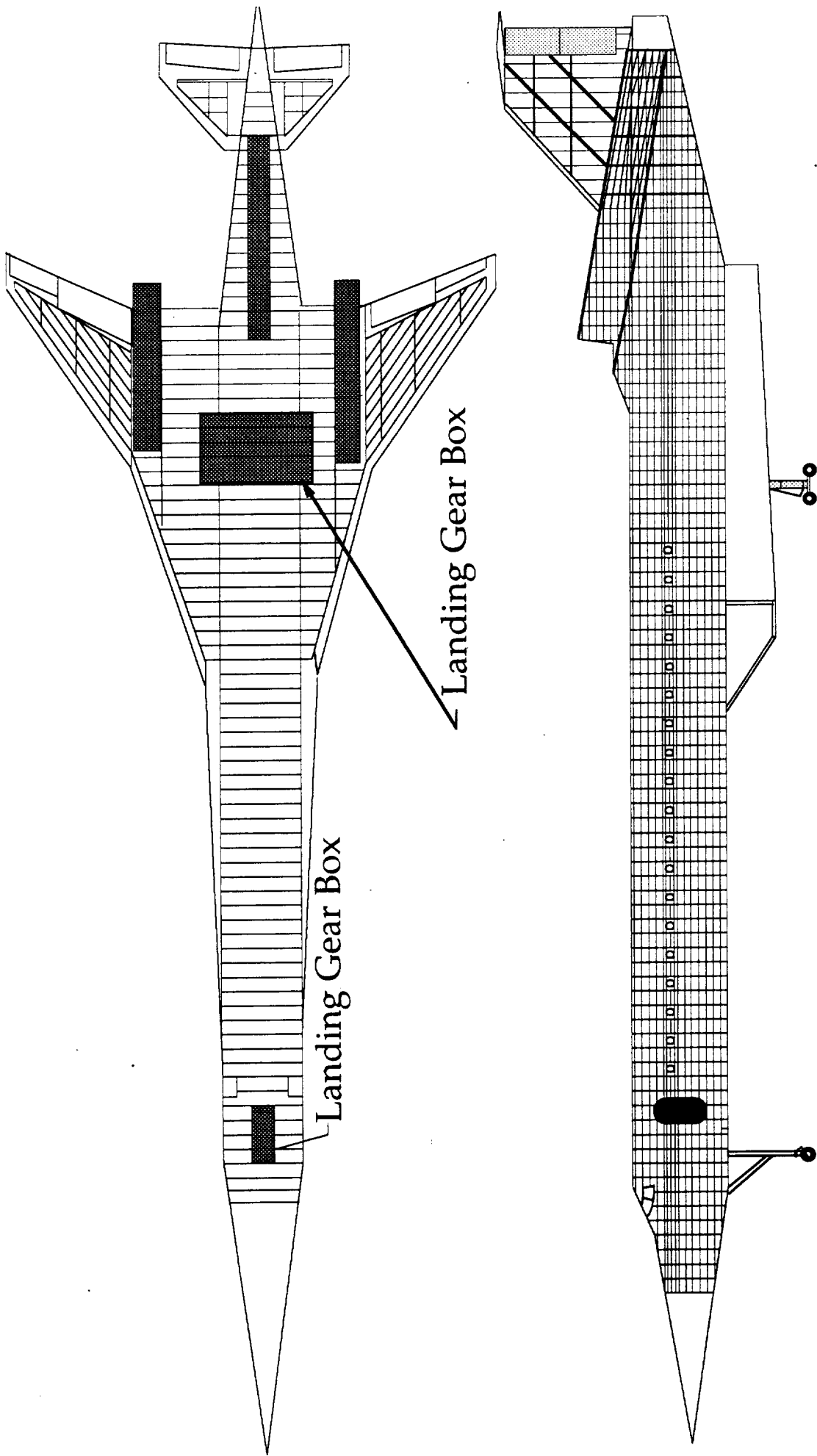


Figure 13.1 Opus 0-001 Structural Layout

13.2 Wing

The wing is constructed in a multi-spar torsion box configuration. The skin panels incorporate stiffening webs. A combination of leading edge spars, transverse spars, and ribs are used. This gives the wing more strength yet still provides enough capacity for the fuel tanks. The transverse spars and ribs are positioned to provide support to the landing gear bay, engine mounts, and trailing edge control surfaces. The structural layout of the wing can be seen in Figure 13.2. A preliminary design of the Opus 0-001's wing was analyzed by finite element analysis, using CAEDS. A wing was constructed, and key elements were defined as the prime loads (landing gear, engine, and fuel tanks). Figure 13.3 shows the expected results, the majority of the stress is concentrated on the inboard part of the wing.

13.3 Empennage

Similar construction techniques used for the wings were used for the vertical tail and the horizontal tail. The empennage was assumed to support lighter loads than the wing. However, the empennage spars were designed with the same cross section as those of the wing to ensure safety. Figure 13.1 shows the structural layout of the horizontal tail and the side view of the vertical tail. The structural layout for the aft of the Opus 0-001 is much more dense, due to the fact that it incorporates an engine, baggage compartment, and the empennage. The leading edge spar of the vertical tail is positioned to give support to the horizontal stabilizer longitudinal trim jack screw. The aft vertical tail spar is positioned to support the rudders, and the pivot for the horizontal stabilizer. The empennage spars are bolted to the fuselage hoop frame mounting brace.

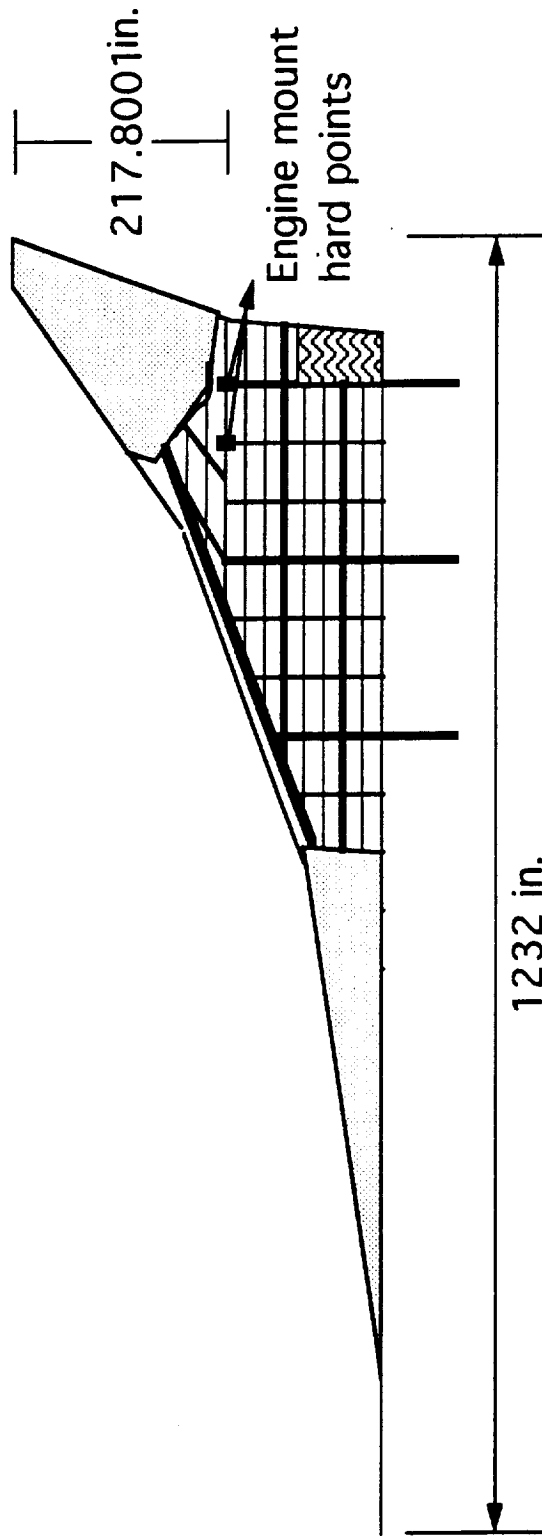


Figure 13.2 Opus 0-001 Wing Structure Layout

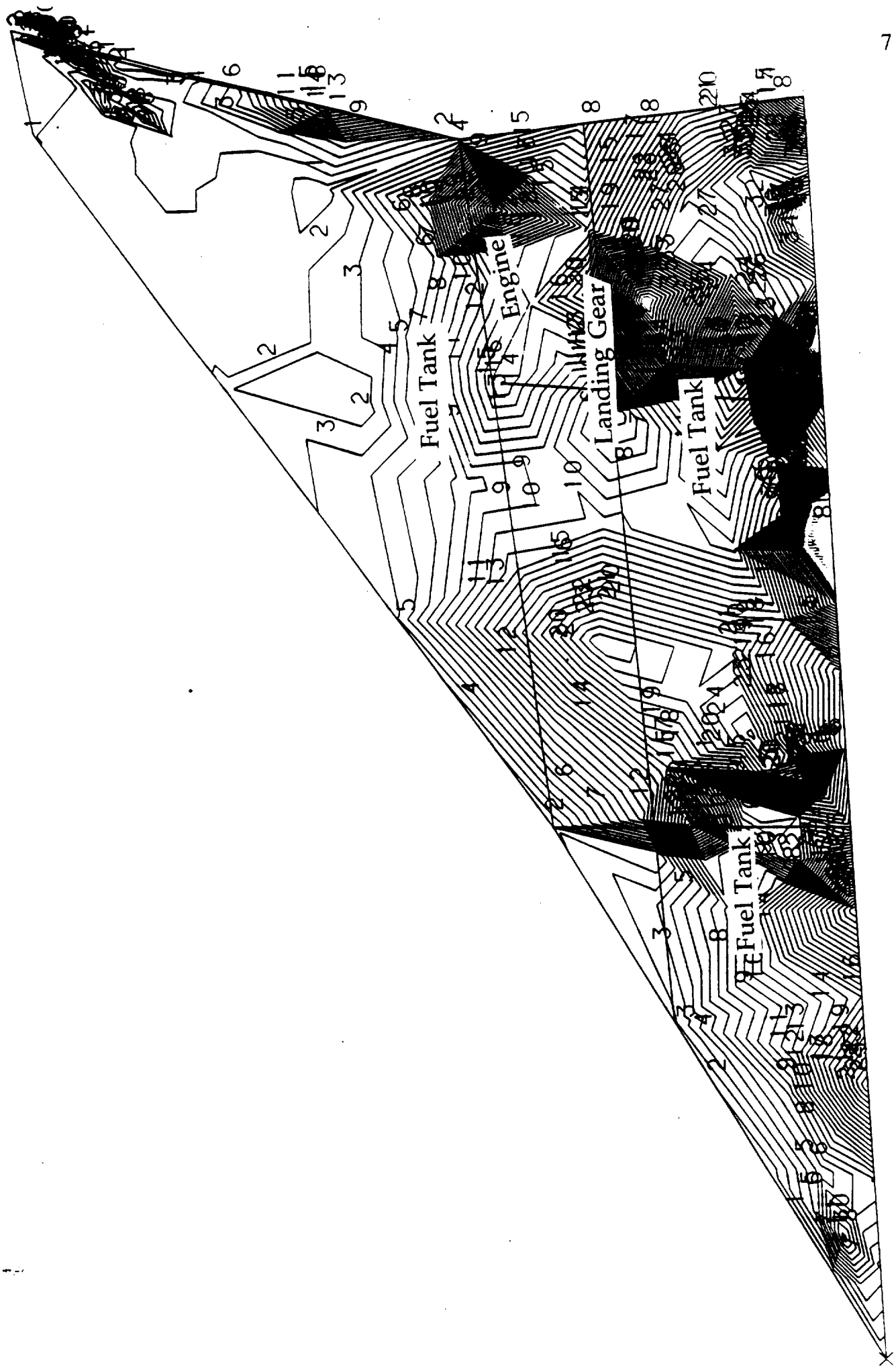


Figure 13.3 Stress Analysis

13.4 Structural Design Limits

The structure of the Opus 0-001 was designed to exceed the structural limitations set forth in the mission specifications. The critical load limit was found by the V-n diagrams shown in Table 13.1, and Figure 13.4. The positive load factor of 2.5 and a maximum negative load factor of -1.0 was used as specified in the Reference 4. Opus 0-001 was designed according to the maneuver envelope of the V-n diagram. Since Opus 0-001 is a commercial transport--absence of excessiv g maneuvers--the load factors prescribed will be sufficient under normal operations.

n - Load Factor		Equivalent Vel (KEAS)	
Positive	2.5	Vs - 1g	70
Negative	-1	Cruise	438
		Maneuver	111
C n, max		Dive Vel	613.3
Positive	1.74		
Negative	-0.71		

Table 13.1 - Design Limits and Design Ultimate Load Factors

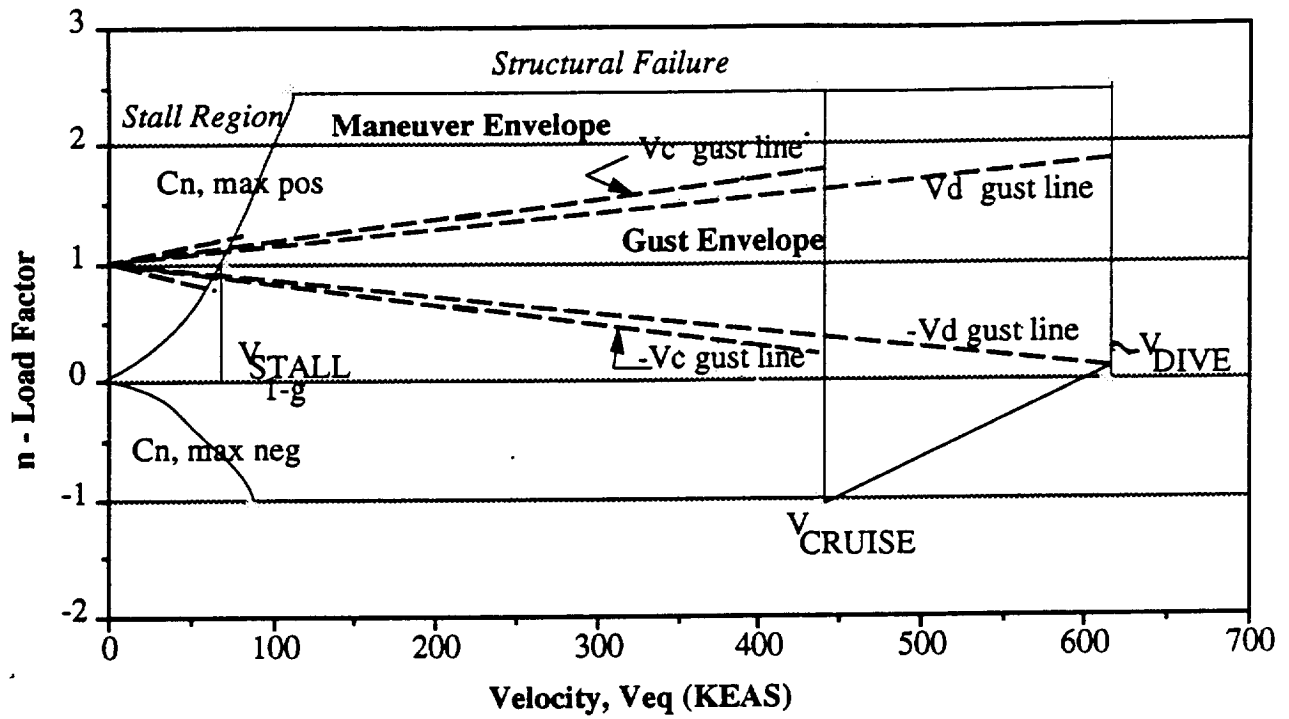


Figure 13.4 Structural Design Limits: V-n Diagram

14.0 Materials

Since the Opus 0-001 will fly at supersonic speeds, the materials chosen will have to provide the high strength to weight characteristics at elevated temperatures. Economic concerns dictate that they must also be cost effective. The Opus 0-001 will be flying at the same Mach number as the Concorde (Mach 2.2), therefore the principle materials selection for the Opus 0-001 was the same as the Concorde, mainly aluminum. The maximum temperatures on the aircraft occur at the nose of the aircraft, under the fuselage, and along the leading edges of the wings. Figure 14.1 shows the temperature variance over the surface of the aircraft, and the materials chosen for Opus 0-001 (Reference 1).

The majority of the aircraft will be constructed out of various aluminum alloys, but for sections subjected to higher temperatures, composites will be used (Reference 29). To conserve weight, honeycomb construction will be employed for the load-carrying skins; This will result in approximately 15% lighter skins. The nose cone and control surfaces will be constructed of an aluminum metal matrix composite which can withstand high temperatures and has a high specific yield strength (160 ksi). The fuselage and the wing skin material will be Al 6061 and Al 2618 due to the airplane's required temperature characteristics, low cost, and rather easy machining characteristics. Al 6061 has a maximum compressive yield stress of 150 ksi at room temperature. Finally, the landing gear struts will be made out of the conventional 300 M steel because of this materials high strength, proven characteristics, and low cost.

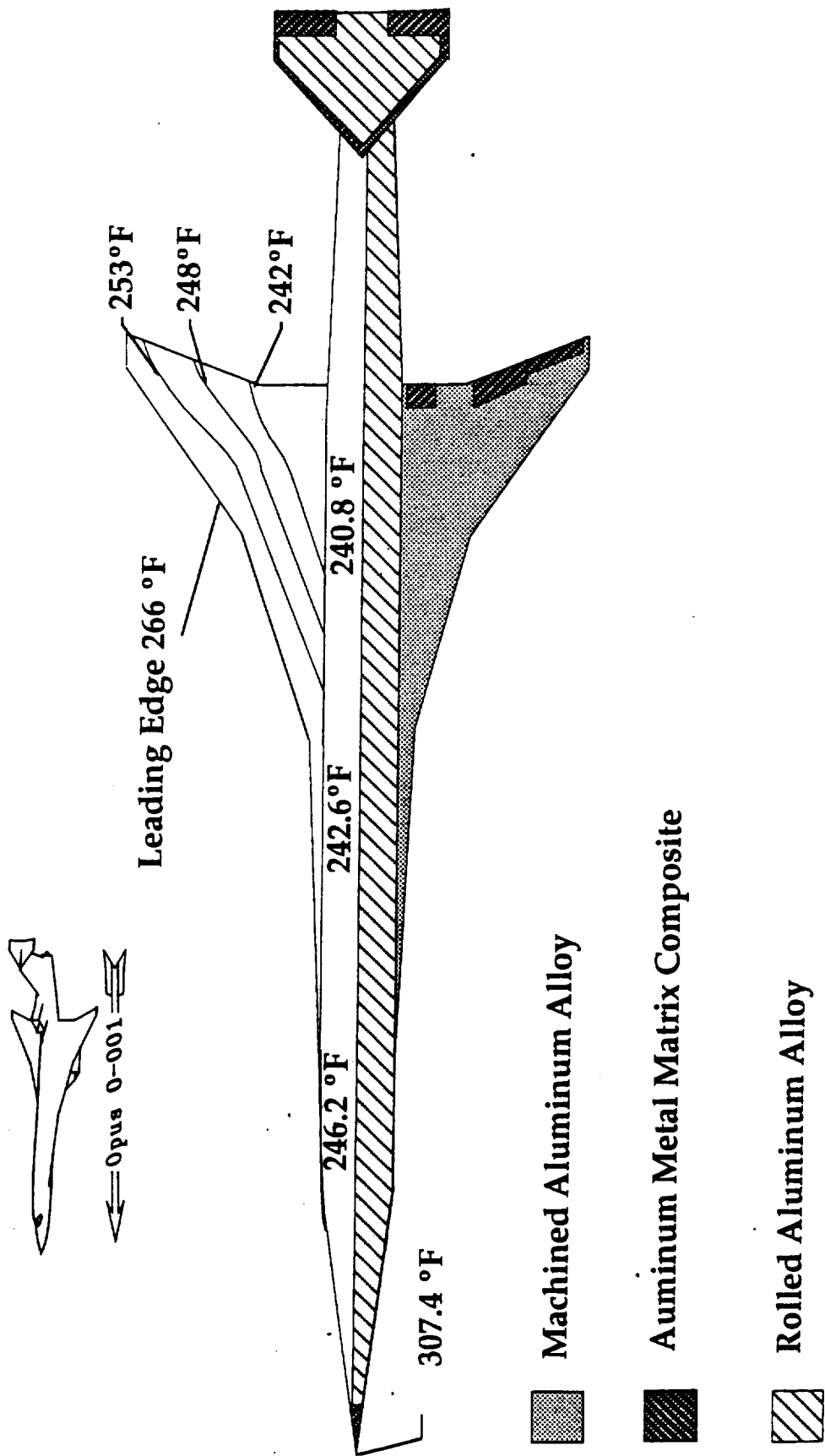
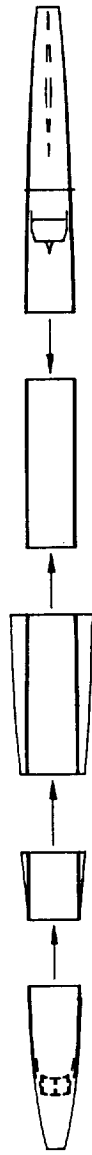
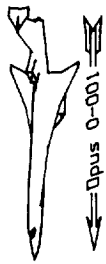


Figure 14.1 Skin Temperatures and Materials at Mach 2.2

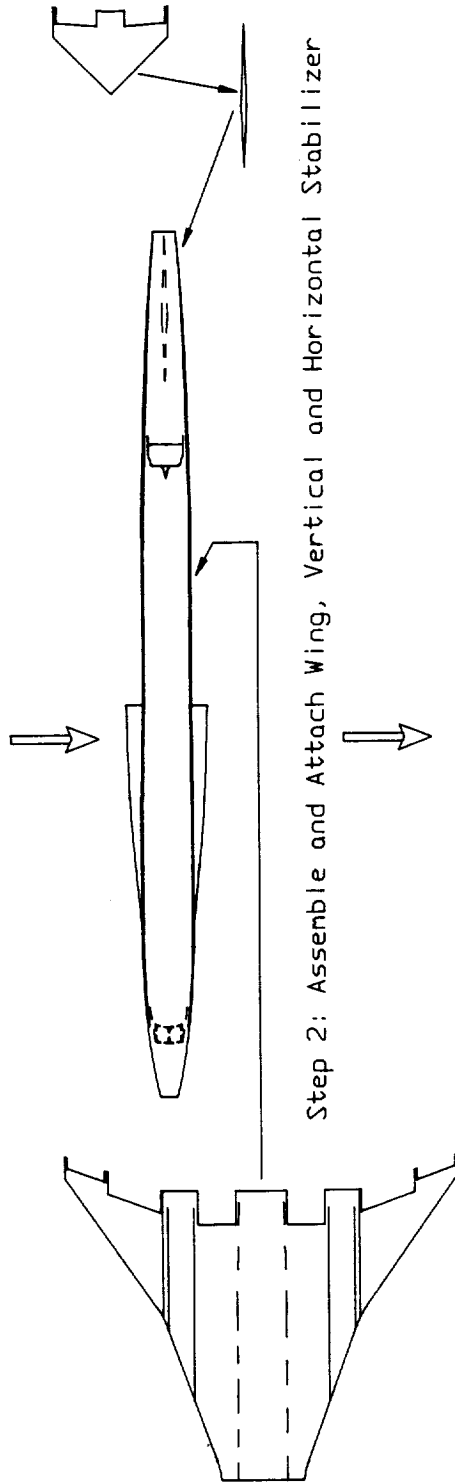
15.0 Manufacturing

The Opus 0-001 aircraft will be manufactured in a similar means to modern subsonic transports. The main objective of the manufacturing is to minimize cost. This will involve the utilization of modern computer aided manufacturing processes as well as management techniques such as "just in time" inventory control. "Just in time" inventory control and factory management involves scheduling the arrival of necessary parts and tools just when needed to avoid the cost of stockpiling unnecessary parts. There will be some advanced manufacturing processes involved in forming the composite parts, including the nose cone and control surfaces, and the titanium parts. These processes will cause a substantial increase in manufacturing cost but could not be avoided. The exotic materials were necessary due to the extreme operating conditions associated with supersonic flight. Figure 15.1 shows a simplified three step assemble diagram. Note that the aircraft is assembled in sections or "barrels." The advantages of using "barrels" is that they allow the relatively easy lengthening of the fuselage at a later date. Also, the construction facilities can be smaller and less costly. The barrels are segmented to allow sections of constant area to be assembled in one piece.

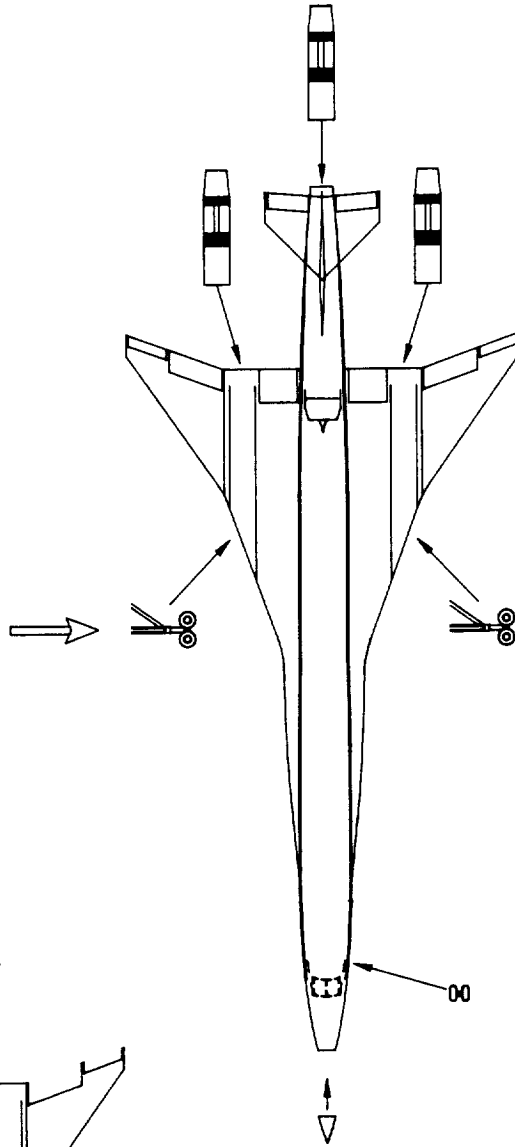
Another advantage of constructing the fuselage in barrels is that the construction of these parts can be distributed to other countries to take advantage of less expensive labor. This is a practice McDonnell Douglas and Boeing are utilizing to differing degrees. Douglas now has China assembling parts, shipped from the US, for the MD-80 aircraft. Boeing has China build sub-assemblies from US supplied materials and then ships the parts back for assembly by Boeing. The difference in pay scale between the Chinese and American work force is on the order of 70 times less, more than covering the costs of shipping all the parts and materials. A less obvious benefit of spreading the construction amongst a number of countries is the positive effect on foreign marketing for the aircraft. Many countries have government subsidized or owned airlines that tend to purchase aircraft that their country participated in building.



Step 1: Manufacture and Assemble Fuselage Barrels



Step 2: Assemble and Attach Wing, Vertical and Horizontal Stabilizer



Step 3: Install Landing Gear, Engines, Systems, Interior, and Composite Parts

Figure 15.1: Manufacturing and Assembly Breakdown

The first step in assembling the aircraft, after the parts and sub-assemblies have been constructed, is to join the barrels to form the fuselage. The wing is then assembled and mounted to the bottom of the fuselage. The outboard wing portion could be added later should space be critical. The horizontal and vertical stabilizer are also joined to fuselage in this second step. Finally the engines ,systems,landing gear, and cabin interior are added. At this time the composite parts of the aircraft are attached, such as the nose cone and control surfaces. This minimizes the chance of damaging these relatively sensitive parts during construction.

This preliminary manufacturing layout will allow an efficient use of manpower and space during the assembly of the aircraft.

16.0 Cost and Profitability Analysis

The Opus 0-001 aircraft is designed to carry sixty passengers for largely economic reasons. An in depth economic trade study revealed that the sixty passenger aircraft stands to have a higher profit margin for the airline (the customer). This peak profitability drove the selection of the sixty passenger size. The result of a highly iterative optimization is a projected fleet of 308 units, with a unit cost of \$92.0 million generating an optimum return on investment of 28% to the airline. Simply put, the reason for the peak in profitability for small aircraft for the HSCT market is fleet size and passenger demand. Research and development funds are a major expense. Increasing the fleet size distributes this cost further, reducing the cost of the aircraft per passenger-mile. The Opus 0-001 can divide its development costs over three hundred aircraft to achieve maximum profitability at approximately 5% market capture. To achieve the same fleet size, a large HSCT would need to capture a much larger segment of the market. To achieve the higher market capture, lower ticket prices would have to be charged. The larger HSCT would, therefore, have lower revenue per passenger mile. The larger HSCT also has a lower cost per passenger mile for a three hundred aircraft fleet. The percent reduction in revenue for the most profitable fleet of larger HSCT's exceeds the percent reduction in costs per passenger mile. This means that profit declines for seating capacities of more than forty passengers.

At the heart of this analysis is the reason behind the economic attractiveness of an HSCT in general and of the Opus 0-001 in particular. Although the costs of building, owning, and operating the Opus 0-001 aircraft are higher than a subsonic aircraft with a similar range, the reduction in travel time of roughly six hours over the design range is valuable in terms of increased passenger convenience and comfort. The difficult issue to predict is how much customers will be willing to pay over the contemporary subsonic airline fares. For the purposes of analysis, the value of the time saved was set to \$50/hour for first class, \$20/hour for business, and \$0/hour for economy class. Ticket prices were computed based on a demand curve. The dollar value of the time savings for each class was added to the respective subsonic fare and the resulting value was adjusted based on desired market capture to represent the variation of demand with ticket price. Advances in technology have brought the operating costs down low enough that a sizeable fleet is possible, resulting in the further division of development costs. Based on projected growth on long, over-

water routes, particularly in the Pacific Rim, an HSCT is definitely a potentially valuable asset. The analysis described above resulted in a comparison of a variety of payload sizes. Since the Opus 0-001 can achieve the cost savings of large fleet sizes without having to slash prices to fill the higher number of seats, it generates a higher profit percentage. The trends of profitability versus payload and cruise Mach number are illustrated in Figure 16.1. Note that the indicated percentages represent ideal market capture for the design range. Thus the relatively high magnitude of profitability indicated in the figure, (28.8%), is not meant to be representative of the actual economic performance for a more complex route structure. The same trends are evident for a wide variety of initial assumptions, and the same forces that would moderate the indicated profit level affect larger aircraft as well.

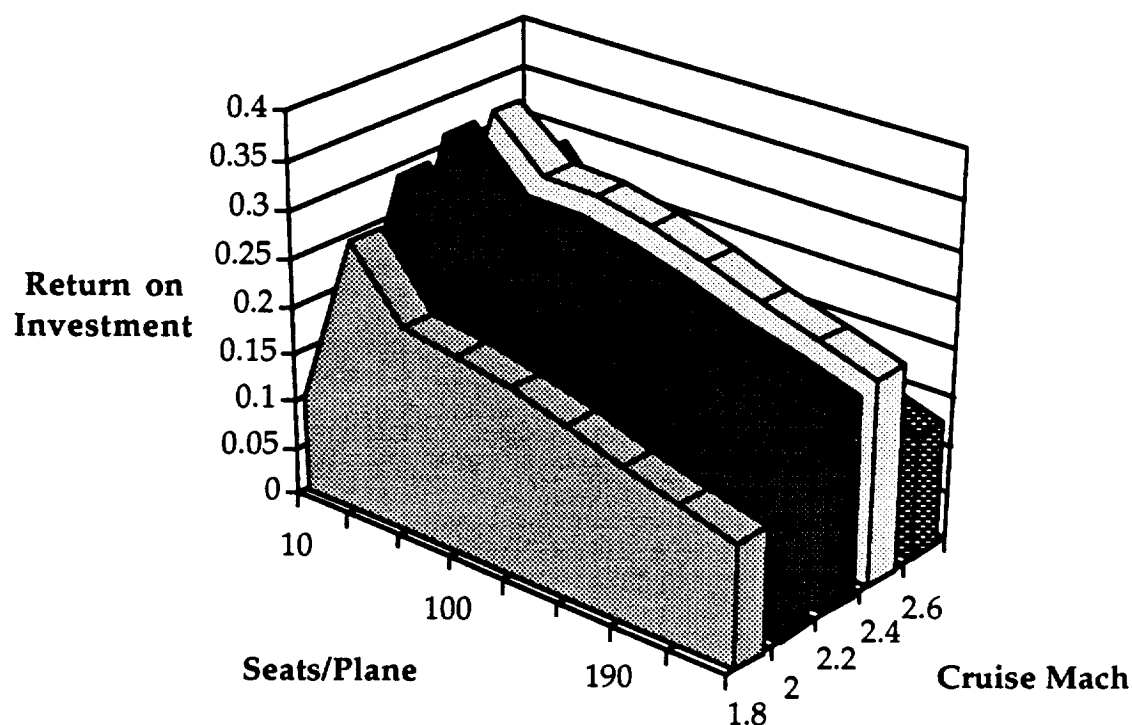


Figure 16.1 Maximum Return on Investment versus Seating Capacity and Mach number.

The costs were computed using both empirical and analytic techniques. The development program is projected to cost approximately \$15.93 billion. The per unit production costs total \$8.41 million, including learning curve effects. The aircraft development costs, shown in Figure 16.2, are based on empirical equations related to aircraft weight and cruise speed (Reference 30), as are the manufacturing costs detailed in Figure 16.3. Development costs are very high for the Opus 0-001 aircraft, as with other HSCT proposals. Thus, the airframer is forced to face a substantial "cash bucket" period prior to the entry of the first units into airline service. Consequently, the total cost computed from the development and manufacturing cost breakdown is marked up to finance the development program and to provide a reasonable return on investment to the airframe manufacturer.

The operating costs per trans-Pacific flight of the aircraft total \$34,000. The direct operating costs are predominated by fuel burn, as shown by Figure 16.4. This is a direct consequence of the required supersonic cruise range of 4,700 nautical miles. In selecting the cruise Mach number, the increased cost for fuel and the increased cost of manufacturing outweigh the advantages of speeds above Mach 2.2.

Note that the optimized parameter in selecting cruise Mach number and passenger size is return on investment. Generally, airframers design for minimum cost per seat-mile. In a highly competitive environment, where there is little differentiation between the service provide by one airline and another competing for the same market, the market capture is highly dependent upon shaving costs to a minimum. The Opus 0-001 aircraft provides a markedly different service from subsonic transports. This differentiation means that it can exploit a niche market. Like Singapore Airlines, SAS, and other subsonic airlines, the HSCT airline can serve a portion of the market with comfort and better service at a slightly higher cost. Due to noise constraints and the use of current technology, the Opus 0-001 will stand alone in the HSCT market for quite some time. Indeed, it is possible that the first manufacturer to market the Opus 0-001 will gain an invaluable foothold in the industry.

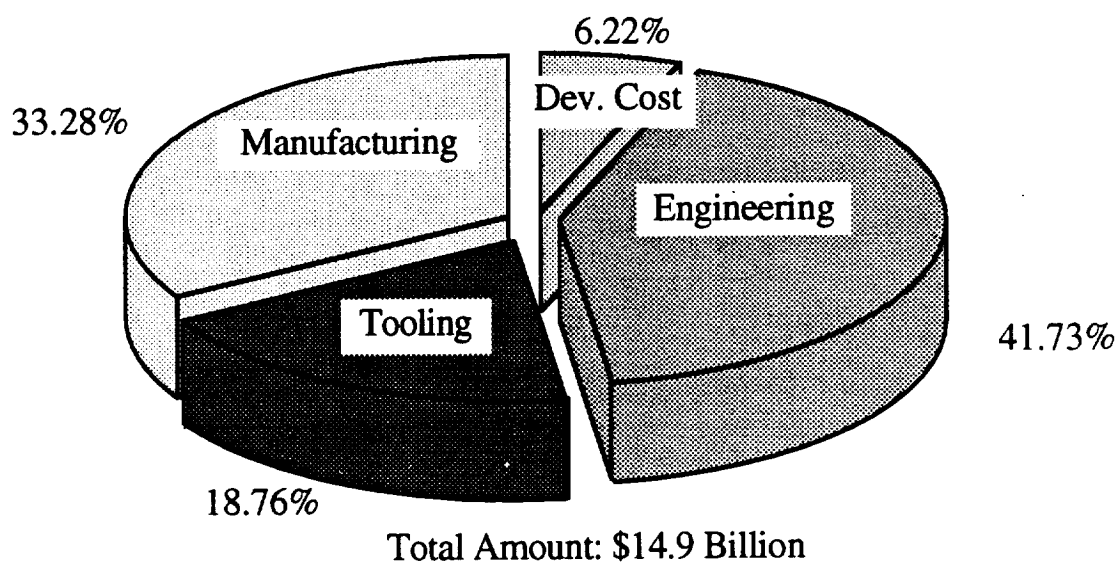


Figure 16.2 Aircraft Development Cost Breakdown

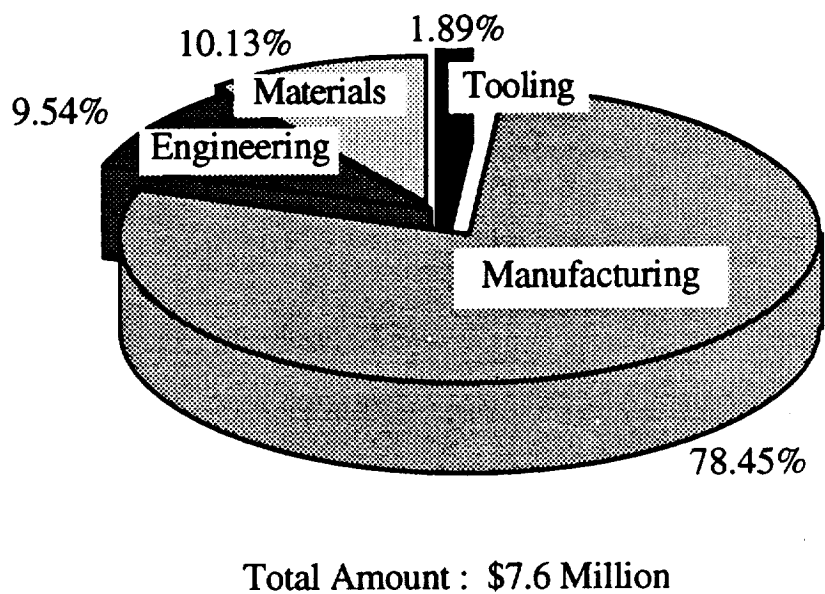


Figure 16.3 Manufacturing Cost Breakdown (per aircraft)

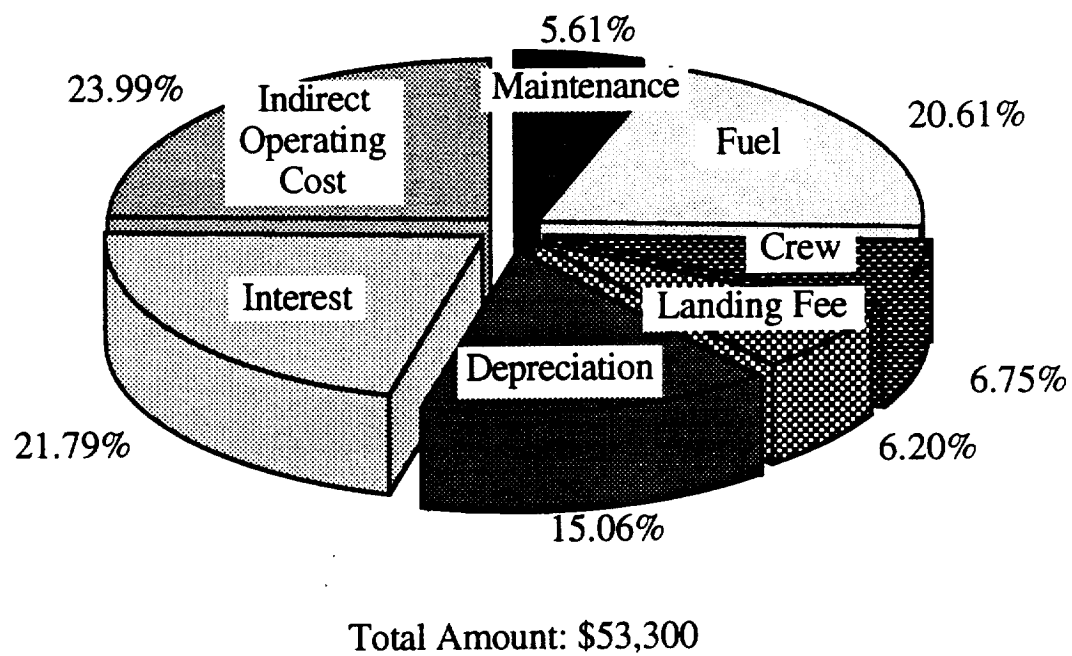


Figure 16.4 Operating Cost Breakdown (per flight)

17.0 Conclusions and Recommendations

The Opus 0-001 is a feasible design for a next generation HSCT. By combining economic realities with the engineering disciplines, the preliminary design of the Opus 0-001 aircraft is both practical and profitable. Current technology and the limited research and development money available make it highly unlikely that more than a single HSCT will see production in the near future. That single HSCT should be the Opus 0-001.

The following areas require further attention in the Opus 0-001 design:

- Design of a control system architecture to provide appropriate handling qualities,
- Aerodynamic data and stability derivatives need to be refined through computational fluid dynamics and wind tunnel investigation.
- Finite element analysis is needed to verify and optimize structural design.

This aircraft was design primarily using a integrated software package written by the Opus 0-001 design team members using Borland's Turbo Pascal, Version 6 programming language. This 5,000-line program contained the capability to analyze weights, aerodynamics, stability and control, and performance. Since the geometry is contained internally, modifications to the design can be universally implemented and rapidly evaluated. This process facilitated design refinement. Because of the generality of the tool, developing the algorithms enhanced the learning value of the design process.

18.0 References

1. Blackall, T.E., Concord: The Story the Facts & Figures, Foulis & Co. Ltd. Oxford, Great Britain. 1989
2. Morris, Charles E. K. Jr., et al., Some Key Considerations for High-Speed-Civil Transports, AIAA 88-4466, Atlanta, Georgia 1988.
3. Mizuno, H., Feasibility Study on the 2nd Generation SST. AIAA Paper. 91-3104, September 1990.
4. Acme Airlines, Request For Proposal, Cal Poly Design Team, 1991.
5. Roskam, J., Preliminary Sizing of Airplanes. Roskam Aviation and Engineering Corp., Kansas 1989.
6. Bonds, R., et al., Editors The Great Book of Modern Warplanes. Portland House, New York, New York 1987.
7. FitzSimmons R.D., et al., Advanced Supersonic Transport Engine Integration Studies for Near-Term Technology Readiness Date. AIAA 78-1052. July 1979.
8. Brown, R. Integration of Variable Cycle Engine Concepts in a Supersonic Aircraft. AIAA Paper 78-1049, July 1978.
9. Federal Aircraft Regulations (FAR), Part 25, Paragraphs 111, 119, 121.
10. Raymer, Daniel P., Aircraft Design: A Conceptual Approach, AIAA, Inc., Washington D.D., 1989.
11. Roskam, J. Component Weight Estimation, Roskam Aviation and Engineering Corp., Kansas 1989.
12. Roskam, J., Preliminary Calculation of Aerodynamic Thrust & Power Characteristics. Roskam Aviation and Engineering Corp. Kansas 1989.
13. Roskam, J., Determination of Stability. Control & Performance Characteristics: FAR and Military Requirements. Roskam Aviation and Engineering Corp., Kansas 1989.
14. Swanbrough, G., Modern Commercial Aircraft, Portland House, New York, New York. 1987.
15. Doenhoff, A., Abbot, I., Theory of Wing Sections, Dover Publications, Inc. New York, New York., 1958.

16. Roskam, J., Layout Design of Cockpit, Fuselage, Wing and Empennage: Cutaways & Inboard Profiles. Roskam Aviation and Engineering Corp., Kansas 1989.
17. Roskam, J., Layout Design of Landing Gear & Systems. Roskam Aviation and Engineering Corp., Kansas 1989.
18. Bushell, K. W., Supersonic Aircraft Power Plant. Lecture Delivered at Cal Poly, February 1992.
19. NASA Lewis Research Center Mixed Flow Turbofan Performance Data. January 1992.
20. FitzSimmons, R. D., et al., Flight & Wind Tunnel Test Results of a Mechanical Jet Noise Suppressor Nozzle, AIAA Paper. 80-0165, January 1989.
21. Roskam, J., Preliminary Configuration Design and Integration of Propulsion Systems. Roskam Aviation and Engineering Corp., Kansas, 1989.
22. Douglas Aircraft Company, Study of High Speed Civil Transport. NASA Contractor Report - 4235, 1989.
23. Schlichting, Hermann, Boudary Layer Theory, Seventh Edition, McGraw-Hill Publishing Co., 1955.
24. Cummings, R. M., et al., Navier Stokes Prediction of the Flow Field Around the F-18 (HARV) Wing and Fuselage at Large Incidence AIAA 90-0099, January 1990.
25. Boeing Commercial Airplanes, High-Speed Civil Transport Study, NASA Contractor Report -4233, 1989.
26. Bushell, K. W., Future Supersonic Transport Noise--Lessons from the Past. AIAA 88-2989, July 1988.
27. Van't Riet, R., Lecture Notes: Aircraft, Cal Poly San Luis Obispo, 1992.
28. Niu, M., Airframe Structural Design. Commilit Press Ltd., Los Angeles, CA, April 1989.
29. ASM International, How to Apply Advanced Composites Technology, ASM International Engineering Society of Detroit, MI. September 1988.

30. Edie. Donald, Cost Estimating Relationships for Airframes in the Development and Production Phases, NASA Technical Memorandum 809229, Hampton, 1980.